Genetic and Morphological Analyses of Three Freshwater Mussel Species in Isolated River Drainages Across Appalachia

Katlyn M. Ortiz

Thesis submitted to the faculty of the Virginia Polytechnic Institute and State University in partial fulfillment of the requirements for the degree of

Master of Science

In

Fish and Wildlife Conservation

Jess W. Jones, Chair

Eric M. Hallerman

Katy Klymus

February 16, 2024

Blacksburg, VA

Keywords: Freshwater Mussels, *Leaunio ortmanni*, *Leaunio vanuxemensis*, *Cambarunio iris*, *Cambarunio taeniatus*, genetic, mitochondrial DNA, nuclear DNA, morphological

Genetic and Morphological Analyses of Three Freshwater Mussel Species in Isolated River Drainages Across Appalachia

Katlyn M. Ortiz

Abstract

The Upper Tennessee River drainage of Virginia and Tennessee, Green River drainage of Kentucky, and Cumberland River drainage of Kentucky and Tennessee are known for their freshwater mussel species diversity. These river systems harbor dense populations of freshwater mussels that have significant impacts on surrounding ecosystems; however, due to their sedentary lifestyles, freshwater mussels are particularly susceptible to many biotic and abiotic stressors. Managers strive to preserve the fragile ecosystems that include freshwater mussels and, hence, study the life-history strategies of endangered and common freshwater mussel species. The goals of this project were to inform management decision-making based on whether *Leaunio ortmanni* is endemic to the Green River drainage and a species distinct from *Leaunio vanuxemensis* based on molecular identification, estimation of genetic diversity, and morphometric analysis, and to screen for cryptic biodiversity of populations of the *Cambarunio iris* species complex in the Upper Tennessee, Cumberland, and Green River drainages. I used the mitochondrial DNA (mtDNA) gene from the first subunit of the NADH dehydrogenase (*ND1*) as a genetic marker for species-level assessment of *L. ortmanni* and *L. vanuxemensis* from the Green and Cumberland River drainages. Additional mtDNA sequences of *L. ortmanni* and *L. vanuxemensis* were added to increase sample sizes and coverage of historical distribution. A Bayesian phylogenetic analysis of mtDNA sequences did not result in monophyletic lineages for either species based on the *ND1* marker. Haplotype networks of mtDNA sequences demonstrated that haplotype sharing is occurring between the two focal taxa, and also among additional taxa, all of which previously belonged to the genus *Villosa*. A total of eight nuclear DNA microsatellites were successfully genotyped for the two focal taxa. The nuclear DNA microsatellites showed a strong phylogeographic signal between *L. ortmanni* of the Green River drainage and *L. vanuxemensis* of the Cumberland River drainage. An assignment-test based analysis in program STRUCTURE and a phylogenetic tree constructed using Nei's *D* genetic distance indicated well-differentiated populations across the two drainages. Additionally, the nuclear DNA microsatellite analysis showed a recent loss of genetic diversity across all populations, including when populations were pooled together at the sub-basin level. Further delineation of the focal taxa was assessed using geometric morphometrics and decision tree and random forest analyses. Decision tree and random forest analyses identified periostracum color, nacre color, overall shape, and sex to be distinguishing factors for field identification of *L. ortmanni* and *L. vanuxemensis*. Geometric morphometrics comparing species, shape, and drainage showed clear differentiation in shell shape between *L. ortmanni* and *L. vanuxemensis*. This study was able to delineate these two taxa, showing that *L. ortmanni* and *L. vanuxemensis* are separate species, and that *L. ortmanni* warrants listing under the Endangered Species Act. Management actions should focus on broodstock collection and propagation strategies to increase genetic diversity within established populations. Additionally, propagation and augmentation should look to reintroduce populations of *L. ortmanni* into its historical geographic range in unoccupied sections of the mainstem Green River. In addition, I assessed genetic diversity and differentiation again using *ND1* and eight nuclear DNA microsatellite loci, and morphological differences among different shell forms of *C. iris* in the Upper Tennessee,

Cumberland, and Green river basins and of the sister species *C. taeniatus* in the Cumberland, and Green river basins. Additional mitochondrial DNA sequences of *C. iris* and *C. taeniatus* were added to increase sample sizes and coverage of historical distribution. Mitochondrial DNA analysis demonstrated haplotype sharing between taxa, but with many unique haplotypes occurring in the upper Tennessee River basin. Nuclear DNA microsatellite loci revealed low levels of genetic diversity within populations of *C. iris* within the Upper Tennessee River basin, but high levels of divergence from *C. iris* and *C. taeniatus* of the Green and Cumberland River basins. The nuclear DNA analysis showed high admixture within and among sampled populations of *C. iris* throughout the Upper Tennessee River Basin with minimal geographic structuring among sub-basins. Further, phenotypic diversity was assessed using geometric morphometrics and decision tree and random forest analysis. Decision-tree and random forest analysis identified maximum height from the umbo to the ventral margin, periostracum color, shell width, and ray coverage to be defining characteristics for field identification of the focal taxa. Geometric morphometrics showed high overlap of shell shape for the focal taxa regardless of locality. While cryptic biodiversity was not detected in the Upper Tennessee River Basin, on a larger geographic level, cryptic biodiversity was detected using the combination of the mtDNA, nuclear DNA, and morphological data, which showed that *C. taeniatus* and *C. iris* from the Green River drainage were distinct from populations of *C. iris* in the upper Tennessee River basin.

Genetic and Morphological Analyses of Three Freshwater Mussel Species in Isolated River Drainages Across Appalachia

Katlyn M. Ortiz

General Audience Abstract

Worldwide, freshwater mussel species diversity is greatest in North America; however, both abundance and diversity have declined in Canada, the United States, Mexico and the countries of Central America. Among rivers of North America, the Ohio River and its large tributaries, which include the Green, Cumberland, and Tennessee River drainages, have been noted for their high levels of biodiversity of freshwater mussels. Freshwater mussels contribute many services to freshwater ecosystems, including nutrient recycling and storage, structural habitat, substrate and food web modification. Dense populations of freshwater mussels have significant impacts on the surrounding ecosystem; however, due to their sedentary lifestyles, freshwater mussels are particularly susceptible to many biotic and abiotic stressors. Examples of stressors include agricultural runoff, temperature fluctuations, and dams which can alter stream conditions into more lake-like conditions and therefore affect the distributions of host fish populations. These stressors put mussels at risk for extirpation, which in turn, reduces the ecological biodiversity of these river drainages. Like other freshwater mussel species, the rainbow mussel *(Cambarunio iris)* of the Upper Tennessee River drainage, Mountain Creekshell *(Leaunio vanuxemensis)* of the Cumberland and Tennessee River drainages, and Kentucky Creekshell *(Leaunio ortmanni)* of the Green River drainage are in danger of decline due to anthropogenic changes in biotic and abiotic factors. Habitat degradation and loss have been of particular concern to managers. Life-history strategies for these three species are still widely unknown, and due to the overlap in their distributions, both phylogenetic and morphological analyses are needed to distinguish between species and populations to determine the best approach for management and conservation. The lack of understanding of taxonomic relationships in combination with morphologically similar characters poses a threat to conservation of these three species. The phylogenetic species concept is defined as an irreducible group whose members are descended from a common ancestor and who all possess a combination of certain defining, or derived traits, whereas the biological species concept is defined as groups or populations that are reproductively isolated from each other, meaning individuals from different groups cannot breed with one another. The results of my study have led to a better understanding of the phylogenetic relationships and species status of individuals collected from different localities of *L. ortmanni* and *L. vanuxemensis* and *C. iris* collected from the Green and Cumberland River drainages and the Upper Tennessee River drainage. In addition, morphological analyses were conducted to identify which traits are best for external identification of these three look-alike species, so they can be more reliably identified in the field.

ACKNOWLEDGEMENTS

The completion of my project would not have been possible if not for the immense support I received from so many people. First, I would like to express my sincerest gratitude to my advisors, Dr. Jess Jones (Committee Chair) and Dr. Eric Hallerman (Committee Member), whose guidance, encouragement, and knowledge were invaluable as they introduced me to the world of freshwater mussels and conservation genetics. I thank my committee member, Dr. Katy Klymus for her insight, knowledge, and support for my project. I extend a special thanks to Michael Compton with the Kentucky Nature Preserves Commission for his exhaustive field sampling, support, and many hours helping me take photographs and record data.

This project was funded by the Kentucky Department of Wildlife Resources, Frankfort, KY through a grant from the U.S. Fish and Wildlife Service, Frankfort, KY. I would like to thank field crews at Kentucky Nature Preserves Commission, Frankfort, KY, who conducted field sampling in the Green and Cumberland River drainages. I would like to thank all those that helped with field sampling in the Upper Tennessee River Basin, including Alissa Ganser and Rebecca Belcher (Virginia Tech Freshwater Mollusk Conservation Center), Tim Lane, Tiffany Leach and Sarah Colletti (Aquatic Wildlife Conservation Center) , Andrew Phipps (White Sulphur Springs National Fish Hatchery), Isabella Boyce (Minnesota Department of Natural Resources), and Kayla Howard (Virginia Department of Natural Resources). I extend a special thanks to Caitlin Carey (Conservation Management Institute at Virginia Tech) for help in the Conservation Genetics Laboratory. I also would like to thank Alexis Schoenlaub with Office of Kentucky Nature Preserves Commission, Frankfort, KY for preparing the maps used for my project.

Lastly, I would like to thank my parents, Charles and Donna Hayden, for their unwavering support, encouragement, and belief in me. I dedicate my thesis to my beloved husband, Andrew Binner, and my cherished son, Charles Andrew Lucas Binner. Without you both, I would not be where I am today.

Table of Contents

List of Tables

List of figures

CHAPTER 1

PHYLOGENETIC, POPULATION GENETIC, AND MORPHOLOGICAL EVALUATION OF KENTUCKY CREEKSHELL *LEAUNIO ORTMANNI* IN THE GREEN RIVER DRAINAGE OF KENTUCKY AND TENNESSEE, U.S.A. SUPPORTS CONTINUED RECOGNITION AS A DISTINCT SPECIES

ABSTRACT

The Kentucky Creekshell (*Leaunio ortmanni*) is endemic to the Green River drainage of Kentucky, U.S.A. and is under review for listing under the Endangered Species Act. A recent mitochondrial DNA (mtDNA)-based study suggested that Mountain Creekshell (*Leaunio vanuxemensis*) of the Cumberland and Tennessee river basins is synonymous with *L. ortmanni*. We tested the validity of these two species utilizing mtDNA, nuclear DNA microsatellites, and morphological characters, and included individuals of *Cambarunio iris* from the upper Tennessee River basin (UTRB) as an outgroup. At the first subunit of the NADH dehydrogenase (*ND1*) mtDNA gene, we sequenced 150 individuals and used 15 sequences from Genbank (*L. ortmanni N*=16, *L. vanuxemensis N*=89, *C. iris N*=59). At 8 nuclear DNA microsatellite loci, we successfully genotyped 254 individuals (*L. ortmanni N*=140*, L. vanuxemensis N*=114). We observed two diverged mtDNA lineages that were not concordant with the geography or species boundaries of the nominal taxa (i.e., both lineages occurred in each basin) and haplotype sharing occurred among all three taxa. Hence, the *ND1* gene did not delineate *L. ortmanni* and *L. vanuxemensis* as phylogenetically distinct from each other, and many of the *C. iris* haplotypes from the UTRB were intermingled in one of the clades containing these taxa. Phylogenetic analysis utilizing nuclear DNA microsatellites clearly divided *L. ortmanni* from *L. vanuxemensis* into two well diverged and distinct clades, as well as admixture analysis in program STRUCTURE also supporting two distinct populations across this drainage divide. Geometric morphometric and classification regression tree analyses of shell shape and external characters also corroborated the nuclear DNA genetic data that these species are different. Our analyses suggest that *L. ortmanni* and *L. vanuxemensis* are closely related but distinct species based on the former's many unique mtDNA haplotypes, divergent nuclear DNA, shell characters and its non-sympatric and endemic distribution in the Green River drainage.

INTRODUCTION

Worldwide, freshwater mussel species diversity is greatest in North America; however, both abundance and diversity have declined in the United States and Canada (Williams et al. 1993; Williams et al. 2017). Of the rivers of North America, the Ohio River and its large tributaries, which include the Green, Cumberland, and Tennessee river drainages, have been noted for their high levels of biodiversity of freshwater mussels (Master et al. 1998; Parmalee and Bogan 1998; Cicerello and Schuster 2003; Jones et al. 2015;). Freshwater mussels contribute many services to freshwater ecosystems, including nutrient recycling and storage, structural habitat, substrate, and food web modification (Vaughn 2018). Dense populations of freshwater mussels have significant impacts on the surrounding ecosystem; however, due to their sedentary lifestyles, freshwater mussels are particularly susceptible to many biotic and abiotic stressors, including runoff from agricultural and urban systems, and temperature and discharge fluctuations from hydroelectric dams, which can cause loss of host fish populations (Baxter 1977; Vaughn et al. 2008; Vaughn 2018). These stressors put freshwater mussels at risk for extirpation and extinction, which in turn, reduces the ecological biodiversity of these Ohio River drainage hotspots, created over millennia by host fish dispersal and colonization of refugial habitat during glacial cycles (Bernatchez and Wilson 2002).

Like other species of freshwater mussels distributed throughout these sub-basins, the rainbow mussel (*Cambarunio iris*) of the Upper Tennessee River drainage, Mountain Creekshell (*Leaunio vanuxemensis*) of the Cumberland and Tennessee River drainages, Dwarf rainbow (*Leaunio pataceus*) of the Cumberland River drainage and Kentucky Creekshell (*Leaunio ortmanni*) of the Green River drainage (Figure 1, Panel A) are in danger of decline due to anthropogenic biotic and abiotic stressors. Habitat degradation and loss have been of particular concern to managers (Williams et al. 1993; COSEWIC 2006). The life history of these four species is still mostly unknown, and due to some overlap in their distributions, both phylogenetic and morphological analyses are needed to distinguish these species and their respective populations to determine the best approaches for management and conservation. The lack of a thorough understanding of the taxonomic relationships in combination with morphologically similar characters poses a challenge to conservation of these three species (Shea et al. 2011; Freshwater Mollusk Conservation Society 2016).

Correct field identification of freshwater mussels is crucial for research, conservation and propagation purposes. For many mussel species, similarity of morphological traits causes taxonomic uncertainty, making field identifications difficult (Figure 2). To prioritize species for recovery, taxonomic relationships must be resolved. However, very little genetic data is available to understand the taxonomy of *L. ortmanni* of the Green River drainage and *L. vanuxemensis* of the Cumberland River drainage. Among them, *L. ortmanni* of the Green River drainage is being considered for listing under the Endangered Species Act by the U.S. Fish and Wildlife Service (ESA 1973, as amended).

There are several small populations of *Leaunio ortmanni* remaining only in the Green River drainage in Kentucky and Tennessee, and these populations need to be characterized genetically before restoration and recovery activities are initiated for the species. Thus, an assessment of genetic diversity within and between populations will help determine source populations for any recovery actions that might be practiced. By utilizing source populations with high genetic diversity, inbreeding and genetic bottlenecks can be avoided in populations with reduced diversity and gene flow.

Individuals of this species inhabit small to large streams in the Green River drainage, typically occurring in riffle or run habitats consisting of sand, gravel, and cobble in water depths of less than two meters (Cicerello and Hannan 1990; Cicerello and Schuster 2003). Possible host fishes for this species include benthic fishes such as Johnny darter *Etheostoma nigrum* (McGregor et al. 2011) and members of the sculpin genus *Cottus* (Haag and Cicerello 2016). Like *L. vanuxemensis* (Zale and Neves 1982), based on collection of gravid female mussels for propagation by Monty McGregor (Kentucky Department of Fish and Wildlife Resources) and Mike Compton (Kentucky Nature Preserves Commission), the males release sperm in late summer and fall to fertilize females, and once spawning is complete, gravid females' over-winter their larvae (glochidia) in their two outer gills for release to host fishes in the late winter and early spring of the following year.

Leaunio vanuxemensis occurs in streams of the Cumberland and Tennessee River drainages (Cicerello et al. 1991; Parmalee and Bogan 1998; Williams et al. 2008), where individuals most often inhabit riffles along *Justicia* beds on gravel or sand substrates. This species also prefers smaller streams with depths of less than one meter (Bogan 2002) and uses various species from the genus *Cottus* as fish hosts (Neves et al. 1985). This species also spawns in the late summer to

early fall and overwinters its glochidia. Where *L. ortmanni* was thought to only occur in the Green River drainage, Watters (2018) identified a specimen from the Red River in the Cumberland River drainage as *Leaunio ortmanni* based on subsequent mitochondrial genetic data from Kuehnl (2009), which clustered phylogenetically with individuals of *L. ortmanni* from the Green River system. Therefore, due to similar life-history strategies and morphological characters and the pending determination on the conservation status of *L. ortmanni*, a deeper look into the genetic relatedness of these two species was needed.

Because of the morphological similarity between *L. ortmanni* and *L. vanuxemensis*, their closely related mtDNA haplotypes, and similar life-history traits, genetic and taxonomic uncertainty needed to be resolved to guide conservation actions for the species. For example, both *L. ortmanni* and *L. vanuxemensis* inhabit similar habitat types, have similar life histories (i.e. timing of spawning and host fish use), and have similar external morphological characteristics (Zale and Neves 1982; Neves et al. 1985; Cicerello and Hannan 1990; Cicerello et al. 1991; Parmalee and Bogan 1998; Bogan 2002; Cicerello and Schuster 2003; Williams et al. 2008; McGregor et al. 2011; Haag and Cicerello 2016). In addition, both species have elongated and subovate forms, and white, purple, or salmon nacre (Figures 2 and 3). Shell color and ray pattern and spacing is also highly variable in individuals of these species (Figure 4). However, differences in mantle lure display have been documented between individuals occurring in the Green and Cumberland River drainages, and in individuals of *L. vanuxemensis* from the Upper Tennessee River Basin populations. The mantle lure for *L. ortmanni* is orange in color with sparse black markings (Figure 5, Panels A and B), whereas the mantle lure for *L. vanuxemensis* of the Cumberland River drainage appears whiter with moderate to dense black markings (Figure 5, Panels C and D) and *L. vanuxemensis* of the Upper Tennessee River Basin appears orange to black pigmented (Figure 5, Panels E and F). Genetic structure and differentiation have been proven to be a factor dependent on migratory/residency behavior of host fish species (Österling et. al 2020). Thus, the purpose of this study was to determine the taxonomic validity of these two morphologically similar mussel species. We used a combination of maternally inherited, non-recombining mitochondrial DNA, along with biparentally inherited recombining nuclear DNA markers, geometric morphometrics and other morphological analyses to test the taxonomic validity of these two species.

METHODS

Collection and preservation

Individuals of *Leaunio ortmanni*, *L. vanuxemensis*, and *Cambarunio iris* were collected from the Green, Cumberland, and Upper Tennessee River Basin from 2018 to 2020. A total of 11 locations were sampled for *L. ortmanni* in the Green River drainage, 6 localities for *L. vanuxemensis* in the Cumberland River drainage, 4 localities in the Cumberland River drainage for *L. pataceus*, and 5 localities in the upper Tennessee River Basin, and at 14 localities for *C. iris* in the Upper Tennessee River Basin (Table 1; Figure 1B). Genetic samples were taken via mantle tissue clip or using buccal swabs (DDK-50, Isohelix, Harrietsham, Kent, UK). Mantle tissue clips were preserved in 100% ethanol and stored at -20˚ C prior to DNA extraction. Individuals were then preserved in specimen jars containing 100% ethanol and stored at -20˚ C for future morphological analysis. DNA was isolated from buccal swabs using the protocol included in the Isohelix DDK-50 kit. The DNA from mantle tissue samples was isolated and extracted using a DNeasy Blood and Tissue Kit (Qiagen, Germantown, MD). The concentration and purity of each sample were assessed using a µLite PC spectrophotometer (Biodrop, Cambridge, UK).

Mitochondrial DNA

Mitochondrial DNA sequences were amplified using primers for the first subunit of NADH dehydrogenase (*ND1*). Primer sequences for *ND1* were: forward: 5'-TGGCAGAAAAGTGCATCAGATTAAAGC-3'; and reverse: 5'-CCTGCTTGGAAGGCAAGTGTACT-3' (Serb et al. 2003). Polymerase chain reaction conditions consisted of H_2O, 5x PCR buffer (Promega, Madison, WI), 2.5 mM $MgCl_2$ (Promega), 2.5 mM dNTPs (ThermoFisher Scientific, Waltham, MA), 1 mg/ml BSA (ThermoFisher Scientific), 5 uM of each primer, 0.1 µl Go Taq polymerase (New England Biolabs, Ipswich, MA), and 1 µl of genomic DNA at 50 ng/µl for a total reaction volume of 22 µl. Polymerase cycling conditions were modified from Eackles and King (2002) and were as follows: 94℃ for 3 minutes; followed by 35 cycles of 94℃ for 40 sec, 59℃ for 40 sec, and 72℃ for 1 min; followed by a final extension at 72℃ for 5 min; and a hold at 4℃. Polymerase chain reaction products were prepared, and sequences were processed by the Virginia Biocomplexity Institute (Blacksburg, VA). Sequences were aligned and edited using Geneious Prime 2022 (Biomatters, Inc., San Diego, CA).

Intraspecific mtDNA genetic diversity indices, including haplotype diversity (*h*), number of polymorphic segregating sites (*s*), mean number of nucleotide differences among sequences (*k*), and nucleotide diversity (π) were assessed using DNAsp 6.12.03X64 (Rozas et al. 2017). All populations from the Green and Cumberland River drainages and the Upper Tennessee River basin were pooled together to assess mitochondrial DNA diversity. MrBayes (version 3.2.6; Ronquist et Al. 2012) was used to construct a tree to assess phylogenetic relatedness using Bayesian inference in the program MrBayes (Huelsenbeck and Ronquist 2001; Ronquist et. al 2012). An individual of *Lampsilis fasciola* and an individual of *Lampsilis ovata* were used as outgroup taxa. FigTree v1.4.4 was used to visualize the phylogenetic tree (Rambaut 2006-2018). A general time- reversible model (Nei and Kumar 2000) with gamma-distributed rate variation included 3,000,000 generations with 4 chains, and a 20,000 burnin. Every 100th-generation tree was saved. Popart (Leigh and Bryant 2015) was used to visualize a haplotype network for the analyzed sequences.

N*uclear DNA microsatellites*

Microsatellite loci and primers were selected from previously developed microsatellite markers (Eackles and King, 2002; Jones et al. 2004; Ortiz et al. 2022) (Table 2), were screened for polymorphism, repeat motif, and ability for use in subsequent multiplexing. Polymerase chain reaction conditions consisted of H_2O, 5x PCR buffer (Promega, Madison, WI), 2.5 mM $MgCl_2$ (Promega), 2.5 mM dNTPs (ThermoFisher Scientific, Waltham, MA), 1 mg/ml BSA (ThermoFisher Scientific), 5 uM of each primer, 0.1 µl Go Taq Polymerase (New England Biolabs, Ipswich, MA), and 1 µl of genomic DNA at 50 ng/µl for a total reaction volume of 22 µl. Polymerase cycling conditions were modified and are as follows: 94℃ for 3 minutes; followed by 30 or 35 cycles of 94℃ for 40 sec, 59℃ for 40 sec, and 72℃ for 1 min; followed by a final extension at 72℃ for 5 minutes; and a hold at 4℃ (Eackles and King 2002). Polymerase chain reaction products were prepared and sent to the Institute of Biotechnology at Cornell University, Ithaca, New York for DNA fragment-size analysis. The resulting fragments were viewed, scored for length, and examined for size polymorphism with Genemarker software (SoftGenetics, State College, PA).

Arlequin v3.0 (Excoffier et al. 2005) was used to calculate expected heterozygosity, observed heterozygosity, number of observed alleles per locus, total number of alleles, number of private alleles, conformance to Hardy-Weinberg equilibrium, linkage disequilibrium (LD), the

Garza-Williams index (*M*-ratio), which indicates evidence of a bottleneck in each population at each locus (Garza and Williamson 2001), and population differentiation metric F_{ST}, which ranges in value from 0 (no differentiation) to 1 (complete differentiation) (Wright 1978; Balloux and Lugon-Moulin 2002) (Table 6). In addition, because F_{ST} will approach zero when gene diversity is high, *D*, — an estimator of actual differentiation developed by Jost (2008) — was estimated using GenAlEx v.6.5 (Peakall and Smouse 2006). The presence of null alleles, allelic dropout, and allelic stuttering was assessed using Microchecker (Van Oosterhout et al. 2004). A phylogenetic tree was constructed using a neighbor-joining (NJ) (Saitou and Nei 1987) method and Nei's standard genetic distance (D_{ST}) (Nei 1972) in program POPTREE2 (Takezaki et al. 2010). STRUCTURE version 2.3.4 (Pritchard and Wen 2003), an assignment test-based algorithm, was used to assess population structure based on common ancestry. Prior population information was not used in the analysis. The number of populations (*K*) was determined by calculating the mean natural logarithm of the probability of *K* [mean Ln*P*(*K*)] with iterations of *K*=2 to *K*=14, which included ten independent runs for each *K*. All runs included 1,000,000 iterations with 100,000 burn-in steps. Lastly, STRUCTURE PLOT was used to create a visualization of the population structure using the highest likelihood estimates (Ramasamy et al. 2014).

Geometric Morphometrics

Photographs of the left valve were used for geometric morphometric analysis. Individuals of *L. ortmanni* (*N*=59) were collected from the Green River drainage (KY); individuals of *Leaunio vanuxemensis* (*N*=125) from the Cumberland River drainage and Upper Tennessee River Basin (KY and TN); and individuals of *Leaunio pataceus* (*N*=12) were collected from the Cumberland River drainage (KY) (Table 1). Mussel shells were fixed within an adhesive square with modeling clay, and photographs were taken using a PULUZ (Shenzhen, PRC) Photo Light Box®. Size-classes were categorized as small (<40 mm), medium (40.1 mm <50 mm), or large (≥50.1 mm). Photographs were overlain with a grid, a 180-degree line on the anterior part of the umbo, and then a digital semicircle was divided into 15-degree increments. The anterior umbo aligned as landmark 1 with the 180-degree angle indicating landmark 5 (Figure 6). Landmarks were obtained using tpsDig2 v 2.25 (Rohlf 2001). MorphoJ version 1.06 (Klingenberg 2011) was used to perform Principal Components Analysis (PCA) and Canonical Variate Analysis (CVA) landmark analyses. The data was checked for outliers, and a covariance matrix was used to assess locations of

landmarks between species and size-classes. The CVA was used to determine differences in all three size-classes between and within species. Procrustes distance among groups and Goodall's *F* which is calculated by adding up sums of squares across all landmarks and then computing the appropriate ratio of the resulting sums in order to test for differences in mean shape between two species relative to variations in shape within all samples (Goodall 1991; Klingenberg 2016).

Decision Trees and Random Forest

Quantitative shell characteristics – including maximum length, hinge length, maximum perpendicular umbo height, maximum perpendicular hinge height, and width – were measured in millimeters with digital calipers (Figure 7). Categorical characters – including shape, periostracum color, ray width, ray spacing, ray pattern, ray coverage, foot color, and nacre color – were documented for each individual (Figures 3 and 4). Individuals of *L. ortmanni* (*N*=64) were collected from the Green River drainage (KY); individuals of *Leaunio vanuxemensis* (*N*=145) from the Cumberland River drainage (*N*=129*)* and Upper Tennessee River Basin (*N*=16) (KY and TN); and individuals of *Leaunio pataceus* (*N*=17) were collected from the Cumberland River drainage (KY) (Table 1). Boxplots with the mean values for each measured quantitative (Figure 8, Panels A and B) and categorical shell characters (Figure 9) for each species are shown. The R packages party 1.3-3 (Hothorn et al. 2019) and rpart 4.1-15 (Therneau et al. 2015) were used for decision tree analysis, with species used as the response variable in the decision tree analysis. Random forest analysis was implemented using randomforest (Liaw 2018) and caret (Kuhn 2012) in R to determine the most prevalent morphological characters for identification of *L. ortmanni*, *L. vanuxemensis*, *L. pataceus* and *C. iris*. For both the decision tree and random forest analyses, the data was partitioned into a training data set (80% with 67 observations) and a validation data set (20% with 28 observations). The confidence level for the decision tree analysis was set to 90% with a branch split of 1, and *K*-fold cross-validation with *K*=10 was used to validate the model. For random forest analysis, the number of trees was set at default *ntree*=500 and then *ntree*=2001 to determine out-of-bag (OOB) error rate and to visualize the decline in the error rate and when it stabilized. Final *ntree*=500 was used for analysis.

RESULTS

Mitochondrial DNA

Using the *ND1* mitochondrial DNA gene, we successfully sequenced 150 individuals, and downloaded 15 sequences from Genbank (*L. ortmanni N*=16, *L. vanuxemensis N*=89, *C. iris N*=59, *C. taeniatus N=1, Lampsilis fasciola N=1,* and *Lampsilis ovata N=1*). The mitochondrial DNA sequences showed a large amount of diversity, with 127 polymorphic segregating sites, and an overall haplotype diversity (*Hd*) of 0.93 and a nucleotide diversity (π) of 0.06. A total of 40 haplotypes were observed between *L. ortmanni, L. vanuxemensis,* and *C. iris*, with 36 haplotypes unique to the recognized taxa; 8 to *L. ortmanni*, 7 to *L. vanuxemensis* (Cumberland River drainage), 2 to *L. vanuxemensis* (Upper Tennessee River Basin), and 19 to *C. iris* in the Upper Tennessee River Basin (Table 4). The remaining 4 haplotypes were shared between taxa, including 1 shared between *C. taeniatus*, *L. vanuxemensis*, *C. iris*, 2 shared between *L. ortmanni* and *L. vanuxemensis* (Cumberland River drainage), and 1 shared between *L. vanuxemensis* and *C. iris* of the Upper Tennessee River basin (Table 5). The number of individuals per haplotype, per population varied greatly depending upon the sample size of the particular population. The haplotype network clearly demonstrates sharing of haplotypes between species across the focal geographical range but also the numerous mutational steps (high divergence) between haplotypes belonging to different clades (Figure 10).

The phylogenetic tree included *N*=164 individuals of all three species collected from their respective drainages in the Green River, Cumberland River, and the Upper Tennessee River basins, with individuals from all localities split into two distinct clades (Figure 11). Individuals of *L. pataceus* were collected after the conclusion of mitochondrial DNA sequencing, and therefore were not included in analysis. Clade 1 included individuals of *C. iris* and *L. vanuxemensis* collected from the Upper Tennessee River Basin, *L. vanuxemensis* from the Cumberland River drainage, and lastly *L. ortmanni* from the Green River drainage. Whereas Clade 2 showed clustering of haplotypes of just *L. ortmanni* and *L. vanuxemensis* with no haplotypes of *C. iris* intermingled in the clade, and additionally, it included four smaller clades, of which individuals of *L. ortmanni* were nested in a sub-clade that included one haplotype from *L. vanuxemensis*. All of the *L. vanuxemensis* sequences obtained from Genbank sequences of *L. ortmanni* and *L. vanuxemensis* from Kentucky and Tennessee formed their own sub-clades and hence fell outside of the sub-clades

of our recently collected individuals, indicating that our samples added significant haplotype diversity for this species than previously understood (Figure 11).

Nuclear DNA microsatellites

A total of 254 individuals (*L. ortmanni N*=140*, L. vanuxemensis N*=114) were successfully genotyped using a suite of 10 nuclear DNA microsatellites (Table 2). Null alleles were observed in at least one locus for each population. Markers *Ecap_4* and *Ecap_7* were omitted from analysis due to excess of null alleles in most populations reducing our loci dataset to eight DNA microsatellites. Based on eight loci, allelic diversity ranged from A=2.43 to A=13.0 for *L. ortmanni* and A=5.75 to A=15.13 for *L. vanuxemensis*. At each locus, all populations demonstrated lower mean observed heterozygosity in comparison to mean expected heterozygosity, suggesting a recent loss of genetic diversity. For *L. ortmanni,* mean observed heterozygosity ranged from H_o=0.29 to H_o=0.65 and mean expected heterozygosity ranged from H_e=0.52 to H_e=0.89. For *L. vanuxemensis,* mean observed heterozygosity ranged from H_o=0.40 to H_o=0.77 and mean expected heterozygosity ranged from H_e=0.82 to H_e=0.89. For *L. ortmanni,* the mean number of observed alleles per locus, allelic diversity ranged from A=2.73 at Green River to A=13.0 at Walters Creek. For *L. vanuxemensis*, the allelic diversity ranged from A=5.75 at Pleasant Run to A=15.13 at Spring Creek. Private alleles were observed in 7 populations of *L. ortmanni* and 5 populations of *L. vanuxemensis*. For populations of *L. ortmanni* and *L. vanuxemensis*, many of which consisted of small sample sizes, 8 of 16 populations had *M*-ratios at 0.70 or below, congruent with the other diversity indices indicating low genetic diversity in all populations in the Green and Cumberland River drainages (Table 4).

The phylogenetic analysis utilizing the DNA microsatellite loci clearly divided the *L. ortmanni* of the Green River drainage and the *L. vanuxemensis* of the Cumberland River drainage into distinct clades with significant bootstrap values (Figure 12). The addition of *L. pataceus* from the Cumberland River drainage and *L. vanuxemensis* from the Upper Tennessee River Basin supports this drainage divide. STRUCTURE, supporting two populations across the drainage divide with the best value at K=2 (Figure 13).

Among populations of *L. ortmanni,* allele frequency divergence values ranged from F_{ST}=0.026 to F_{ST}=0.259 and D of effectively 0 to D=0.735, with the majority of D values <0.5. Among populations of *L. vanuxemensis* allele frequency divergence values ranged from F_{ST}=

0.023 to F_{ST}=0.089 and D=0.018 to D=0.424. Between populations of *L. ortmanni* and *L. vanuxemensis,* F_{ST}=0.177 to F_{ST}=0.570 and D=0.25 to D=0.719. Overall, F_{ST} and D divergence values ranged from moderate to high between populations of *L. ortmanni* in the Green River drainage, *L. pataceus*, and *L. vanuxemensis* in the Cumberland River drainage, and *L. vanuxemensis* and *C. iris* of the Upper Tennessee River Basin (Table 7). When populations were combined by subbasin in order to increase sample sizes, allele divergency values decreased and generally ranged from F_{ST}=0.019 to F_{ST}=0.208 and D=0.064 to 0.497 within the Green River drainage, F_{ST}=0.069 and D=0.398 within the Cumberland River drainage, then F_{ST}=0.061 to F_{ST}=0.170 and D=0.406 to 0.659 between the Green and Cumberland River drainages (Table 8).

Geometric Morphometrics

The first CVA comparing species and drainage without size classification demonstrated high morphological overlap with most individuals falling within the 0.90 confidence ellipses (Figure 14, Panel A). The exceptions were five individuals of *L. ortmanni* from the Green River drainage, five individuals of *L. pataceus* from the Cumberland River drainage, and four individuals of *L. vanuxemensis* from the Cumberland River drainage. The CVA with predetermined small size class (<40 mm) showed little to no morphological overlap, with three *L. ortmanni* from the Green River drainage and two *L. pataceus* form the Cumberland River drainage falling outside of the 0.90 confidence ellipses (Figure 14, Panel B). There was some morphological overlap in the medium size class (40.1 mm — 50 mm), which had the largest sample size of N=93, with three *L. pataceus* from the Cumberland River Drainage and 5 *L. ortmanni* from the Green River drainage falling outside of the 0.90 confidence ellipses (Figure 14, Panel C). Lastly, there was no morphological overlap in the large size class ($\geq$ 50.1mm) between taxa, with three *L. pataceus* and three *L. vanuxemensis*, both from the Cumberland River drainage, falling outside of the 0.90 confidence ellipses (Figure 14, Panel D). We combined individuals of *L. ortmanni*, *L. vanuxemensis*, *L. pataceus* from the Green and Cumberland River drainages with 16 individuals of *L. vanuxemensis* from the Upper Tennessee River drainage in the medium size class which yielded some morphological overlap between drainages with two *L. vanuxemensis* from the Cumberland River drainage, four from the Powell River subbasin, two from the Holston subbasin and four *L. ortmanni* from the Green River drainage falling outside of the 0.90 confidence ellipses

(Figure 14. Panel E). Procrustes distances among group *p*-values ranged from effectively 0 to 0.60, and Goodall's F *p*-values ranged from effectively 0 to 0.30 (Table 2).

Decision Trees and Random Forest

In the decision tree analysis, the misclassification error rate for the training data set and validation data set was 14% and 9%, respectively when *ntree*=500. After adjusting the *ntree* value to *ntree*=2100, the out-of-box error rate of decreased to 10.67% and did not decrease thereafter. Thus, the *ntree*=2100 was taken as adequate for this data set. The training data set had an accuracy of 1 (0.98, 1), whereas the validation data set had an accuracy of 0.88 (0.76, 0.95). When including posterior and anterior nacre color, anterior nacre color was determined to be a crucial character with the largest mean decrease accuracy and largest mean decrease gini (Figure 15, Panel A). However, when those characters were omitted the periostracum color was the main character with the largest mean decrease accuracy and largest mean decrease gini (Figure15, Panel B) The decision tree including characters posterior nacre color and anterior nacre color identified the anterior nacre color, periostracum color, and ray spacing as defining characters for species identification (Figure 16, Panel A). However, when anterior and posterior nacre color were omitted, still including main shell or umbo nacre color, the decision tree included periostracum color, nacre color, overall shape, and sex as defining characters for species identification (Figure 16, Panel B).

DISCUSSION

The main findings of our phylogenetic, population genetic and morphological analyses of *Leaunio ortmanni* and *L. vanuxemensis* were the following: (1) mitochondrial DNA (mtDNA) failed to delineate between the study taxa, and findings based solely on mtDNA can be misleading when closely related taxa are not strongly diverged at this molecular marker, (2) nuclear DNA microsatellites delineated these two taxa and demonstrated strong phylogeographic distinctiveness between *L. ortmanni* of the Green River drainage and *L. vanuxemensis* of the Cumberland River drainage, (3) diversity indices indicated low genetic diversity in those populations with small sample sizes in the Green and Cumberland River drainages; however, when populations were pooled by subbasin genetic diversity indices increased, and (4) morphological data supports the

nuclear DNA genetic dataset by showing different groupings of *L. ortmanni* and *L. vanuxemensis* individuals based on species, size class, and drainage.

Mitochondrial DNA

Using concatenated sequences of mitochondrial *COI* and *ND1*, Kuehnl (2009) showed that individuals of *L. ortmanni* (*N*=7) and *L. vanuxemensis* were phylogenetically distinct but closely related, suggesting that *L. ortmanni* is a valid species. While our findings using just *ND1* were similar our sample sizes for both species were much larger than Kuehnl's. Thus, we observed a much higher number of *ND1* haplotypes for both species, especially for *L. vanuxemensis*, with much greater corresponding clade complexity in our phylogenetic tree. For example, Clade 2 was further divided into smaller sub-clades where most *L. ortmanni* haplotypes clustered together into their own single sub-clade, but one that exhibited shallow divergence relative to the numerous *L. vanuxemensis* individuals forming their own respective sub-clades. One haplotype of *L. vanuxemensis* even clustered with the haplotypes of *L. ortmanni*, and one haplotype of *L. ortmanni* clustered into Clade 1 with numerous haplotypes of *L. vanuxemensis*, *C. iris* and *C. taeniata* (Figure 4), indicating that some haplotype sharing occurs between these species. More broadly in the phylogenetic tree, ~10% of the mtDNA haplotypes were shared between the two species of *Leaunio* (*ortmanii* and *vanuxemensis*) and the two species of *Cambarunio* (*iris* and *taeniatus*), and thus mitochondrial *ND1* did not definitively differentiate taxa in these two genera. Again, this haplotype sharing among these four species is evident in Clade 1 (Figure 4). Therefore, while we did observe mostly unique mtDNA sequences for *L. ortmanni*, the analyzed individuals were not recovered as monophyletic. Further, our finding of shared mtDNA haplotypes among these species does not support Watters (2018) preliminary assessment that these species should be classified separately in the genera *Cambarunio* and *Leaunio*.

Haplotype sharing between mussel taxa previously has been observed in morphologically well-differentiated species in North America. For example, Morrison et al. (2021) showed that *Pleurobema clava* shares haplotypes with morphologically distinct forms of *Pleurobema oviforme* in the upper Tennessee River basin, and Jones et al. (2006) showed that several species of *Epioblasma* in the Cumberland and Tennessee River basin were well differentiated based on shell and mantle-lure morphology, mantle-lure behavior, and fish-host usage, but shared some mtDNA haplotypes among taxa. Therefore, given the low observed mtDNA haplotype divergence among

our study species, one plausible scenario is that *L. ortmanni* and *L. vanuxemensis* evolved from a recent single common ancestor residing in the Cumberland River glacial refugia that eventually over time crossed into the headwaters of the Barren River or other tributaries to the Green River system either through a stream capture event or an underground karst passage, for which the headwaters of both drainage systems are well known (Simpson 2009; Meiman et al. 2001). Hybridization is another plausible explanation for the observed haplotype sharing among these taxa, a process which is known to occur in unionids (Porto-Hannes et al. 2021). For example, Cyr et al. (2007), found two previously undetected lineages in species of *Pyganodon*, which they suggested that the presence of one lineage at distinct sites was due to hybridization that occurred before postglacial colonization. Our study species co-occur in shallow and small 2nd- and 3rd-order streams, providing ideal conditions for sperm from one species to drift and fertilize the eggs of another species to allow for hybridization.

Other studies of mussels distributed in the Ohio, Cumberland and Tennessee river systems have reported similar results regarding shared mtDNA haplotypes among their focal species (Lane et. al 2016; Inoue et al. 2014; Jones et al. 2015). Thus, we caution against the use of mtDNA solely to assess phylogenetic and taxonomic relationships among mussel species, especially among closely related species. Incongruence between mtDNA and other molecular and morphological datasets is not unique to freshwater mussels. For example, mtDNA failed to discriminate morphologically distinct forms of northern and southern red snapper *Lutjanus campechanus* and *L. purpureus* in the Western Atlantic as independent evolutionary groups; however, RAD sequencing recognized these two forms as independent evolutionary lineages, resulting in recognition as distinct species (Pedraza-Marrón et. al 2019). While phylogenetically informative, mtDNA did not uphold our initial expectations of *L. ortmanni* and *L. vanuxemensis* being well-delineated monophyletic lineages. Rather, our mtDNA tree suggests closely related species with shallow and hence recent divergence, perhaps as recently as the late Pleistocene. Finally, most of the mtDNA haplotypes we observed for *L. ortmanni* were geographically unique to the species and only occur in the Green River system, further supporting the validity of the species.

Nuclear DNA Microsatellites

In contrast to the mtDNA, the nuclear DNA microsatellites showed a strong phylogeographic signal between *L. ortmanni* of the Green River Drainage and *L. vanuxemensis* of

the Cumberland River Drainage. For example, the STRUCTURE analysis exhibited clear geographic structure between the two species across this geographic divide, which is concordant with their historical distributions. Interestingly, results of our STRUCTURE analysis demonstrated some admixture in a few individuals from the upper Red River of the Cumberland River drainage, especially Sulphur Spring, suggesting shared ancestry with individuals from the Green River drainage. Geographically, the Red River System includes the Sulphur Spring population, which borders closely with the upper Gasper and Barren River systems in the Green River drainage. The Sulphur Spring drainage is ~17 aerial miles from West Fork Drakes Creek of the Green River Drainage. Further support comes from our phylogenetic tree constructed using Nei's *D*, which clearly shows two distinct clades with moderately high bootstrap support, further indicating differentiated populations across the two drainages. Thus, a possible hypothesis would be historical stream capture in the headwaters of these two basins resulting in a secondary contact event that caused interbreeding of individuals and ultimately a population of mixed ancestry, or a dispersal event from the Cumberland River basin into the Green River basin, establishing the ancestral population in this drainage. Hence, our nuclear DNA analyses leads us to believe that populations in the Green and Cumberland River drainages were connected in the past, and with time, due to paleo-environmental factors ultimately became isolated populations from each other, resulting in *L. ortmanni* becoming genetically distinct at nuclear DNA loci from *L. vanuxemensis.*

Overall, heterozygosity values indicated low genetic diversity for most populations of *L. ortmanni* and *L. vanuxemensis*. The mean *M*-ratio values were <0.70 for half of the populations, generally indicating recent bottlenecks and loss of genetic diversity. However, some population sample sizes were small and genetic diversity values generally are sample size dependent. For example, when larger samples sizes were obtained and analyzed in our study — Walter's (*N*=39) and Russell (*N*=31) creeks for *L. ortamnni* in the Green River drainage or Spring (*N*=50) and Sulphur Spring (*N*=25) creeks for *L. vanuxemensis* in the Cumberland River drainage — genetic diversity values were higher and likely provide a better estimate of overall genetic diversity of the respective population. In contrast, when smaller sample sizes were obtained in our study, a select and smaller amount of genetic diversity was captured to estimate genetic diversity, hence potentially introducing a downward bias in the estimates. This poses a challenge when studies are designed to determine the population genetic diversity of small and scarce populations, which of course was one of the main objectives of this study. Our field collections to obtain specimens of

both species were very intensive and represent hundreds of hours of field time, especially in the Green and Cumberland River drainages, and thus it is unlikely that for some populations with smaller sample sizes that the number of specimens collected from certain streams could have been greatly increased. Therefore, some of the genetic diversity indices, such as allelic diversity (*A*) and some of the pairwise allele frequency divergence values for F_{ST} and *D* among populations of *L. ortmanni* and *L. vanuxemensis* could be affected by low sample sizes. In order to mitigate for the smaller sample sizes of some populations, we combined populations by subbasins to obtain additional F_{ST} and *D* values utilizing larger sample sizes, which increased the respective genetic diversity values and decreased the F_{ST} and *D* values (Table 8) These additional analyses with larger sample sizes further demonstrated that *L. ortmanni* is genetically distinct from *L. vanuxemensis*.

Morphology

Accurate identification of freshwater mussel species is a foundational basis for which biologists make management and conservation decisions. Without a set of diagnostic or distinguishing characters for understanding morphological among variation species, the conservation community run the risk of over or under describing taxonomic relationships. For example, Lane et al. (2019) determined that nacre color was not a reliable characteristic for distinguishing *Venustaconcha trabalis* from *V. troostensis*. Whereas in the past, nacre color was considered a diagnostic trait for identifying these two species. Diagnostic traits become even more important when the study species is highly variable within and among populations. Another multidata set study showed that phenotypic plasticity in the Chinese freshwater mussel *Lamprotula caveata* was high and that robust genetic and morphological data were needed to accurately delineate individuals from other species (Liu et al. 2022). For many closely related species, one external shell character is not enough to reliably identify the species, thus for many species a set of several or more characters are needed for distinguishing taxa.

In our study, we used a suite of morphological characters and analyses to better understand which ones were best suited to discriminate the study species. The CVA for example demonstrated the morphological overlap in shell shape between *L. ortmanni* and *L. vanuxemensis* when all size classes were combined. However, when the CVA was conducted to comparesize classes between drainages, there was a clear difference between shell shape in the Green River drainage versus shell shape in the Cumberland River drainage, which was further corroborated by the Procrustes

distances among these groups. We then used the CART analysis to determine the best characteristics for identifying these species. During our initial assessment and identification of shell characters, differences in anterior and posterior nacre color for *L. vanuxemensis* in the Cumberland River drainage were seen as important traits for identifying this species. Many individuals had a strong color change in nacre from purple to white on the anterior margin. We further explored this trait in the analyses, considering that historically nacre color was used as a diagnostic trait. However, nacre color was highly variable among individuals and populations depending on geographical location. Therefore, we conducted a second Decision-tree and Random Forest analysis that was much more informative. The key morphological characteristics outlined by this analysis included: (1) Periostracum color (2) nacre color (3) over all shape and (4) sex. These traits can be difficult to discern in a field setting if the practitioner is not experienced in how to use these traits to identify these two species. Based on our analysis, over shape is that character that is the most descriptive for field application. However, this characteristic can be problematic when individuals are small (<40 mm) or medium (40.1 mm to 50 mm). The large size class ($\geq$50.1 mm) showed distinct groupings of *L. ortmanni*, *L. vanuxemensis*, and *L. pataceus*. Confusion matrices obtained from decision tree analysis showed high correct identification based on species for both the training and validation data sets. When viewed integrated with the genetic datasets, these morphological characters help support the continued recognition of *L. ortmanni* in the Green River drainage as a separate species from *L. vanuxemensis* of the Cumberland River drainage.

Summary and Management Implications

First, while our Bayesian mtDNA phylogenetic analysis clustered these species together within distinct clades and sub-clades, we did not observe monophyletic lineages for each species congruent with initial expectations. We did observe a large number of unique haplotypes among our study species, but generally mtDNA failed to delineate between these taxa, even for species as morphologically distinct as *L. vanuxemensis* and *C. iris*. It is important to emphasize here that these two species are easily recognizable morphologically, especially based on differences in their mantle lure displays and associated mantle lure behaviors. Further, these two species use completely different families of fish hosts, the former using benthic dwelling fishes in the families Cottidae and Percidae, while the latter uses hosts in the Centrarchidae, illustrating major life history differences between the two mussel species. Thus, we consider both *L. vanuxemensis* and

C. iris as good biological species that co-occur in sympatry throughout large parts of each species respective range but share some mtDNA haplotypes perhaps due to introgression and/or incomplete haplotype sorting. The addition of more mtDNA gene markers would perhaps help resolve some of the uncertainty, but due to low divergence among haplotypes within one of the clades it is unlikely to remove all uncertainty within the tree.

Second, nuclear DNA microsatellites demonstrated strong population divergence across the Green and Cumberland river drainage divide, and thus support continued recognition of the two taxa as separate species. Third, genetic diversity indices indicated low diversity within populations with small population sizes in the Green and Cumberland river drainages, but at the subbasin level within each drainage genetic diversity was higher. Based on our mtDNA and nuclear DNA data and analyses, our recommendation is that *L. ortmanni* remain recognized as a separate species from *L. vanuxemensis*. Future work should include the addition of mtDNA marker *CO1*, and nuclear DNA analysis of additional individuals of *L. ortmanni* from West Fork Drakes Creek, Simpson County, KY, *L. vanuxemensis* from Bushman Creek, Rutherford County, TN, select localities within the Upper Tennessee River Basin, and other populations and species of interest from the Cumberland and Green River drainages. Additional samples may help to further delineate these taxa and aid in our understanding of the genetic diversity of remaining populations throughout their respective distributions. Propagation and augmentation should focus on reintroduction of populations throughout *L. ortmanni's* geographic range. Hence, broodstock collection and propagation strategies to increase genetic diversity in newly established populations should be considered and developed. One strategy would be a "synthetic population" approach, where progeny from different populations within a subbasin are combined to introduce populations with higher genetic diversity at sites where *L. ortmanni* was historically present at the subbasin level. A second approach would be to introduce progeny only from the closest viable population to the historical population location. Both strategies could be used in combination to protect potential unique variation occurring in parental populations (i.e., the broodstock sources) but when establishing new populations, mix progeny from different broodstock sources to maximize genetic diversity.

LITERATURE CITED

Balloux, F., and N. Lugon-Moulin. 2002. The estimation of population differentiation with microsatellite markers. Molecular Ecology 11:155–165.

Baxter, R.M. 1977. Environmental effects of dams and impoundments. Annual Review of Ecology and Systematics 8:255–283.

Bernatchez, L., and C.C. Wilson. 1998. Comparative phylogeography of Nearctic and Palearctic fishes. Molecular Ecology 7:431–452.

Bogan, A.E. 2002. Workbook and key to the freshwater bivalves of North Carolina. North Carolina Museum of Natural Sciences: Raleigh, North Carolina. 101 pp.

Cicerella, R.R., and R.R. Hannan. 1990. Survey of the freshwater unionids (mussels) (Bivalvia: Margaritiferidae and Unionidae) in the Green River in Mammoth Cave National Park, Kentucky. Technical Report, Mammoth Cave National Park.

Cicerello, R.R., M.L. Warren Jr., and G.A. Schuster. 1991. A distributional checklist of the freshwater unionids (Bivalvia: Unionoidea) of Kentucky. American Malacological Bulletin 8:113–129.

Cicerello, R.R. and G.A. Schuster. 2003. A guide to the freshwater mussels of Kentucky. Kentucky State Nature Preserves Commission Scientific and Technical Series 7:1–62.

COSEWIC. 2006. COSEWIC assessment and status report on the rainbow mussel *Villosa iris* in Canada. Committee on the Status of Endangered Wildlife in Canada. Ottawa, Canada. 38pp.

Cyr, F., A. Paquet, A.L. Martel, B. Angers. 2007. Cryptic lineages and hybridization in freshwater mussels of the genus *Pyganodon* (Unionidae) in northeastern North America. Canadian Journal of Zoology 85:1216–1227.

Eackles, S.M., and T.L. King. 2002. Isolation and characterization of microsatellite loci in *Lampsilis abrupta* (Bivalvia: Unionidae) and cross-species amplification within the genus. Molecular Ecology Notes 2:559–562.

[ESA] US Endangered Species Act of 1973, as amended, Pub. L. No. 93-205, 87 Stat. 884 (Dec. 28, 1973).

Excoffier, L., G. Laval, S. Schneider. 2005. Arlequin ver. 3.0: An integrated software package for population genetics data analysis. Evolutionary Bioinformatics Online 1:47–50.

Falush, D., M. Stephens, J.K. Pritchard. 2003. Inference of population structure using multilocus genotype data: linked loci and correlated allele frequencies. Genetics 164:1567–1587.

Freshwater Mollusk Conservation Society. 2016. A national strategy for the conservation of native freshwater mollusks. Freshwater Mollusk Biology and Conservation. 19:1–21.

Garza, J.C., and E.G. Williamson. 2001. Detection of reduction in population size using data from microsatellite loci. Molecular Ecology 10:305–318.

Goodall, C., 1991. Procrustes Methods in the Statistical Analysis of Shape. Journal of the Royal Society, Series B 53: 285–239.

Haag, W.R., and R.R. Cicerello. 2016. A distributional atlas of the freshwater mussels of Kentucky. Scientific and Technical Series 8. Kentucky State Nature Preserves Commission, Frankfort, KY. 299 pp.

Hothorn, T., A. Zeileis, and K. Hornik. 2019. Package 'party'. Available online: cran.r-project.org/web/packages/party/party.pdf.

Huelsenbeck, J.P., and F. Ronquist 2001. MrBayes: Bayesian inference of phylogenetic trees. Bioinformat 17:754–755.

Inoue, K., E.M. Monroe, C.L. Elderkin, and D.J. Berg. 2014. Phylogenetic and population genetic analyses reveal Pleistocene isolation followed by high gene flow in a wide ranging, but endangered, freshwater mussel. Heredity 112:282–290.

Jones, J.W., M. Culver, V. David, J. Struthers, N.A. Johnson, R.J. Neves, S.J. O'Brien, E.M. Hallerman. 2004. Development and characterization of microsatellite loci in the endangered oyster mussel *Epioblasma capsaeformis* (Bivalvia: Unionidae). Molecular Ecology 4:649–652.

Jones, J.W., R.J. Neves, S.A. Ahlstedt, E.M. Hallerman. 2006. A holistic approach to taxonomic evaluation of two closely related endangered freshwater mussel species, the oyster mussel *Epioblasma capsaeformis* and tan riffle shell *Epioblasma florentina walkeri* (Bivalvia: Unionidae). Journal of Molluscan Studies 72:267–283.

Jones, J.W., R.J. Neves, E.M. Hallerman. 2015. Historical demography of freshwater mussels (Bivalvia: Unionidae): genetic evidence for population expansion and contraction during the late Pleistocene and Holocene. Biological Journal of the Linnean Society 114:376–397.

Jost, L. 2008. G_{ST} and its relatives do not measure differentiation. Molecular Ecology 17, 4015–4026.

Klingenberg, C.P., 2011. MorphoJ: an integrated software package for geometric morphometrics. Molecular Ecology Resources 11:353–357.

Klingenberg, C.P., 2016. Size, shape, and form: concepts of allometry in geometric morphometrics. Development Genes and Evolution 226:113–137.

Kuehnl, K. 2009. Exploring levels of genetic variation in the freshwater mussel genus *Villosa* (Bivalvia Unionidae) at different spatial and systematic scales: Implications for biogeography, taxonomy, and conservation. Ph.D. Dissertation, Ohio State University, Columbus, Ohio.

Kuhn, M. 2012. The caret package. Available online: cran.r-project.org/package=caret.

Lane, T.W., E.M. Hallerman, J.W. Jones. 2016. Phylogenetic and taxonomic assessment of the endangered Cumberland bean, Villosa trabalis and purple bean, *Villosa perpurpurea* (Bivalvia: Unionidae). Conservation Genetics 17: 1109–1124.

Leigh, J.W., and D. Bryant. 2015**.** PopART: Full-feature software for haplotype network construction. Methods Ecol Evol 6:1110–1116.

Liaw, A. 2018. Package 'randomForest'. Available online: cran.r-project.org/web/packages/randomForest/randomForest.pdf.

Master, L.L., S.R. Flack, and B.A. Stein. 1998. Rivers of life: critical watersheds for protecting freshwater biodiversity. Nature Conservancy, Arlington, Virginia. 71 pp.

McGregor, M., J. Culp, A. Shepard, F. Vorisek, B. Davis, and T. Bailey. 2011. Fish host determined for the Kentucky Creekshell, *Villosa ortmanni* and a new fish host found for the Cumberland Combshell, *Epioblasma brevidens*. Kentucky Department of Fish and Wildlife Resources 2010 Annual Research Highlights IV. P 58.

Meiman, J., C. Groves, and S. Herstein. 2001. In-cave dye tracing and drainage basin divides in the Mammoth Cave karst aquifer, Kentucky. U.S. Geological Survey Karst Interest Group Proceedings, Water-Resources Investigations Report. 179–185.

Morrison, C.L., N.A. Johnson, J.W. Jones, M.S. Eackles, A.W. Aunins, D.B. Fitzgerald, E. H. Hallerman, T.L. King. 2021. Genetic and morphological characterization of the freshwater mussel clubshell species complex (*Pleurobema clava* and *Pleurobema oviforme*) to inform conservation planning. Ecology and Evolution 11:15325–15350.

Nei, M. 1972. Genetic distance between populations. The American Naturalist. 106:949.

Nei, M., and S. Kumar. 2000. Molecular Evolution and Phylogenetics. Oxford University Press, New York.

Neves, R.J., L.R. Weaver, A.V. Zale. 1985. An evaluation of host fish suitability for glochidia of *Villosa vanuxemi* and *V. nebulosi* (Pelecypoda: Unionidae). The American Midland Naturalist 113:13–19.

Ortiz, K., J.W. Jones, and E.M. Hallerman. 2022. Development and characterization of microsatellite loci in the Purple Cat's Paw Pearlymussel *Epioblasma obliquata* (Bivalvia:Unionidae). Freshwater Mollusk Biology and Conservation 25:1–6.

Österling, M., M. Lopes-Lima, E. Froufe, A.H. Hadzihalilovic, B. Arvidsson. 2020. The genetic diversity and differentiation of mussels with complex life cycles and relations to host fish migratory traits and densities. Scientific Reports 10:17435.

Parmalee, P.W., and A.E. Bogan. 1998. The Freshwater Mussels of Tennessee. University of Tennessee Press: Knoxville, Tennessee. 328 pp.

Peakall, R., and P.E. Smouse. 2006. GENALEX 6: Genetic analysis in Excel. Population genetic software for teaching and research. Molecular Ecology Notes:6 288–295.

Pedraza-Marrón, C., R. Silva, J. Deeds, S.M. Van Belleghem, A. Mastretta-Yanes, O. Domínguez-Domínguez, R.A. Rivero-Vega, L. Lutackas, D. Murie, D. Parkyn, L.H. Bullock, K. Foss, H. Ortiz-Zuazaga, J. Narváez- Barandica, A. Acero, G. Gomes, and R. Betancur-R. 2019. Genomics overrules mitochondrial DNA, siding with morphology on a controversial case of species delimitation. Proceedings of the Royal Society B 286: 20182924.

Porto-Hannes, I., L.E. Burlakova, D.T. Zanatta, H.R. Lasker. 2021.Boundaries and hybridization in a secondary contact zone between freshwater mussel species (Family: Unionidae) Heredity 126: 955–973.

Pritchard, J.K., and W. Wen. 2003. Documentation for STRUCTURE Software: Version 2. Chicago: University of Chicago Press. Retrieved from: http://web.stanford.edu/group/pritchardlab/software/structure2_1.html.

Ramasamy, R.K., S. Ramasamy, B.B. Bindroo, V.G. Naik. 2014. STRUCTURE PLOT: a program for drawing elegant STRUCTURE bar plots in user friendly interface. SpringerPlus 3:431.

Rambaut, A. 2006–2018. FigTree v1.4.4. Institute of Evolutionary Biology. University of Edinburgh.

Rohlf, F.J. 2001. TPSDig2: a program for landmark development and analysis. http://life.bio.sunysb.edu/morph/index. Html.

Ronquist, F., M. Teslenko, P. van der Mark, D.L. Ayres, A. Darling, S. Hohna, B. Larget, L. Liu, M. A. Suchard, J. P. Huelsenbeck. 2012. MrBayes 3.2: Efficient Bayesian phylogenetic inference and model choice across a large model space. Systematic Biology 61:539–542.

Rozas, J., A. Ferrer-Mata, J.C. Sánchez-DelBarrio, S. Guirao-Rico, P. Librado, S.E. Ramos-Onsins, A. Sánchez-Gracia. 2017. DnaSP v6: DNA Sequence Polymorphism Analysis of Large Datasets. Molecular Biology and Evolution 34:3299–3302.

Saitou, N., and M. Nei. 1987. The neighbor-joining method: a new method for reconstructing phylogenetic trees. Molecular Biology and Evolution 4:406-425.

Serb, J.M., J.E. Buhay, C. Lydeard. 2003. Molecular systematics of the North American freshwater bivalve genus *Quadrula* (Unionidae: Ambleminae) based on mitochdonrial ND1 sequences. Molecular Phylogenetics and Evolution. 28:1–11.

Shea, C.P., J.T. Peterson, J.M. Wisniewski, N.A. Johnson. 2011. Misidentification of freshwater mussel species (Bivalvia: Unionidae): Contributing factors, management implications, and potential solutions. The North American Benthological Society 30:446–458.

Simpson, L.C. 2009. The Cumberland Plateau of Eastern Kentucky. Caves and Karst of America: 70–79.

Takezaki, N., M. Nei, and K. Tamura. 2010. POPTREE2: Software for constructing population trees from allele frequency data and computing other population statistics with Windows-interface. Molecular Biology and Evolution 27:747–752.

Therneau, T., B. Atkinson, B. Ripley, and Ripley, M.B. 2015. Package 'rpart'. Available online:cran.r-project.org/web/packages/rpart/rpart.pdf.

Van Oosterhout, C., B. Hutchinson, D. Wills, P. Shipley. 2004. Micro-checker: a software for identifying and correcting genotyping errors in microsatellite data. Molecular Ecology Notes 4:535–538.

Vaughn, C.C., S.J. Nichols, D. Spooner. 2008. Community and food web ecology of freshwater mussels. Journal of the North American Benthological Society 27:409–423.

Vaughn, C.C. 2018. Ecosystem services provided by freshwater mussels. Hydrobiologia 810:15–27.

Watters, G.T. 2018. A preliminary review of the nominal Genus *Villosa* of freshwater mussels (Bivalvia, Unionidae) in North America. Conchology, Inc. ConchBooks, Harxheim, Germany.

Williams, J.D., M.L. Warren Jr., K.S. Cummings, J.L. Harris, and R.J. Neves. 1993. Conservation status of freshwater mussels of the United States and Canada. Fisheries 18:622.

Williams, J.D., A.E. Bogan, J.T. and Garner. 2008. Freshwater Mussels of Alabama & the Mobile Basin in Georgia, Mississippi & Tennessee. University of Alabama Press, Tuscaloosa, Alabama. 908 pp.

Williams, J.D., A.E. Bogan, R.S. Butler, K.S. Cummings, J.T. Garner, J.L. Harris, N.A. Johnson, G.T. Watters. 2017. A revised list of the freshwater mussels (Mollusca: Bivalvia: Unionida) of the United States and Canada. Freshwater Mollusk Biology and Conservation 20:33–58.

Wright, S. 1978. Evolution and the Genetics of Populations, Vol. 4: Variability Within and Among Natural Populations. University of Chicago Press, Chicago, IL.

Zale, A.V., and R.J. Neves. 1982. Reproductive biology of four freshwater mussel species (Mollusca: Unionidae) in Virginia. Freshwater Invertebrate Biology. 1:17—28.

Table 1. Species, river drainage, sub-basin system, site location and year sampled and site coordinates for DNA samples obtained for study species *Leaunio ortmanni*, *Leaunio vanuxemensis*, *Cambarunio iris*, *Cambarunio taeniatus*, and *Leaunio pataecus* from 2018-2022 in the Green, Cumberland and upper Tennessee River basin.

Species	River Drainage	Sub-basin system	Site Location name	Year(s) sampled	Latitude	Longitude	Collectors
L. ortmanni	Green	Rough	Meeting Creek, Hardin County, KY	2018	37.57589	-86.21584	M. Compton and L. Phelps
			Rough River, Hardin County, KY	2018	37.64184	-86.19804	M. Compton and L. Phelps
			Rough River, Hardin County, KY	2021	37.67553	-86.17361	M. Compton and K. Howard
		Nolin	Nolin River, Larue County, KY	2021	37.58384	-85.91549	M. Compton and J. Day
			Walters Creek, Larue County, KY	2020	37.50968	-85.74759	M. Compton and V. Jones
		Barren	West Fork Drakes Creek, Simpson County, KY	2020	36.81139	-86.46045	M. Compton and V. Jones
			West Fork Drakes Creek, Simpson County, KY	2021	36.81355	-86.45813	M. Compton and K. Howard
			West Fork Drakes Creek, Simpson County, KY	2022	36.80881	-86.45611	M. Compton and B. Dorsett
			Salt Lick Creek, Macon County, TN	2021	36.55167	-85.85698	M. Compton, K. Howard, G. Dinkins, A. Rosenberger, and K. Irwin
			Lick Creek, Simpson County, KY	2021	36.79165	-86.49169	M. Compton and K. Howard
			Trammel Fork, Allen County, KY	2021	36.71473	-86.26036	M. Compton and K. Howard
			Trammel Fork, Allen County, KY	2021	36.71592	-86.26119	M. Compton and K. Howard
		Gasper	Clear Fork Creek, Logan County, KY	2021	36.90719	-86.65491	M. Compton and K. Howard
			Wiggington Creek, Logan County, KY	2019	36.91036	-86.75076	M. Compton and D. Smith
		Russell	Russell Creek, Adair County, KY	2020, 2021	37.08715	-85.28662	M. Compton, V. Jones and K. Howard
		Green	Green River, Hart County, KY	2022	37.28812	-85.82958	M. Compton, C. Lewis, J.C. Miller, C. Lawlis and S. McGlinchy
			Green River, Hart County, KY	2022	37.29074	-85.85275	M. Compton, C. Lewis, J.C. Miller, C. Lawlis, L. Sneed, and S. McGlinchy
L. vanuxemensis	Cumberland	Red	Montgomery Creek, Tood County, KY	2022	36.78551	-87.33784	M. Compton and R. Watson
			Pleasant Run, Logan County, KY	2019	36.7687	-86.78897	M. Compton and D. Smith
			Spring Creek, Simpson County, KY	2018, 2019, 2021, 2022	36.7619	-86.72015	M. Compton, L. Phelps, D. Smith and K. Howard
			Sulphur Spring Creek, Simpson County, KY	2019	36.6957	-86.72829	M. Compton and D. Smith
			Whippoorwill Creek, Logan County, KY	2020	36.78515	-86.99621	M. Compton
		Stones	Bushman Creek, Rutherford County, TN	2022	35.90559	-86.35014	M. Compton and G. Dinkins
			West Fork Stones River, Rutherford County, TN	2022	35.72173	-86.44735	M. Compton and J.C. Miller
	Tennessee	Clinch	Bennett Island, Russel County, VA	2019	36.9597	-82.097206	K. Ortiz and R. Belcher
			Richlands, Tazewell County, VA	2019	37.0940717	-81.8026221	K. Ortiz, D. Phipps, D. Neves, A. Ganser and B. Henley

		Holston	Beech Creek, Greene County, TN	2019	36.4097	-82.7638	K. Ortiz, A. Ganser, T. Lane and T. Leach
			North Fork Holston, Smyth County, VA	2020	36.9248886	-81.6260268	K. Ortiz and A. Binner
			North Fork Holston, Smyth County, VA	2022	36.9562594	-81.4928233	K. Ortiz, I. Boyce and K. Howard
			Locust Cove Creek, Smyth County, VA	2020	36.9459366	-81.5913793	K. Ortiz, A. Binner, I. Boyce and K. Howard
		Powell	Wallen Creek, Lee County, VA	2022	36.936871	-82.166001	K. Ortiz and K. Howard
C. taeniatus	Green	Barren	West Fork Drakes Creek, Simpson County, KY	2020	36.81139	-86.46045	M. Compton and V. Jones
			West Fork Drakes Creek, Simpson County, KY	2022	36.80881	-86.45611	M. Compton and K. Howard
	Cumberland	Rockcastle	Sinking Creek, Laurel County, KY	2022	37.09785	-84.22369	M. Compton and J.C. Miller
		Red	Sulphur Spring Creek, Simpson County, KY	2019	36.6957	-86.72829	M. Compton and D. Smith
			Sulphur Spring Creek, Simpson County, KY	2022	36.69581	-86.72647	M. Compton, J.C. Miller and L. Massar
		Stones	West Fork Stones River, Rutherford County, TN	2022	35.72173	-86.44735	M. Compton and J.C. Miller
			Middle Fork Stones River, Rutherford County, TN	2022	35.76713	-86.37588	M. Compton and J.C. Miller
L. pataecus	Cumberland	Little River	Riverside Creek, Christian County, KY	2022	36.86883	-87.58648	M. Compton
			Rock Bridge Branch, Christian County, KY	2021	36.79472	-87.47356	M. Compton and K. Howard
			Rock Bridge Branch, Christian County, KY	2022	36.79421	-87.47321	M. Compton and J.C. Miller
			Sinking Fork, Christian County, KY	2022	36.87762	-87.60765	M. Compton
C. iris	Green	Rough	Rough River, Hardin County, KY	2021	37.67553	-86.17361	M. Compton and K. Howard
		Russell	Russell Creek, Adair County, KY	2021	37.07182	-85.25097	M. Compton and K. Howard
	Cumberland	Rockcastle	Sinking Creek, Laurel County, KY	2022	37.09785	-84.22369	M. Compton and J.C. Miller
	Tennessee	Clinch	Bennett Island, Russell County, VA	2019, 2022	36.9597	-82.097206	K. Ortiz, R. Belcher and K. Howard
			Cavitts Creek, Tazewell County, VA	2018	37.1458558	-81.5449801	K. Ortiz, A. Ganser and J. Jones
			Copper Creek, Scott County, VA	2018	36.7286	-82.4684	K. Ortiz, A. Ganser, T. Lane, S. Colletti, T. Leach
			Indian Creek, Tazewell County, VA	2018	37.088	-81.7591	K. Ortiz and A. Ganser
			Kyles Ford, Hancock County, TN	2021	36.566368	-83.04182	J. Jones and Z. Taylor
			Richlands, Tazewell County, VA	2019	37.0940717	-81.8026221	K. Ortiz, D. Phipps, D. Neves, A. Ganser and B. Henley
		Holston	Beech Creek, Greene County, TN	2019	36.4097	-82.7638	K. Ortiz, A. Ganser, T. Lane and T. Leach
			Middle Fork Holston, Smyth County, VA	2020	36.807357	-81.67143	K. Ortiz and A. Binner
			North Fork Holston, Smyth County, VA	2020	36.8956034	-81.7462632	K. Ortiz and A. Binner

			North Fork Holston, Smyth County, VA	2020	36.9248886	-81.6260268	K. Ortiz and A. Binner
			North Fork Holston, Smyth County, VA	2020	36.9562594	-81.4928233	K. Ortiz and A. Binner
			Locust Cove Creek, Smyth County, VA	2020	36.9459366	-81.5913793	K. Ortiz and A. Binner
		Powell	Powell River, Lee County, VA	2020	36.621005	83.284522	K. Ortiz, T. Lane and T. Leach
			Wallen Creek, Lee County, VA	2022	36.936871	-82.166001	K. Ortiz and K. Howard
			South Fork Powell River, Wise County, VA	2022	36.865529	-82.7714967	K. Ortiz and K. Howard

Table 2. Nuclear DNA microsatellite loci, primer sequences, melting temperature (˚C), repeat motif, and base-pair size range, from Eackles & King (2002), Jones et al. (2004), and Ortiz et al. (2022) used to amplify loci for the study species.

Locus	Primer Sequence (5'-3')	Melting Temp. ˚C	Repeat Motif	Size Range (bp)	Source
EOO_8	F: TATCCCTCCGCTGCTGTAAG	59.7	$ACT_{(16)}$	125-173	Ortiz et al. 2022
	R:CCCTGGCCTGTAACAATCTTG	59.7			
EOO_10	F:CTGGTTGTTCGGTCTTGTGG	59.4	$ATC_{(8)}$	137-161	Ortiz et al. 2022
	R:ACTTTACATCCTGTCCAACTGC	59.8			
EOO_22	F:CAGTCCAAGTCATCTCTCAGG	58.4	$AGAT_{(15)}$	91-151	Ortiz et al. 2022
	R:GCATACGTGTAGCTTTATCGTG	58.2			
EOO_24	F:TCACAAGTCCTACACCCTCTC	59	$AATC_{(6)}$	169-193	Ortiz et al. 2022
	R:TCTTATCAGTTGGGTTTGGTGG	59.2			
EOO_46	F:CAGTCGGGCGTCATCACTGTAACGAG	58.9	$ATCC_{(6)}$	223-247	Ortiz et al. 2022
	R:GTTTGTTAGTTGGGCGGATGGTTG	59.9			
ECAP_8	F: TGCAGACATCGTAGCGATATG	59.9	$(CA)_{15}$	127-159	Jones et al. 2004
	R: ATTTCCAGTTGCAAGTCTCATT	57.9			
ECAP_7	F: ACGAAAAATGTTGTCATCCATT	58.4	$(CA)_{25}$	106-130	Jones et al. 2004
	R: GCCTAGACGACAAGCAAACC	59.9			
ECAP_5	F: TTTGAACACATTCGCCTCAG	59.8	$(GT)_{29}$	176-224	Jones et al. 2004
	R: GAATTTGCCTCATCAGCCAC	60.6			
ECAP_4	F: GTGCCCCAGTGCTAGACATT	60.1	$(CA)_{10}$	98-120	Jones et al. 2004
	R: AGAACAAAACACCCGTGTCC	59.9			
LAB_206	F: AAGTGTAGAGGCAGAGAACTGAC	58*	$(ATCT)_9$	191-231	Eackles & King 2002
	R: TCACTGATACAGCATACATAATATAC	58*			

Table 3. Total sample sizes (*N*) of individuals genotyped from 2018-2022 per mitochondrial DNA (mtDNA) sequences and number of DNA microsatellites (nDNA) loci for Kentucky Creekshell (*Leaunio ortmanni*), Mountain Creekshell (*Leaunio vanuxemensis*), Dwarf Rainbow (*Leaunio pataecus*), and Rainbow Mussel (*Cambarunio iris*). Individuals were collected from Meeting Creek (MC), Nolin River (NR), West Fork Drakes Creek (WFD), Salt Lick Creek (SLC), Rough River (RR), Clear Fork Creek (CFC), Walters Creek (WC), Lick Creek (LIC), and Trammel Fork (TF) in the Green Drainage. Individuals were collected from Spring Creek (SPC), Pleasant Run (PR), Sulphur Spring Creek (SULP), Whippoorwill Creek (WHIP), and Rock Bridge Branch (RBB) in the Cumberland Drainage. Individuals were collected from Beech Creek (BC), Rich Valley (RV), Locust Cove Creek (LCC), Ceres (CE), Chilhowie (CHIL), Saltville (SAL), Bennett Island (BEN), Cavitts Creek (CAVC), Copper Creek (COPC), and Richlands (RICH) in the Upper Tennessee River Drainage. – means locus not analyzed for population.

				mtDNA	nDNA Microsatellite Loci									
Species	***N***	**Site**	**Year**	***ND1***	***Eoo08***	***Eoo10***	***Eoo22***	***Eoo24***	***Eoo46***	***Ecap08***	***Ecap07***	***Ecap05***	***Ecap04***	***LAB206***
L. ortmanni	10	MC	2018	2	10	9	10	9	10	10	10	8	9	10
L. ortmanni	3	NR	2021	3	3	3	3	3	3	3	3	3	3	3
L. ortmanni	5	WFD	2020, 2021, 2022	–	7	7	7	7	7	7	7	7	7	7
L. ortmanni	16	SLC	2021	1	16	16	16	16	16	16	16	16	16	14
L. ortmanni	19	RR	2018, 2021	1	19	19	18	19	19	18	19	19	19	18
L. ortmanni	5	CFC	2021	–	5	5	5	5	5	5	5	5	5	5
L. ortmanni	39	WC	2020	–	39	39	39	39	39	39	39	39	39	37
L. ortmanni	2	LIC	2021	–	2	2	2	2	2	2	2	1	2	2
L. ortmanni	3	TF	2021	–	3	3	3	2	3	3	3	3	3	3
L. ortmanni	1	WIG	2019	1	1	0	1	0	1	1	1	1	1	1
L. ortmanni	32		2020, 2021	–	32	31	32	28	31	32	31	31	31	16
L. ortmanni	3	GR	2022	–	3	2	3		3	3	3	3	2	2
L. vanuxemensis	50	SPC	2018, 2019, 2021, 2022	30	47	49	50	47	50	50	49	47	50	36
L. vanuxemensis	6	PR	2019	5	6	6	6	5	6	6	5	6	6	6
L. vanuxemensis	26	SULP	2019	23	25	24	23	25	25	25	25	22	25	20
L. vanuxemensis	6	WHIP	2020	4	6	6	5	6	6	6	6	6	6	2
L. vanuxemensis	1	BC	2019	1	–	–	–	–	–	–	–	–	–	–
L. vanuxemensis	3	RV	2020	3	–	–	–	–	–	–	–	–	–	–
L. vanuxemensis	10	LCC	2020	2	8	8	8	8	7	8	8	8	8	8
L. vanuxemensis	18	WFS	2022	–	19	19	18	18	19	19	19	19	19	19
L. pataecus	1	RBB	2021, 2022	–	0	1	1	1	1	1	1	1	1	1
L. pataecus	15	SINKF	2022	–	8	8	8	8	8	8	8		6	8
C. taeniatus	5	WFD	2020, 2022	–	3	3	3	3	3	3	3	3	2	3
C. taeniatus	3	SINKC	2022	–	3	3	3	3	3	3	3	3	3	3

C. iris	3	RC	2021	–	3	3	3	3	3	3	3	3	3	
C. iris	3	SINKC	2022	–	3	3	3	3	3	3	3	3	3	3
C. iris	8	BC	2019	8	–	–	–	–	–	–	–	–	–	–
C. iris	11	CER	2020	11	–	–	–	–	–	–	–	–	–	–
C. iris	3	CHIL	2020	3	–	–	–	–	–	–	–	–	–	–
C. iris	6	RV	2020	6	–	–	–	–	–	–	–	–	–	–
C. iris	18	SAL	2020	18	8	8	7	8	8	8	8	8	8	8
C. iris	5	BEN	2019	5	–	–	–	–	–	–	–	–	–	–
C. iris	5	CAVC	2018	5	–	–	–	–	–	–	–	–	–	–
C. iris	3	COPC	2018	3	–	–	–	–	–	–	–	–	–	–
C. iris	3	RICH	2018	3	–	–	–	–	–	–	–	–	–	–

Table 4. Observed haplotypes and polymorphic sites for mitochondrial DNA sequences using the *ND1* gene for *Leaunio ortmanni, Leaunio vanuxemensis, Cambarunio taeniatus, Cambarunio iris.* Individuals were obtained from Meeting Creek, Nolin River, West Fork Drakes Creek, Salt Lick Creek, Rough River, Clear Fork Creek, Walters Creek, and Wiggington Creek in the Green River drainage; Spring Creek, Pleasant Run, Sulphur Spring Creek, and Whippoorwill Creek in the Cumberland River drainage; Holston River system to include Beech Creek, Rich Valley, Locust Cove Creek, Ceres, Chilhowie, Saltville, and the Clinch River system to include Bennett Island, Cavitts Creek, Copper Creek, Richlands, all streams of in the Upper Tennessee River drainage. All individuals were collected from 2018 to 2022.

	Polymorphic sites and Base Pair Positions																																							
Haplotype	4	6	7	10	11	13	15	17	19	22	26	31	38	40	43	46	49	55	56	58	59	61	64	70	73	76	83	84	86	89	98	102	110	117	122	125	131	132	134	137
Haplotype 1	A	T	A	G	G	C	C	T	G	C	C	C	T	A	C	A	C	A	T	A	A	C	A	T	A	C	A	T	A	C	C	C	C	A	T	T	C	T	G	T
Haplotype 2	.	.	.	.	.	.	.	.	.	.	.	.	.	.	.	.	.	.	.	.	.	.	.	.	.	.	.	.	.	.	.	.	.	.	.	.	.	.	.	.
Haplotype 3	.	.	.	A	.	.	.	.	A	.	T	.	.	.	T	.	.	.	C	.	G	T	.	.	.	T	.	.	.	T	T	T	.	.	.	.	.	C	A	.
Haplotype 4	.	.	.	A	.	.	.	.	A	.	T	.	.	.	T	.	.	.	C	.	G	T	.	.	.	T	.	.	.	T	T	T	.	.	.	.	.	C	A	.
Haplotype 5	.	.	.	.	.	.	.	.	.	.	.	.	.	.	.	.	.	G	.	.	.	.	.	.	.	.	.	.	.	.	.	.	.	.	.	.	.	.	.	.
Haplotype 6	.	.	.	.	.	.	.	.	.	.	.	.	.	.	.	.	.	G	.	.	.	.	.	.	.	.	.	.	.	.	.	.	.	.	.	.	.	.	.	.
Haplotype 7	.	.	.	.	.	.	.	.	.	.	.	.	.	.	.	.	.	G	.	.	.	.	.	.	.	.	.	.	.	.	.	.	.	.	.	.	.	.	.	.
Haplotype 8	.	.	.	.	.	.	.	.	.	.	.	.	.	.	.	.	.	G	.	.	.	.	.	.	.	.	.	.	.	.	.	A	.	.	.	.	.	A	.	.
Haplotype 9	.	.	.	.	.	.	.	.	.	.	.	.	.	.	.	.	.	G	.	.	.	.	.	.	.	.	.	.	.	.	.	.	.	.	.	.	.	.	.	.
Haplotype 10	.	.	.	.	.	.	.	.	.	.	.	.	.	.	.	.	.	G	.	.	.	.	.	.	.	.	.	.	.	.	.	.	.	.	.	.	.	.	.	.
Haplotype 11	.	.	.	.	.	.	.	.	.	.	A	.	.	.	A	.	.	G	A	.	T	.	.	.	.	A	.	.	.	G	G	.	.	.	.	.	.	A	C	.
Haplotype 12	.	.	.	.	.	.	.	.	.	.	.	.	.	.	.	.	.	G	.	.	.	.	.	.	.	.	.	.	.	.	.	.	.	.	.	.	.	.	.	.
Haplotype 13	.	.	.	.	.	.	.	.	.	.	.	.	.	.	.	.	.	G	.	.	.	.	.	.	.	.	.	.	.	.	.	.	.	.	.	.	.	.	.	.
Haplotype 14	.	.	.	A	.	.	.	.	A	.	T	.	.	.	T	.	.	.	C	.	G	T	.	.	.	T	.	.	.	T	T	T	.	.	.	.	.	C	A	.
Haplotype 15	.	.	.	.	.	.	.	.	.	.	.	.	.	.	.	.	.	.	.	.	.	.	.	.	.	.	.	.	.	.	.	.	.	.	.	.	.	.	.	.
Haplotype 16	.	.	.	.	.	.	.	.	.	.	.	.	.	.	.	.	.	.	.	.	.	.	.	.	.	.	.	.	.	.	.	.	.	.	.	.	.	.	.	.
Haplotype 17	.	.	.	.	.	.	.	.	.	.	.	.	.	.	.	.	.	.	.	.	.	.	.	.	.	.	.	.	.	.	.	.	.	.	.	.	.	.	.	.
Haplotype 18	.	.	.	A	.	.	.	.	A	.	T	.	.	.	T	.	.	.	.	.	G	T	.	.	.	T	.	.	.	T	T	T	.	.	.	.	.	C	A	.
Haplotype 19	.	.	.	A	.	.	.	.	A	.	T	.	.	.	T	.	.	.	C	.	G	T	.	.	.	T	G	.	.	T	T	T	.	.	.	.	.	C	A	.
Haplotype 20	.	.	.	A	.	.	.	.	A	.	T	.	.	.	T	.	.	.	.	.	G	T	.	.	.	T	.	.	.	.	T	T	.	.	.	.	.	C	A	.
Haplotype 21	.	.	.	A	.	.	.	.	A	.	T	.	.	.	T	.	.	.	.	.	G	T	.	.	.	T	.	.	.	.	T	T	.	.	.	.	.	C	A	.
Haplotype 22	G	.	.	A	.	.	.	.	A	.	T	.	.	.	T	.	.	.	.	.	G	T	.	.	.	T	.	.	.	.	T	T	.	.	.	.	.	C	A	.
Haplotype 23	G	.	.	A	.	.	.	.	A	.	T	.	.	.	T	.	.	.	.	.	G	T	.	.	.	T	.	.	.	.	T	T	.	.	.	.	.	C	A	.
Haplotype 24	.	.	.	A	.	.	.	.	A	.	T	.	.	.	T	.	.	.	.	.	G	T	.	.	.	T	.	.	.	.	T	T	.	.	.	.	.	C	A	.
Haplotype 25	.	.	.	A	.	.	.	.	A	.	T	.	.	.	T	.	.	.	.	.	G	T	.	.	.	T	.	.	.	.	T	T	.	.	.	C	.	C	A	.
Haplotype 26	.	.	.	A	.	.	.	.	A	.	T	.	.	.	T	.	.	.	.	.	G	T	.	.	.	T	.	.	.	.	T	T	.	.	.	.	.	C	A	.
Haplotype 27	.	.	.	A	.	T	.	.	A	.	T	.	.	.	T	.	T	.	C	G	.	T	.	.	.	.	.	C	.	T	T	T	.	.	.	.	T	C	A	C
Haplotype 28	.	.	.	A	.	.	.	.	A	.	.	.	.	.	T	.	.	.	.	.	G	T	.	.	.	T	.	.	.	.	T	T	.	.	.	.	.	C	A	.
Haplotype 29	.	.	.	A	.	.	.	.	A	.	T	.	.	.	T	.	.	.	.	.	G	T	.	.	.	T	.	C	.	.	T	T	.	.	.	.	.	C	A	.
Haplotype 30	.	.	G	A	.	.	.	.	A	.	T	.	.	.	T	.	.	.	C	.	G	T	.	.	.	T	G	.	.	T	T	T	.	.	.	.	.	C	A	.
Haplotype 31	.	.	.	A	.	.	.	.	A	.	T	.	.	.	T	.	.	.	.	.	.	T	.	.	.	T	.	.	.	.	T	T	.	.	.	.	.	C	A	.
Haplotype 32	.	.	.	A	.	.	.	.	A	.	T	.	.	.	T	.	.	.	C	.	G	T	.	.	.	T	.	.	.	.	T	T	.	.	.	.	.	C	A	.
Haplotype 33	G	.	.	.	.	.	.	G	A	T	.	.	C	.	T	.	T	.	C	.	.	.	.	.	.	.	.	C	G	T	.	.	.	.	.	C	.	.	.	.
Haplotype 34	G	.	.	.	.	.	.	G	A	T	.	.	C	.	T	.	T	.	C	.	.	.	.	.	.	.	.	C	G	T	.	.	.	.	.	C	.	.	.	.
Haplotype 35	.	.	.	.	.	.	.	.	A	T	.	.	.	.	T	.	T	.	C	.	.	.	.	C	.	.	.	C	.	T	.	.	.	G	.	.	.	.	.	C
Haplotype 36	G	.	.	.	.	.	.	G	A	T	.	.	.	.	T	.	T	.	C	.	.	.	.	.	.	.	.	C	G	T	.	.	.	.	.	.	.	.	.	.
Haplotype 37	.	.	.	A	.	.	.	.	A	.	T	.	.	.	T	.	.	.	C	.	G	T	.	.	G	T	.	.	.	T	T	T	.	.	.	.	.	C	A	.
Haplotype 38	.	.	.	A	.	.	.	.	A	.	T	.	.	.	T	.	.	.	C	.	G	T	.	.	.	T	.	.	.	.	T	T	.	.	.	.	.	C	A	.
Haplotype 39	.	C	.	A	A	.	T	.	A	.	.	A	.	G	.	G	T	.	C	.	.	.	G	C	.	.	.	.	G	.	.	.	A	G	.	.	T	.	.	.
Haplotype 40	.	.	.	A	.	.	.	.	A	.	T	.	.	.	T	.	.	.	C	.	G	T	.	.	.	T	.	.	.	T	T	T	.	.	.	.	.	C	A	.

Table 4. continued.

Haplotype	Polymorphic Sites and Base Pair Positions																																						
	138	140	144	146	149	152	153	158	160	161	167	182	194	203	209	217	218	219	222	224	230	232	131	233	236	239	242	248	251	254	256	264	275	278	281	282	287	302	306	308
Haplotype 1	C	A	A	T	C	C	T	C	T	C	A	C	C	C	C	C	C	A	C	G	A	C	C	T	A	C	C	C	G	T	C	C	C	C	T	C	C	A	A	A
Haplotype 2	.	.	.	.	.	.	.	.	.	.	.	.	.	.	.	.	.	.	.	.	.	.	.	.	.	.	.	.	.	.	.	.	.	.	.	.	.	.	.	.
Haplotype 3	T	.	.	C	.	.	C	T	.	T	.	.	T	T	.	.	T	.	.	A	.	.	.	C	.	.	.	.	A	.	.	T	T	T	C	T	T	.	.	G
Haplotype 4	T	.	.	C	.	.	C	T	.	T	.	.	T	T	.	.	T	.	.	A	.	.	.	.	.	.	.	.	A	.	.	T	T	T	C	T	T	.	.	G
Haplotype 5	.	.	.	.	.	.	.	.	.	.	.	.	.	.	.	.	.	.	.	.	.	.	.	C	.	.	.	.	.	.	.	.	.	.	.	.	.	.	.	.
Haplotype 6	.	.	.	.	.	.	.	.	.	.	.	.	.	.	.	.	.	.	.	.	.	.	.	C	.	.	.	.	.	.	.	.	.	.	.	.	.	.	.	.
Haplotype 7	.	.	.	.	.	.	.	.	.	.	.	T	.	.	.	.	.	.	.	.	.	.	.	C	.	.	.	.	.	.	.	.	.	.	.	.	.	.	.	.
Haplotype 8	.	T	.	.	.	.	A	.	.	G	.	.	.	G	.	.	A	T	A	A	.	G	.	C	T	.	.	.	.	.	.	.	.	.	.	.	.	.	.	.
Haplotype 9	.	.	.	.	.	.	.	.	.	.	.	.	.	.	.	.	.	.	.	.	.	.	.	C	.	.	.	.	.	.	.	.	.	.	.	.	.	.	G	.
Haplotype 10	.	.	.	.	.	.	.	.	.	.	.	.	.	.	.	.	.	.	.	.	.	.	.	.	.	.	.	.	.	.	.	.	.	.	.	.	.	.	.	.
Haplotype 11	.	.	.	.	.	.	A	.	.	G	.	.	A	A	.	A	A	.	.	.	.	.	.	C	.	.	.	.	.	A	.	A	.	.	.	A	.	.	.	G
Haplotype 12	.	.	.	.	.	.	.	.	.	.	C	.	.	.	.	.	.	.	.	.	.	.	.	.	.	.	.	.	.	.	.	.	.	.	.	.	.	.	.	.
Haplotype 13	.	.	.	.	.	.	.	.	.	.	.	.	.	.	.	.	.	.	.	.	.	.	.	.	.	.	.	.	.	.	.	.	.	.	.	.	.	.	.	.
Haplotype 14	T	.	.	C	.	.	C	T	.	.	.	.	.	T	.	.	T	.	.	A	.	.	.	.	.	.	.	.	A	.	.	T	T	T	C	T	.	.	.	G
Haplotype 15	.	.	.	.	.	.	.	.	.	.	.	.	.	.	.	.	.	.	.	.	.	.	.	.	.	.	.	.	A	.	.	.	.	.	.	.	.	.	.	.
Haplotype 16	.	.	.	.	.	.	.	.	.	.	.	.	.	.	.	.	.	.	.	.	.	.	.	.	.	.	.	.	.	.	.	.	.	.	.	.	.	.	.	.
Haplotype 17	.	.	.	.	.	.	.	.	.	.	.	.	.	.	.	.	.	.	.	.	.	.	.	.	.	.	.	.	.	.	.	.	.	.	.	.	.	.	.	.
Haplotype 18	T	.	.	C	.	.	C	T	.	T	.	.	T	T	.	.	T	.	.	A	.	.	.	.	.	.	.	.	A	.	.	T	T	T	C	T	T	.	.	G
Haplotype 19	T	.	.	C	.	.	C	T	.	T	.	.	T	T	T	.	T	.	.	A	.	.	.	.	.	.	.	.	A	.	.	T	T	T	C	T	T	.	.	G
Haplotype 20	T	.	.	.	.	.	C	T	.	T	.	.	T	T	.	.	T	.	.	A	.	.	.	.	.	.	.	.	A	.	.	T	T	T	C	T	.	.	.	G
Haplotype 21	T	.	.	C	.	.	C	T	.	T	.	.	T	T	.	.	T	.	.	A	.	.	.	.	.	.	.	.	A	.	.	T	T	T	.	T	.	.	.	.
Haplotype 22	T	.	.	.	.	.	C	T	.	T	.	.	T	T	.	.	T	.	.	A	.	.	.	.	.	.	.	.	A	.	.	T	T	T	C	T	.	.	.	G
Haplotype 23	T	.	.	.	.	.	C	T	A	T	.	.	T	T	.	.	T	.	.	A	.	.	.	.	.	.	.	.	A	.	.	T	T	T	C	T	.	.	.	G
Haplotype 24	T	.	.	.	.	.	C	T	.	T	.	.	T	T	.	.	T	.	.	A	.	.	.	.	.	.	.	.	A	.	.	T	T	T	C	T	.	.	.	G
Haplotype 25	T	.	.	.	.	.	C	T	.	T	.	.	T	T	.	.	T	.	.	A	.	.	.	.	.	.	.	.	A	.	.	T	T	T	C	T	.	.	.	G
Haplotype 26	T	.	.	.	.	.	C	T	.	T	.	.	T	T	.	.	T	.	.	A	.	.	.	.	.	.	.	.	A	.	T	T	T	T	C	T	.	.	.	G
Haplotype 27	T	.	.	C	.	G	.	T	.	T	.	.	T	T	.	.	T	.	.	A	.	.	T	.	.	.	T	T	A	.	.	T	T	T	C	T	T	.	G	G
Haplotype 28	T	.	.	.	.	.	C	T	.	T	.	.	T	T	.	.	T	.	.	A	.	.	.	.	.	.	.	.	A	.	.	T	T	T	C	T	.	.	.	G
Haplotype 29	T	.	.	.	.	.	C	T	.	T	.	.	T	T	.	.	T	.	.	A	.	.	.	.	.	.	.	.	A	.	.	T	T	T	C	T	.	.	.	G
Haplotype 30	T	.	.	C	.	.	C	T	.	T	.	.	T	T	T	.	T	.	.	A	.	.	.	.	.	.	.	.	A	.	.	T	T	T	C	T	T	.	.	G
Haplotype 31	T	.	.	.	.	.	C	T	.	T	.	.	T	T	.	.	T	.	.	A	.	.	.	.	.	.	.	.	A	.	.	T	T	T	C	T	.	.	.	G
Haplotype 32	T	.	.	.	.	.	C	T	.	T	.	.	T	T	.	.	T	.	.	A	.	.	.	.	.	.	.	.	A	.	.	T	T	T	C	T	.	.	.	G
Haplotype 33	.	.	.	.	T	.	.	.	.	.	.	.	T	T	T	.	.	.	.	A	G	.	.	.	.	.	.	.	A	.	.	.	.	.	C	.	T	.	.	.
Haplotype 34	.	.	.	.	T	.	.	.	.	.	.	.	T	.	T	.	.	.	.	.	G	.	.	.	.	.	.	.	A	.	.	.	.	.	C	.	T	.	.	.
Haplotype 35	.	.	.	.	T	.	.	.	.	.	.	.	T	.	T	.	.	.	.	.	G	.	.	.	.	.	T	.	A	.	.	.	.	.	C	.	T	.	.	.
Haplotype 36	.	.	.	.	T	.	.	.	.	.	.	.	T	T	T	.	.	.	.	.	G	.	.	.	.	.	.	.	A	.	.	.	.	.	C	.	T	.	.	.
Haplotype 37	T	.	.	C	.	.	C	T	.	T	.	.	T	T	.	.	T	.	.	A	.	.	.	C	.	.	.	.	A	.	.	T	T	T	C	T	T	.	.	G
Haplotype 38	T	.	.	.	.	.	C	T	.	T	.	.	T	T	.	.	T	.	.	A	.	.	.	.	.	T	.	.	A	.	.	T	T	T	C	T	.	.	.	G
Haplotype 39	.	G	G	.	.	.	C	T	.	.	.	.	.	.	T	.	T	.	.	.	.	.	T	C	.	.	T	.	.	C	.	.	T	T	C	T	T	G	.	.
Haplotype 40	T	.	.	.	.	.	C	T	.	T	.	.	T	T	.	.	T	.	.	A	.	.	.	.	.	.	.	.	A	.	.	T	T	T	C	T	T	.	.	G

Table 4. continued.

	Polymorphic Sites and Base Pair Positions																																					
	3	3	3	3	3	3	3	3	3	3	3	3	3	3	3	3	3	3	3	3	3	3	3	3	3	3	3	3	4	4	4	4	4	4	4	4	4	4
	1	1	1	1	2	2	2	2	2	2	2	3	3	3	3	4	5	5	5	5	5	5	6	7	7	7	7	8	8	8	0	1	1	1	1	2	2	3	3	4
Haplotype	1	2	7	9	0	1	4	6	7	8	9	1	2	5	8	1	0	1	3	6	7	9	3	0	1	4	9	0	5	6	4	2	6	8	9	2	8	1	4	1
Haplotype 1	A	A	T	G	C	C	A	T	A	A	T	T	T	G	A	T	C	C	C	A	T	A	C	T	T	A	T	C	T	C	C	C	T	A	C	C	G	A	A	C
Haplotype 2	.	.	.	.	A	.	.	.	.	.	.	.	.	.	.	.	T	.	.	.	.	.	.	.	.	.	.	.	.	.	.	.	.	.	.	.	.	.	.	.
Haplotype 3	.	.	.	.	A	T	.	.	.	.	C	.	C	C	.	.	T	.	T	C	C	.	.	.	.	.	C	A	.	A	T	.	.	.	T	T	A	G	.	T
Haplotype 4	.	.	.	.	A	T	.	.	.	.	C	.	C	C	.	.	T	.	T	C	C	.	.	.	.	.	C	A	.	A	T	.	.	.	T	T	A	G	.	T
Haplotype 5	.	.	.	.	.	.	.	.	.	.	.	.	.	.	.	.	.	.	A	.	.	.	.	.	.	.	.	.	.	.	.	.	.	.	.	.	.	.	.	.
Haplotype 6	.	.	.	.	.	.	.	.	.	.	.	.	.	.	.	.	.	.	A	.	.	.	.	.	.	.	.	.	.	.	.	.	.	.	.	.	.	.	G	.
Haplotype 7	.	.	.	.	.	.	.	.	.	.	.	.	.	.	.	.	.	.	A	.	.	.	.	.	.	.	.	.	.	.	.	.	A	.	.	.	.	.	.	.
Haplotype 8	.	.	.	.	.	.	.	.	.	.	.	.	.	.	.	.	A	.	A	.	.	C	.	.	.	.	.	.	.	.	.	T	.	.	.	.	.	.	.	.
Haplotype 9	.	.	.	.	.	.	.	.	.	.	.	.	.	.	.	.	.	.	A	.	.	.	.	.	.	.	.	.	.	.	.	.	.	.	.	.	.	.	.	.
Haplotype 10	.	.	.	.	.	.	.	.	.	.	.	.	.	.	.	.	.	T	A	.	.	.	.	.	.	.	.	.	.	.	.	.	.	.	.	.	.	.	.	.
Haplotype 11	.	G	.	.	T	A	.	.	.	.	A	.	.	.	.	.	T	.	A	T	.	.	.	.	.	.	.	.	C	.	T	.	.	T	.	.	.	.	.	.
Haplotype 12	.	.	.	.	.	.	.	.	.	.	.	.	.	.	.	.	.	.	.	.	.	.	.	.	.	.	.	.	.	.	.	.	.	.	.	.	.	.	.	.
Haplotype 13	.	.	.	.	.	.	.	.	.	.	.	.	.	.	.	.	.	.	.	.	.	.	.	.	.	.	.	.	.	.	.	.	.	.	.	.	.	.	.	.
Haplotype 14	.	.	.	.	A	T	.	.	.	.	C	.	C	C	.	.	T	.	T	C	C	.	.	.	.	.	C	A	.	A	T	.	.	.	T	T	A	.	.	T
Haplotype 15	.	.	.	.	.	.	.	.	.	.	.	.	.	.	.	.	.	.	.	.	.	.	.	.	.	.	.	.	.	.	.	.	.	.	.	.	.	.	.	.
Haplotype 16	.	.	.	.	.	.	.	.	.	.	.	.	.	.	.	.	.	.	.	.	.	.	.	.	C	.	.	.	.	.	.	.	.	.	.	.	.	.	.	.
Haplotype 17	.	.	G	T	A	T	G	A	G	G	.	G	.	.	.	.	.	.	.	.	.	.	.	.	C	.	.	.	.	.	.	.	.	.	.	.	.	.	.	.
Haplotype 18	.	.	.	.	A	T	.	.	.	.	C	.	C	C	.	.	T	.	T	C	C	.	.	.	.	.	C	A	.	A	T	.	.	.	T	T	A	G	.	T
Haplotype 19	.	.	.	.	-	-	G	.	.	.	C	.	C	C	.	.	T	.	T	C	C	.	.	.	.	.	-	A	.	A	T	.	.	.	T	T	A	G	.	.
Haplotype 20	.	.	.	.	-	-	.	.	.	.	C	.	C	C	.	.	T	.	T	C	C	.	.	.	.	.	-	A	.	A	T	.	.	.	T	T	A	G	.	T
Haplotype 21	.	.	.	.	-	-	.	.	.	.	C	.	C	C	.	.	T	.	T	C	C	.	.	.	.	.	-	A	.	A	T	.	.	.	T	T	A	G	.	T
Haplotype 22	.	.	.	.	-	-	.	.	.	.	C	.	C	C	.	.	T	.	T	C	C	.	.	.	.	.	-	A	.	A	T	.	.	.	T	T	A	G	.	T
Haplotype 23	.	.	.	.	-	-	.	.	.	.	C	.	C	C	.	.	T	.	T	C	C	.	.	.	.	.	-	A	.	A	T	.	.	.	T	T	A	G	.	T
Haplotype 24	.	.	.	.	-	-	.	.	.	.	C	.	C	C	.	.	T	.	T	C	C	.	.	C	.	.	-	A	.	A	T	.	.	.	T	T	A	G	.	T
Haplotype 25	.	.	.	.	-	-	.	.	.	.	C	.	C	C	.	.	T	.	T	C	C	.	.	.	.	.	-	A	.	A	T	.	.	.	T	T	A	G	.	T
Haplotype 26	.	.	.	.	-	-	.	.	.	.	C	.	C	C	.	.	T	.	T	C	C	.	.	.	.	.	-	A	.	A	T	.	.	.	T	T	A	G	.	T
Haplotype 27	.	.	.	.	-	-	.	.	.	.	C	.	C	C	.	.	T	.	T	C	C	.	T	.	.	.	-	A	.	.	T	.	.	.	T	T	A	.	.	.
Haplotype 28	.	.	.	.	-	-	.	.	.	.	C	.	C	C	.	.	T	.	T	C	C	.	.	.	.	.	-	A	.	A	T	.	.	.	T	T	A	G	.	T
Haplotype 29	.	.	.	.	-	-	.	.	.	.	C	.	C	C	.	.	T	.	T	C	C	.	.	C	.	.	-	A	.	A	T	.	.	.	T	T	A	G	.	T
Haplotype 30	.	.	.	.	-	-	G	.	.	.	C	.	C	C	.	.	T	.	T	C	C	.	.	.	.	.	-	A	.	A	T	.	.	.	T	T	A	G	.	.
Haplotype 31	.	.	.	.	-	-	.	.	.	.	C	.	C	C	.	.	T	.	T	C	C	.	.	.	.	.	-	A	.	A	T	.	.	.	T	T	A	G	.	T
Haplotype 32	.	.	.	.	-	-	.	.	.	.	C	.	C	C	.	.	T	.	T	C	C	.	.	.	.	.	-	A	.	A	T	.	.	.	T	T	A	G	.	T
Haplotype 33	.	.	.	.	-	-	.	.	.	.	.	.	.	.	G	C	T	.	T	C	C	.	.	.	.	.	-	A	.	.	.	.	.	.	T	T	.	.	G	.
Haplotype 34	.	.	.	.	-	-	.	.	.	.	.	.	.	.	G	C	T	.	T	.	C	.	.	.	.	.	-	A	.	.	.	.	.	.	T	T	.	.	G	.
Haplotype 35	T	.	.	.	-	-	.	.	.	.	.	.	.	.	G	C	.	.	T	.	C	.	A	.	.	.	-	A	.	.	.	.	.	.	T	T	.	.	G	.
Haplotype 36	.	.	.	.	-	-	.	.	.	.	.	.	.	.	G	C	T	.	T	.	C	.	.	.	.	.	-	A	.	.	.	.	.	.	T	T	.	.	G	.
Haplotype 37	.	.	.	.	-	-	.	.	.	.	C	.	C	C	.	.	T	.	T	C	C	.	.	.	.	.	-	A	.	A	T	.	.	.	T	T	A	G	.	T
Haplotype 38	.	.	.	.	-	-	.	.	.	.	C	.	C	C	.	.	T	.	T	C	C	.	.	.	.	.	-	A	.	A	T	.	.	.	T	T	A	G	.	T
Haplotype 39	.	.	C	.	-	-	.	.	.	.	C	.	C	T	.	.	T	.	T	.	C	.	T	.	.	G	-	A	.	.	.	.	.	.	T	T	A	.	.	.
Haplotype 40	.	.	.	.	-	-	.	.	.	.	C	.	C	C	.	.	T	.	T	C	C	.	.	.	.	.	-	A	.	A	T	.	.	.	T	T	A	G	.	T

Table 4. continued.

	Polymorphic Sites and Base Pair Positions																					
Haplotype	446	452	458	461	467	470	473	479	482	483	486	489	494	496	497	499	503	506	509	513	515	518	mtDNA Lineage
Haplotype 1	T	G	T	T	T	T	A	C	C	G	T	C	T	T	A	C	A	T	A	A	C	G	*L. vanuxemensis*
Haplotype 2	.	.	.	.	.	.	.	.	.	.	.	.	.	.	.	.	.	.	.	.	.	.	*L. vanuxemeneis*
Haplotype 3	C	A	.	.	C	C	G	T	.	.	.	.	.	.	G	.	.	.	G	.	T	A	*L. vanuxemensis, C. taeniatus, C. iris*
Haplotype 4	C	A	.	.	C	C	G	T	.	.	.	.	.	.	G	.	.	.	G	.	T	A	*L. ortmanni, L. vanuxemensis*
Haplotype 5	.	.	.	.	.	.	.	.	.	.	.	.	.	.	.	.	.	.	.	.	.	.	*L. ortmanni*
Haplotype 6	.	.	.	.	.	.	.	.	.	.	.	.	A	.	.	.	.	.	.	.	.	.	*L. ortmanni*
Haplotype 7	.	.	.	.	.	.	.	.	.	.	.	T	.	.	.	.	.	.	.	.	.	.	*L. ortmanni*
Haplotype 8	.	.	.	.	.	.	.	.	.	A	.	T	.	A	.	.	.	.	.	T	.	.	*L. ortmanni*
Haplotype 9	.	.	.	.	.	.	.	.	.	.	.	A	.	.	.	.	.	C	.	.	.	.	*L. ortmanni*
Haplotype 10	.	A	.	.	.	.	.	.	.	.	.	A	.	.	.	.	.	.	.	.	.	.	*L. ortmanni*
Haplotype 11	.	.	.	.	.	.	.	.	.	.	.	.	.	.	.	G	.	.	.	.	.	.	*L. ortmanni*
Haplotype 12	.	.	.	.	.	.	.	.	.	.	A	.	.	.	.	.	.	.	.	.	.	.	*L. ortmanni*
Haplotype 13	.	.	.	.	.	.	.	.	.	.	.	.	-	-	-	-	-	-	-	-	-	-	*L. ortmanni, L. vanuxemensis*
Haplotype 14	C	A	.	.	C	C	.	T	.	.	.	.	.	.	G	.	.	.	G	.	T	A	*L. vanuxemensis*
Haplotype 15	.	.	.	.	.	.	.	.	.	.	.	.	.	.	.	.	.	.	.	.	.	.	*L. vanuxemensis*
Haplotype 16	.	.	.	.	.	.	.	.	.	.	.	.	.	.	.	.	.	.	.	.	.	.	*L. vanuxemensis*
Haplotype 17	.	.	.	.	.	.	.	.	.	.	.	.	.	.	.	.	.	.	.	.	.	.	*L. vanuxemensis*
Haplotype 18	C	A	.	.	C	C	G	T	.	.	.	.	.	.	G	.	.	.	G	.	T	A	*L. vanuxemensis*
Haplotype 19	C	A	.	.	-	C	G	T	.	.	.	.	.	.	G	.	.	.	G	.	T	A	*L. vanuxemensis, C. iris*
Haplotype 20	C	A	.	.	-	C	G	T	.	.	.	.	.	.	G	.	.	.	G	.	T	A	*C. iris*
Haplotype 21	C	A	.	.	-	C	G	T	.	.	.	.	.	.	G	.	.	.	G	.	T	A	*C. iris*
Haplotype 22	C	A	.	.	-	C	G	T	.	.	.	.	.	.	G	.	.	.	G	.	T	A	*L. vanuxemensis, C. iris*
Haplotype 23	C	A	.	.	-	C	G	T	.	.	.	.	.	.	G	.	.	.	G	.	T	A	*C. iris*
Haplotype 24	C	A	.	.	-	C	G	T	.	.	.	.	.	.	G	.	.	.	G	.	T	A	*C. iris*
Haplotype 25	C	A	.	.	-	C	G	T	.	.	.	.	.	.	G	.	.	.	G	.	T	A	*C. iris*
Haplotype 26	C	A	.	.	-	C	G	T	.	.	.	.	.	.	G	.	.	.	G	.	T	A	*C. iris*
Haplotype 27	.	A	.	.	-	C	G	.	T	.	.	.	.	.	G	.	.	.	G	.	T	A	*C. iris*
Haplotype 28	C	A	.	.	-	C	G	T	.	.	.	.	.	.	G	.	.	.	G	.	T	A	*C. iris*
Haplotype 29	C	A	.	.	-	C	G	T	.	.	.	.	.	.	G	.	.	.	G	.	T	A	*C. iris*
Haplotype 30	C	A	.	.	-	C	G	T	.	.	.	.	.	.	G	.	.	.	G	.	T	A	*L. vanuxemensis, C. iris*
Haplotype 31	C	A	.	.	-	C	G	T	.	.	.	.	.	.	G	.	.	.	G	.	T	A	*C. iris*
Haplotype 32	C	A	.	.	-	C	G	T	.	.	.	.	.	.	G	.	.	.	G	.	T	A	*C. iris*
Haplotype 33	.	A	C	.	-	.	.	.	.	.	.	.	.	.	.	.	.	C	.	.	.	.	*L. vanuxemensis*
Haplotype 34	.	A	C	.	-	.	.	.	.	.	.	.	.	.	.	.	.	C	.	.	.	.	*L. vanuxemensis*
Haplotype 35	.	A	.	.	-	.	.	.	.	.	.	.	.	.	.	.	.	C	.	.	.	.	*L. vanuxemensis*
Haplotype 36	.	A	C	.	-	.	.	.	.	.	.	.	.	.	.	.	.	C	.	.	.	.	*L. vanuxemensis*
Haplotype 37	C	A	.	.	-	C	G	T	.	.	.	.	.	.	G	.	.	.	G	.	T	A	*C. iris*
Haplotype 38	C	A	.	.	-	C	G	T	.	.	.	.	.	.	G	.	.	.	G	.	T	A	*C. iris*
Haplotype 39	.	A	.	C	-	.	G	.	.	.	.	.	.	.	G	.	G	.	.	.	T	A	*L. vanuxemensis*
Haplotype 40	C	A	.	.	-	C	G	T	.	.	.	.	.	.	G	.	.	.	G	.	T	A	*L. vanuxemensis*

Table 5. Observed haplotypes and polymorphic sites for mitochondrial DNA sequences of the *ND1* gene per population of *Leaunio ortmanni, Leaunio vanuxemensis, Cambarunio taeniatus, Cambarunio iris* collected from 2018 to 2022. Individuals were obtained from Meeting Creek (MC), Nolin River (NR), West Fork Drakes Creek (WFD), Salt Lick Creek (SLC), Rough River (RR), Clear Fork Creek (CFC), Walters Creek (WC), and Wiggington Creek (WIG) in the Green River drainage; Spring Creek (SPC), Pleasant Run (PR), Sulphur Spring Creek (SULP), and Whippoorwill Creek (WHIP) in the Cumberland River drainage; Beech Creek (BC), Rich Valley (RV), Locust Cove Creek (LCC), Ceres (CER), Chilhowie (CHIL), Saltville (SAL), Bennett Island (BEN), Cavitts Creek (CAV), Copper Creek (COP), Richlands (RICH) in the Upper Tennessee River drainage.

	Number of Individuals Per Haplotype Per Population																						
	Green								Cumberland				Upper Tennessee										
	Leaunio ortmanni							*Cambarunio taeniatus*	*Leaunio vanuxemensis*							*Cambarunio iris*							
Haplotype	MC	NR	WFD	SLC	RR	RC	WIG	WFD	SPC	PR	SULP	WHIP	RV	LCC	BC	BC	RV	CER	CHIL	SAL	BEN	CAV	COP	RICH	Total
Haplotype 1									1	3	10	4													18
Haplotype 2										1															1
Haplotype 3								1	1	1										2		1		1	7
Haplotype 4			1								10														11
Haplotype 5	1																								1
Haplotype 6	1																								1
Haplotype 7					1																				1
Haplotype 8		1																							1
Haplotype 9		1																							1
Haplotype 10		1																							1
Haplotype 11						1																			1
Haplotype 12							1																		1
Haplotype 13				1							1														2
Haplotype 14											1														1
Haplotype 15											1														1
Haplotype 16									26																26
Haplotype 17									1																1
Haplotype 18									1																1
Haplotype 19														3	1	2		3				1			10
Haplotype 20																2	2	3	2	6	2			1	18
Haplotype 21																1									1
Haplotype 22															1					1					2
Haplotype 23																1									1
Haplotype 24																		1		1	2		2	1	7
Haplotype 25																	1	2			1				4
Haplotype 26																						1			1
Haplotype 27																						1			1
Haplotype 28																						1			1
Haplotype 29																							1		1
Haplotype 30														1				1							2
Haplotype 31																		1							1
Haplotype 32																	2		1	6					9
Haplotype 33														1											1
Haplotype 34														3											3

Haplotype 35															2	2													4
Haplotype 36																1													1
Haplotype 37																								1					1
Haplotype 38																								1					1
Haplotype 39																	1												1
Haplotype 40															2	1													3
Total	2	3	1	1	1	1	1		1		30	5	23	4	4	12	3	6	5	11	3	18	5	5	3	3	151		

Table 6. Summary of genetic variation among eight microsatellite DNA loci examined for *Leaunio ortmanni* in the Green River drainage and *Leaunio vanuxemensis* and *Leaunio pataceus* in the Cumberland River drainage collected in Kentucky from 2018 to 2022; and *Cambarunio iris* from the Holston River drainage collected in Virginia in 2020. *N*=number of individuals genotyped per locus, H_o=mean observed heterozygosity, H_e=mean expected heterozygosity, *A*=mean number of observed alleles per locus, *Ap*=total number of private alleles observed per locus, mean *M*-ratio=ratio of *A* and number of alleles possible within the range of nucleotide base-pair differences between the shortest and longest microsatellite alleles observed per locus.

Species	Drainage	Subbasin	Population	N	H_e	H_o	A	Ap	Mean M-ratio
L. ortmanni	Green	Rough	Meeting Creek	10	0.86	0.65	7.63	0	0.71
	Green	Rough	Rough River	19	0.86	0.52	11.50	5	0.71
	Green	Rough	SUB-BASIN TOTAL	29	0.88	0.57	13.63	5	0.77
	Green	Nolin	Nolin River	3	0.80	0.63	3.88	0	0.49
	Green	Nolin	Walters Creek	39	0.88	0.52	13.00	2	0.72
	Green	Nolin	SUB-BASIN TOTAL	42	0.89	0.52	14.13	2	0.72
	Green	Barren	West Fork Drakes Creek	7	0.89	0.59	8.13	2	0.50
	Green	Barren	Salt Lick Creek	16	0.87	0.48	9.25	2	0.76
	Green	Barren	Trammel Fork	3	0.86	0.56	4.00	2	0.40
	Green	Barren	SUBBASIN TOTAL	26	0.90	0.52	14.00	6	0.73
	Green	Gasper	Clear Fork Creek	5	0.88	0.52	6.00	4	0.53
	Green	Russell	Russell Creek	31	0.87	0.51	12.13	3	0.71
	Green	Green	Green River	3	0.52	0.29	2.43	0	0.74
L. vanuxemensis	Cumberland	Red	Spring Creek	50	0.89	0.53	15.13	7	0.85
	Cumberland	Red	Pleasant Run	6	0.82	0.57	5.75	0	0.67
	Cumberland	Red	Sulphur Spring	25	0.88	0.59	14.25	4	0.68
	Cumberland	Red	Whippoorwill Creek	6	0.87	0.77	7.13	4	0.45
	Cumberland	Red	SUB-BASIN TOTAL	87	0.90	0.57	20.63	15	0.78
	Cumberland	Stones	West Fork Stones River	19	0.87	0.40	10.50	7	0.59
	Holston	Holston	Locust Cove Creek	8	0.85	0.55	6.63	5	0.80
L. pataecus	Cumberland	Little River	Sinking Fork	8	0.85	0.73	7.29	3	0.56
C. iris	Holston	Holston	Saltville	8	0.91	0.60	9.38	10	0.51

Table 7. Pairwise allelic differentiation F_{ST} values (below diagonal) and pairwise D_{est} values (above diagonal) between populations based on eight microsatellite loci for *Leaunio ortmanni* in Meeting Creek (MC), Russell Creek (RC), Nolin River (NR), West Fork Drakes Creek (WFD), Trammel Fork (TF), Salt Lick Creek (SLC), Rough River (RR), Clear Fork Creek (CFC), and Walters Creek (WC) in the Green River drainage in Kentucky and Spring Creek (SPC), Pleasant Run (PR), Sulphur Spring Creek (SUL), Whippoorwill Creek (WHIP), West Fork Stones River (WFS), for *Leaunio vanuxemensis* in the Cumberland River drainage in Kentucky for *Leaunio pataceus* in Sinking Fork, *Leaunio vanuxemensis* in Locust Cove Creek (LCC), and *Cambarunio iris* in the North Fork Holston River (NFH) in the Upper Tennessee River Basin . All individuals were collected from 2018 to 2022.

Drainage		Green										Cumberland						Upper Tennessee	
Species		*Leaunio ortmanni*										*Leaunio vanuxemensis*					*Leaunio pataceus*	*Leaunio vanuxemensis*	*Cambarunio iris*
		MC	RC	NR	WFD	TF	SLC	RR	CFC	WC	GR	SPC	PR	SUL	WHIP	WFS	SF	LCC	NFH
Leaunio ortmanni	MC	—	0.352	0.504	0.567	0.661	0.735	0.338	0.300	0.338	—	0.542	0.554	0.698	0.552	0.522	0.510	0.678	0.404
	RC	0.053	—	0.306	0.294	0.398	0.444	0.464	0.108	0.215	—	0.557	0.601	0.663	0.451	0.643	0.745	0.682	0.363
	NR	0.132	0.083	—	—	—	0.722	0.675	0.489	0.488	—	0.535	0.689	0.626	0.69	0.696	0.679	0.552	0.602
	WFD	0.086	0.068	0.102	—	—	0.421	0.316	0.553	0.416	—	0.325	0.250	0.333	0.452	0.577	0.400	0.418	0.283
	TF	0.141	0.109	0.172	0.105	—	—	-0.006	-0.201	0.380	—	0.667	0.452	0.589	0.494	0.829	0.753	0.633	0.473
	SLC	0.114	0.084	0.131	0.058	0.050	—	—	0.260	0.483	—	0.718	0.719	0.707	0.614	0.807	0.718	0.776	0.620
	RR	0.055	0.056	0.135	0.072	0.091	0.075	—	-0.060	0.197	—	0.450	0.532	0.527	0.608	0.599	0.507	0.595	0.483
	CFC	0.071	0.053	0.114	0.091	0.055	0.063	0.026	—	0.002	—	0.390	0.543	0.520	0.297	0.678	0.505	0.565	0.320
	WC	0.050	0.041	0.098	0.067	0.086	0.073	0.034	0.029	—	—	0.539	0.710	0.660	0.570	0.729	0.647	0.579	0.433
	GR	0.147	0.131	0.259	0.130	0.225	0.136	0.123	0.161	0.107	—	—	—	—	—	—	—	—	—
Leaunio vanuxemensis	SPC	0.083	0.076	0.102	0.057	0.115	0.098	0.063	0.066	0.070	0.134	—	0.181	0.108	0.378	0.521	0.636	0.473	0.525
	PR	0.118	0.113	0.161	0.068	0.131	0.124	0.096	0.111	0.113	0.200	0.044	—	0.018	0.424	0.427	0.702	0.662	0.525
	SULP	0.107	0.094	0.122	0.056	0.113	0.104	0.079	0.083	0.087	0.150	0.023	0.025	—	0.420	0.585	0.698	0.477	0.683
	WHIP	0.097	0.076	0.135	0.077	0.106	0.093	0.090	0.063	0.080	0.164	0.058	0.090	0.070	—	0.407	0.797	0.645	0.601
	WFS	0.091	0.094	0.132	0.094	0.142	0.116	0.085	0.101	0.100	0.124	0.071	0.085	0.086	0.071	—	0.535	0.577	0.427
Leaunio pataceus	SF	0.104	0.114	0.141	0.080	0.144	0.108	0.081	0.089	0.090	0.182	0.087	0.128	0.100	0.121	0.088	—	0.532	0.486
Leaunio vanuxemensis	LCC	0.118	0.107	0.122	0.090	0.130	0.117	0.098	0.097	0.086	0.177	0.075	0.125	0.080	0.103	0.093	0.094	—	0.434
Cambarunio iris	NFH	0.067	0.061	0.107	0.072	0.096	0.081	0.065	0.063	0.058	0.089	0.062	0.089	0.081	0.079	0.061	0.070	0.067	—

Table 8. Pairwise allelic differentiation F_{ST} values (below diagonal) and pairwise D_{est} values (above diagonal) between populations pooled at the subbasin level based on eight microsatellite loci for *Leaunio ortmanni* in Rough River (RR), Russell Creek (RC), Nolin River (NR), Barren River (BR), Gasper River (GS), and Green River (GR) in the Green River drainage in Kentucky and Red River (RD) and Stones River (SR) for *Leaunio vanuxemensis* in the Cumberland River drainage in Kentucky and Tennessee and for *Leaunio pataceus* in Little River (LR), and *Leaunio* vanuxemensis and *Cambarunio iris* in the North Fork Holston River (HR) in the Upper Tennessee River Basin in Virginia. All individuals were collected from 2018 to 2022.

Drainage		Green						Cumberland			Holston	
Species		*Leaunio ortmanni*						*Leanunio vanuxemensis*		*Leaunio pataceus*	*Leaunio vanuxemensis*	*Cambarunio iris*
		RR	RC	NR	BR	GS	GR	RD	ST	LR	HR	HR
Leaunio ortmanni	RR	—	0.302	0.253	0.407	0.161	—	0.415	0.406	0.480	0.558	0.387
	RC	0.050	—	0.177	0.497	0.232	—	0.563	0.563	0.738	0.664	0.330
	NR	0.029	0.044	—	0.471	0.064	—	0.584	0.659	0.631	0.571	0.366
	BR	0.071	0.075	0.063	—	0.427	—	0.516	0.638	0.560	0.685	0.562
	GS	0.035	0.054	0.019	0.068	—	—	0.497	0.576	0.489	0.525	0.434
	GR	0.141	0.158	0.137	0.151	0.197	—	—	—	—	—	—
Leaunio vanuxemensis	RD	0.061	0.080	0.076	0.073	0.079	0.169	—	0.398	0.481	0.394	0.636
	ST	0.076	0.093	0.102	0.101	0.105	0.170	0.069	—	0.513	0.624	0.434
Leaunio pataceus	LR	0.088	0.120	0.091	0.085	0.078	0.208	0.093	0.109	—	0.479	0.573
Leaunio vanuxemensis	HR	0.073	0.090	0.064	0.074	0.075	0.201	0.060	0.108	0.088	—	0.531
Cambarunio iris	HR	0.043	0.051	0.053	0.059	0.051	0.115	0.070	0.062	0.071	0.058	—

Table 9. Procrustes distance and *p*-values among groups of *Leaunio ortmanni* of the Green River drainage, *Leaunio vanuxemensis* of the Cumberland River drainage and UTRB, and *L. pataceus* of the Cumberland River drainage.

Size Class	Drainage		Green	Cumberland		Powell	Goodall's F	*p-value*
		Species	*Leaunio ortmanni*	*Leaunio vanuxemensis*	*Leaunio pataceus*	*Leaunio vanuxemensis*	—	—
Small	Cumberland	*Leaunio vanuxemensis*	0.24 (p=0.03)	—	—	—	—	—
	Cumberland	*Leaunio pataceus*	0.65 (p=0.04)	0.38 (p=0.27)	—	—	1.17	p=0.28
Medium	Cumberland	*Leaunio vanuxemensis*	0.03 (p=0.23)	—	—	—	—	—
	Cumberland	*Leaunio pataceus*	0.08 (p=0.08)	0.09 (p=0.01)		—	2.87	p=0.02
Medium	Cumberland	*Leaunio vanuxemensis*	0.03 (p=0.22)	—	—	—	—	—
	Cumberland	*Leaunio pataceus*	0.08 (p=0.08)	0.09 (p=0.01)	—	—	—	—
	Powell	*Leaunio vanuxemensis*	0.12 (p=0)	0.13 (p=0)	0.06 (p=0.16)	—	—	—
	Holston	*Leaunio vanuxemensis*	0.08 (p=0)	0.09 (p=0)	0.05 (p=0.29)	0.07 (p=0.02)	6.92	*p=0*
Large	Cumberland	*Leaunio vanuxemensis*	0.02 (p=0.60)	—	—	—	—	—
	Cumberland	*Leaunio pataceus*	0.05 (p=0.14)	0.04 (p=0.25)	—	—	1.16	p=0.30

Table 10. Decision tree analysis confusion matrix for *L. ortmanni* of the Green River drainage, *L. vanuxemensis* of the Cumberland River srainage, and *L. pataceus* of the Cumberland River drainage. Data validations included Hold-Out validation which splits the data into training (80%, 67 observations) and validation data (20%, 28 observations). The matrix shows predicted and actual identification to demonstrate the misclassifications for each species. The misclassification error rates for training data were 14% and 9% for the validation data.

			Actual		
			Leaunio ortmanni	*Leaunio pataceus*	*Leaunio vanuxemensis*
Prediction	Training data	*Leaunio ortmanni*	52	8	10
		Leaunio pataceus	0	0	0
		Leaunio vanuxemensis	3	4	98
	Validation Data	*Leaunio ortmanni*	9	1	2
		Leaunio pataceus	0	0	0
		Leaunio vanuxemensis	0	0	20

FIGURES

Figure 1. **Panel A**. View of the Green, Cumberland, French Broad River Drainages and the Upper Tennessee River Basin. **Panel B**. Historical and Current distributions of *Leaunio ortmanni* in the Green River Drainage and *Leaunio vanuxemensis* in the Cumberland River Drainage.

Figure 1, Panel A.

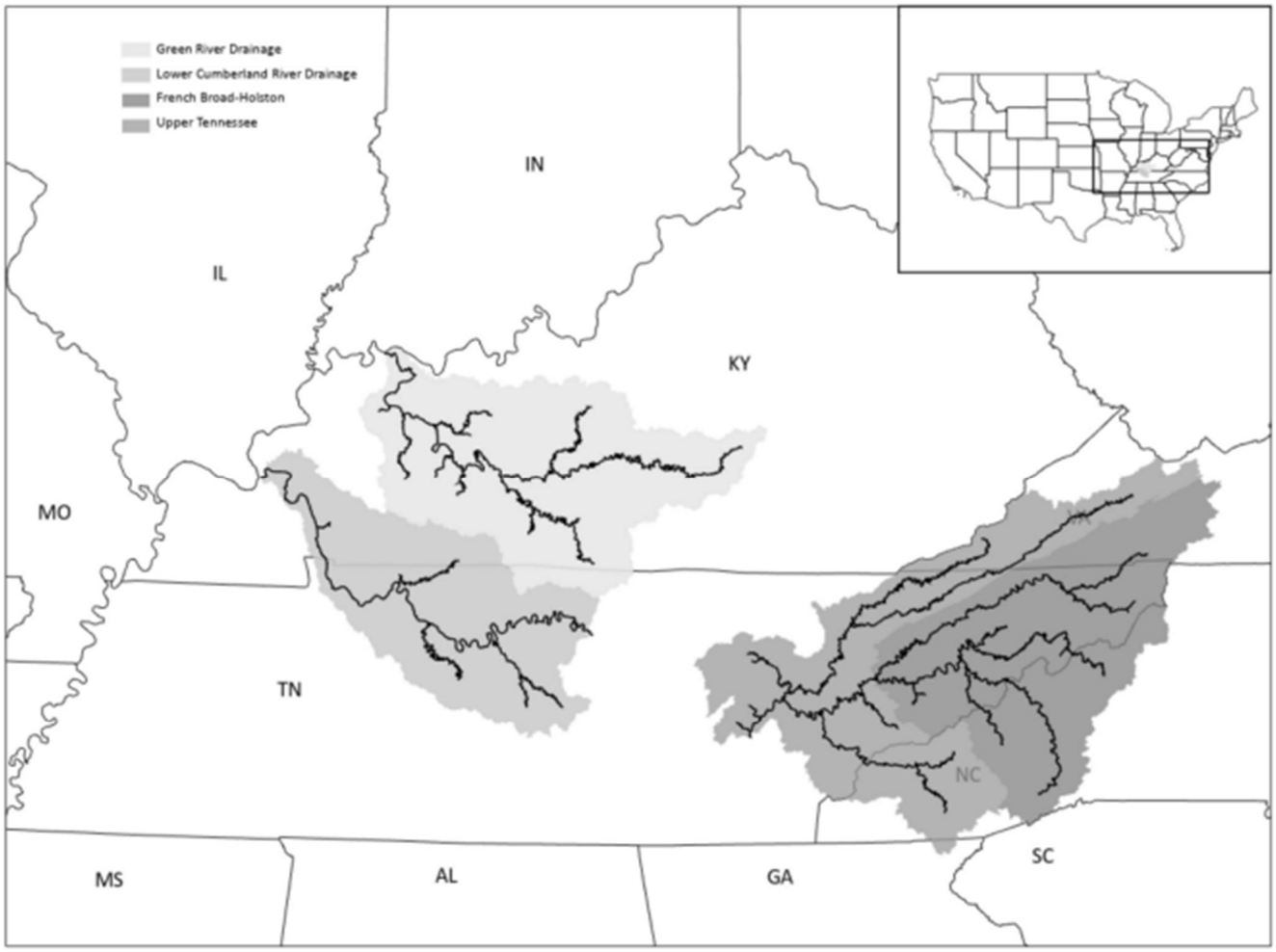

Figure 1. **Panel B.**

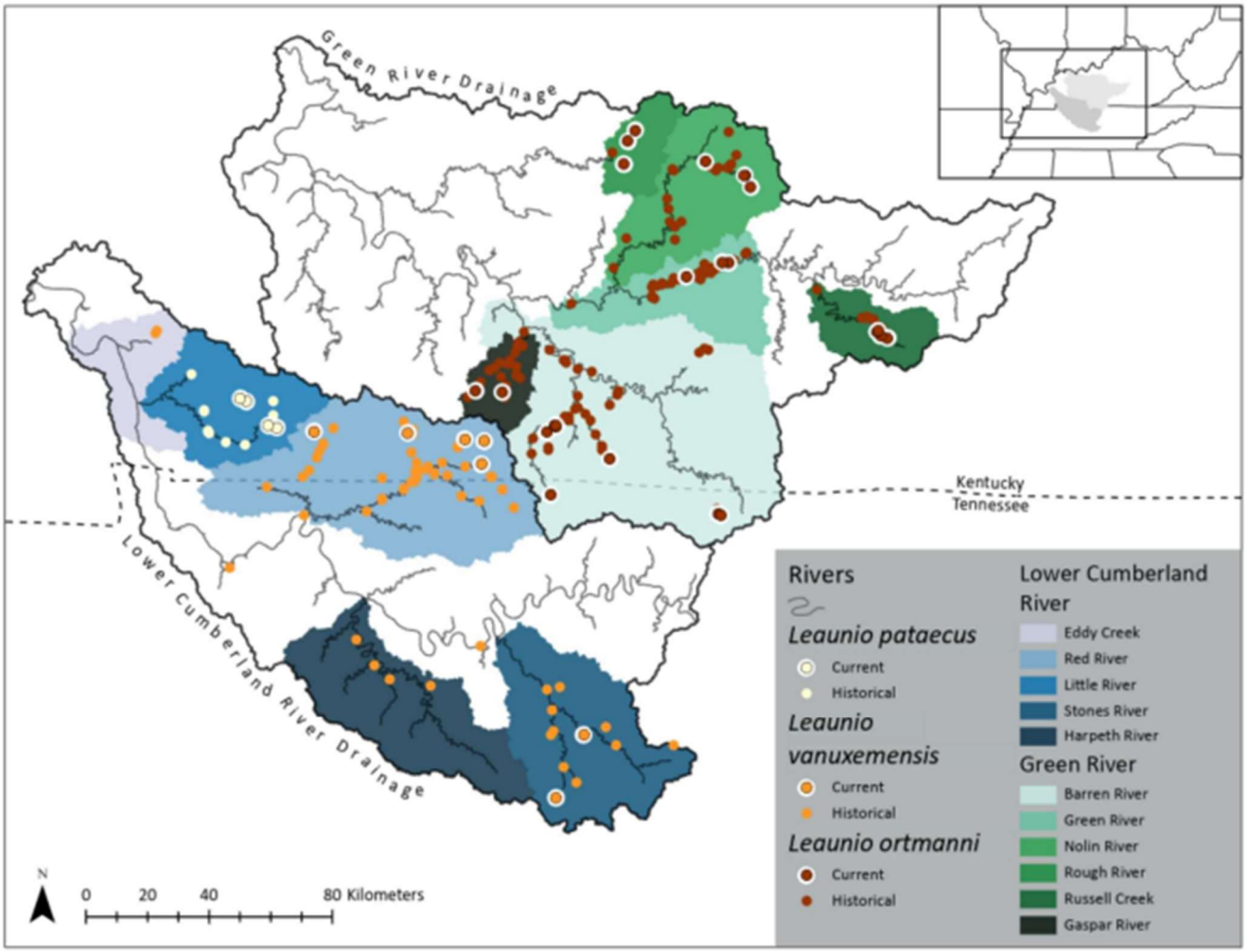

Figure 2. Photographs of *Leaunio vanuxemensis* collected from the Cumberland River drainage from 2018-2022 outlined in blue. *Leaunio pataecus* collected from the Cumberland River drainage in 2022 outlined in blue. *Leaunio ortmanni* collected from the Green River drainage from 2018-2021 outlined in Green showing morphological variation of the study species. Row A, Columns 1 and 2 indicate outershell periostricum and innershell nacre for one individual, columns 3 and 4 indicate periostracum and nacre for the next individual.

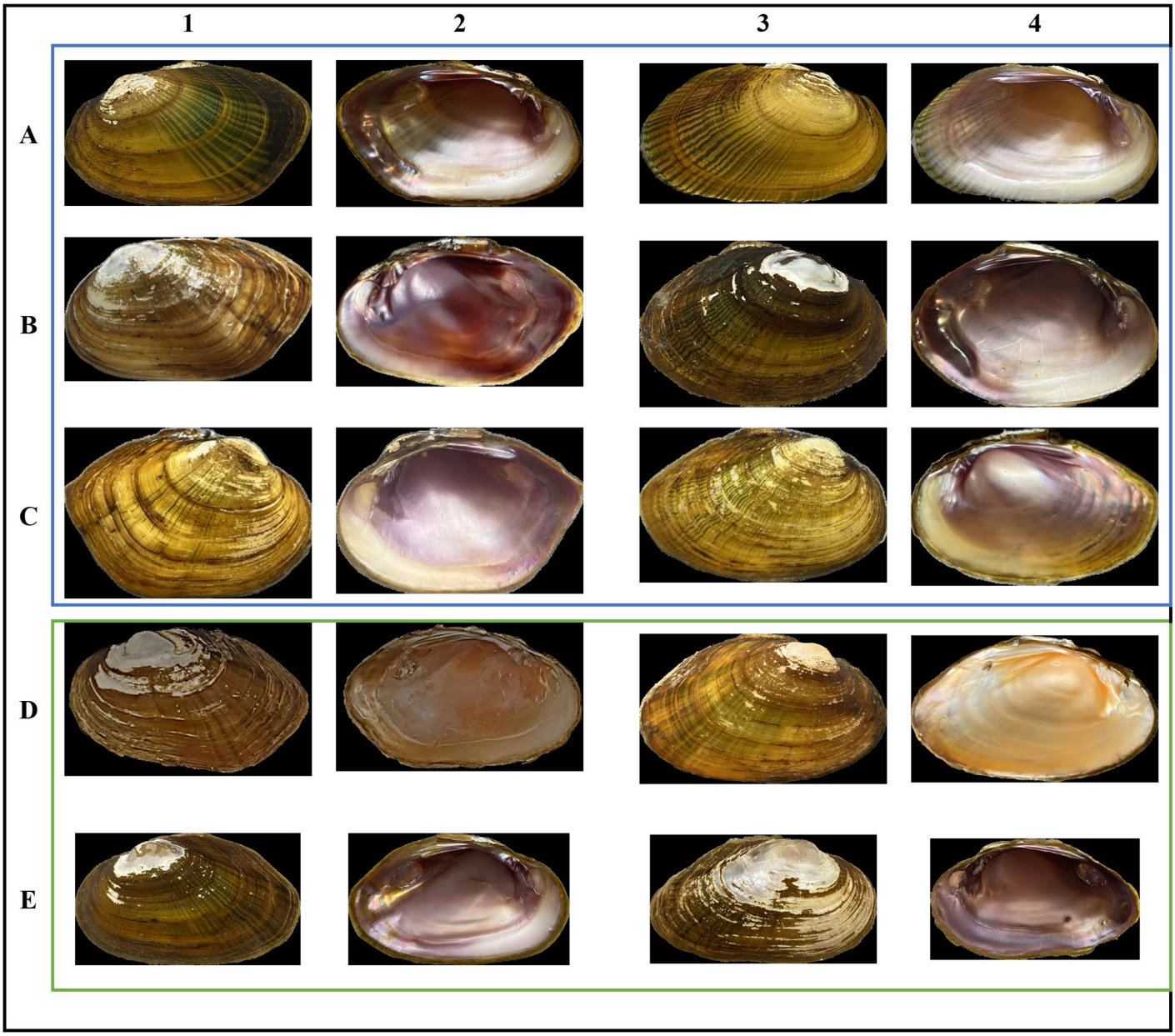

Figure 3. Morphological categorical characteristics. Shell shape categorized as elliptical or subovate, ray pattern categorized as interrupted or uninterrupted, and ray width categorized as fine, wide, or mixed.

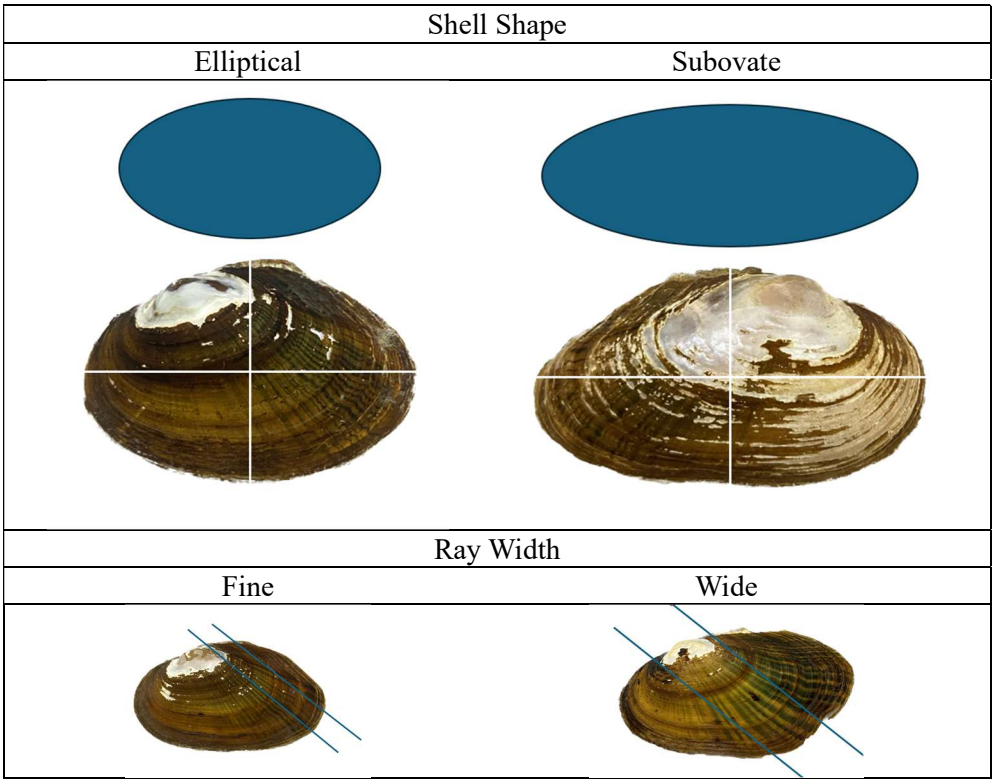

Figure 4. Morphological categorical characteristics. Periostracum color categorized as brown or yellow and nacre color categorized as white, purple, or salmon.

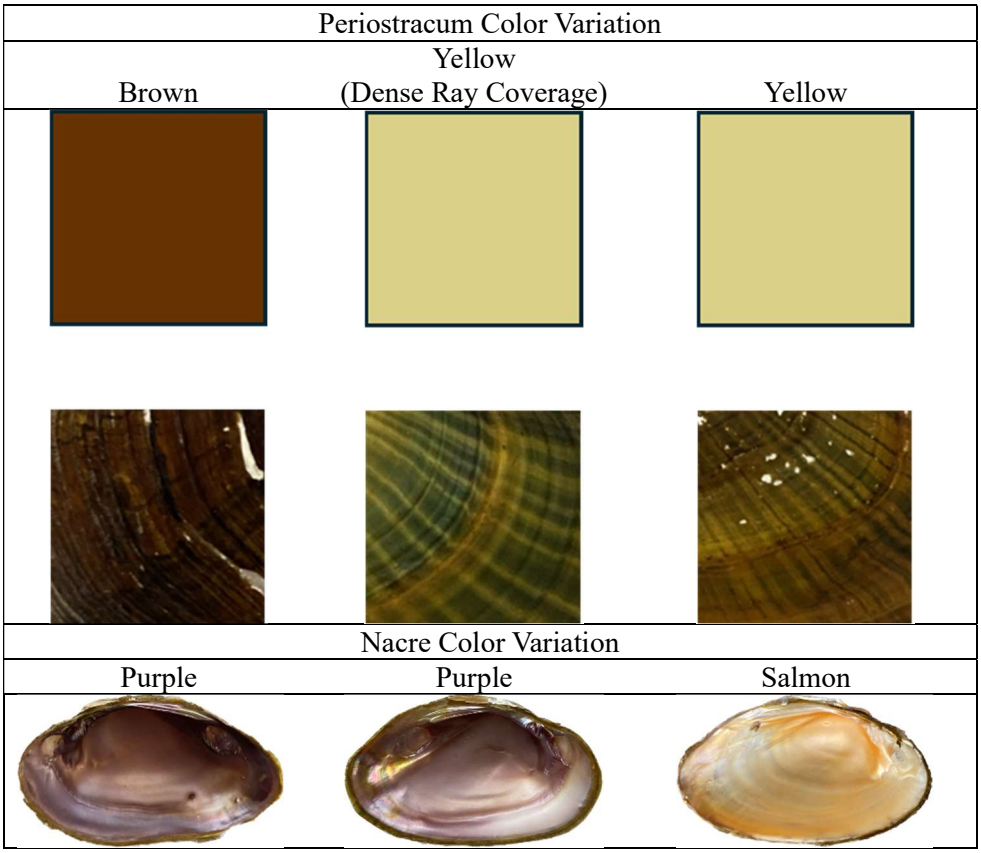

Figure 5. Photographs of mantle-lure display for *L. ortmanni* in the Rough River (Panel A) and Walters Creek (Panel B) of the Green River drainage, *L. vanuxemensis* in Sulphur Spring (Panel C) and the West Fork Stones River (Panel D) of the Cumberland River drainage, and *L. vanuxemensis* in the North Fork Holston River of the UTRB (Panel E and F).

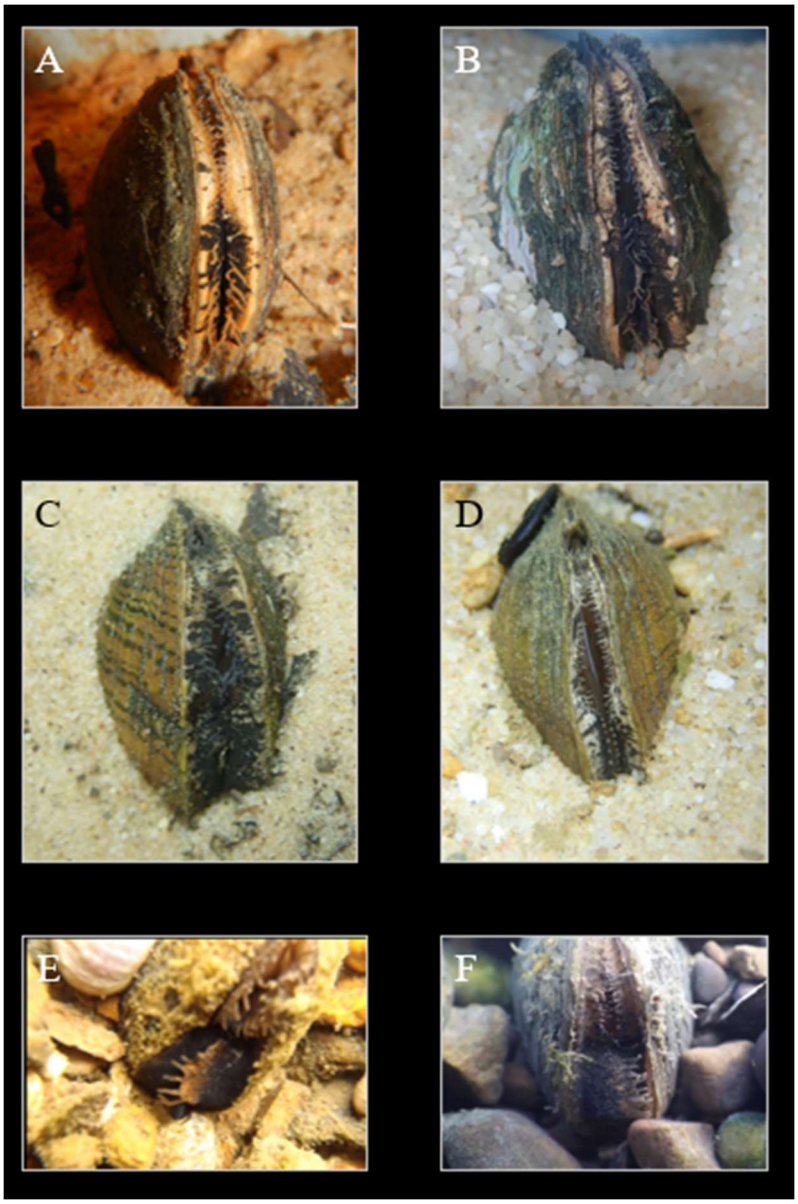

Figure 6. Landmarks used for the geometric morphometric analysis. Two main landmarks were aligned to the anterior part of the umbo (Point 1) and 180 degrees to the longest, posterior of the shell (Point 5). A total of 15 landmarks separated by 15 degrees were used for obtaining shell measurement data.

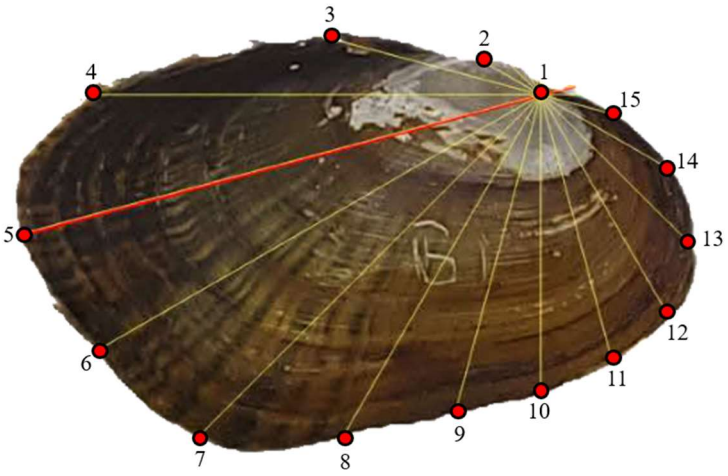

Figure 7. The morphology of freshwater mussel showing Max Length, Max hinge height, Max umbo height, and Hinge length used for decision-tree and forest-tree analyses are illustrated. A. Interior of right valve. B. Exterior of left valve.

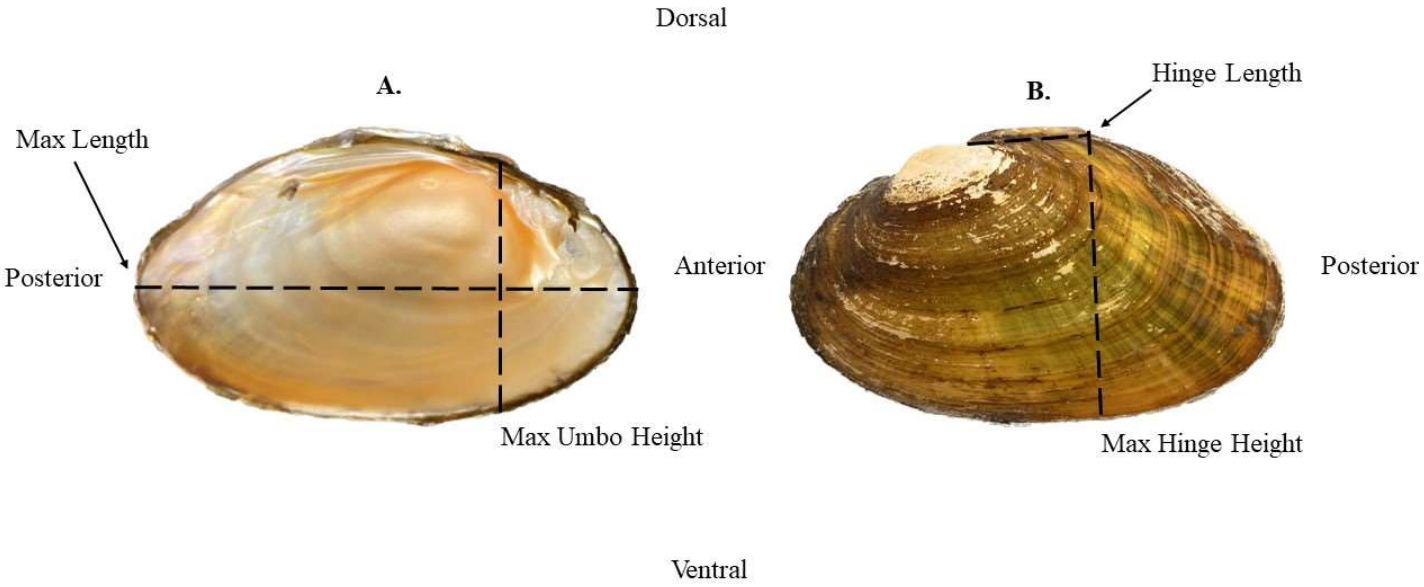

Figure 8. Morphological categorical characteristics showing shell shape as elliptical or subovate, ray pattern categorized as interrupted or uninterrupted, and ray width categorized as fine, wide, or mixed.

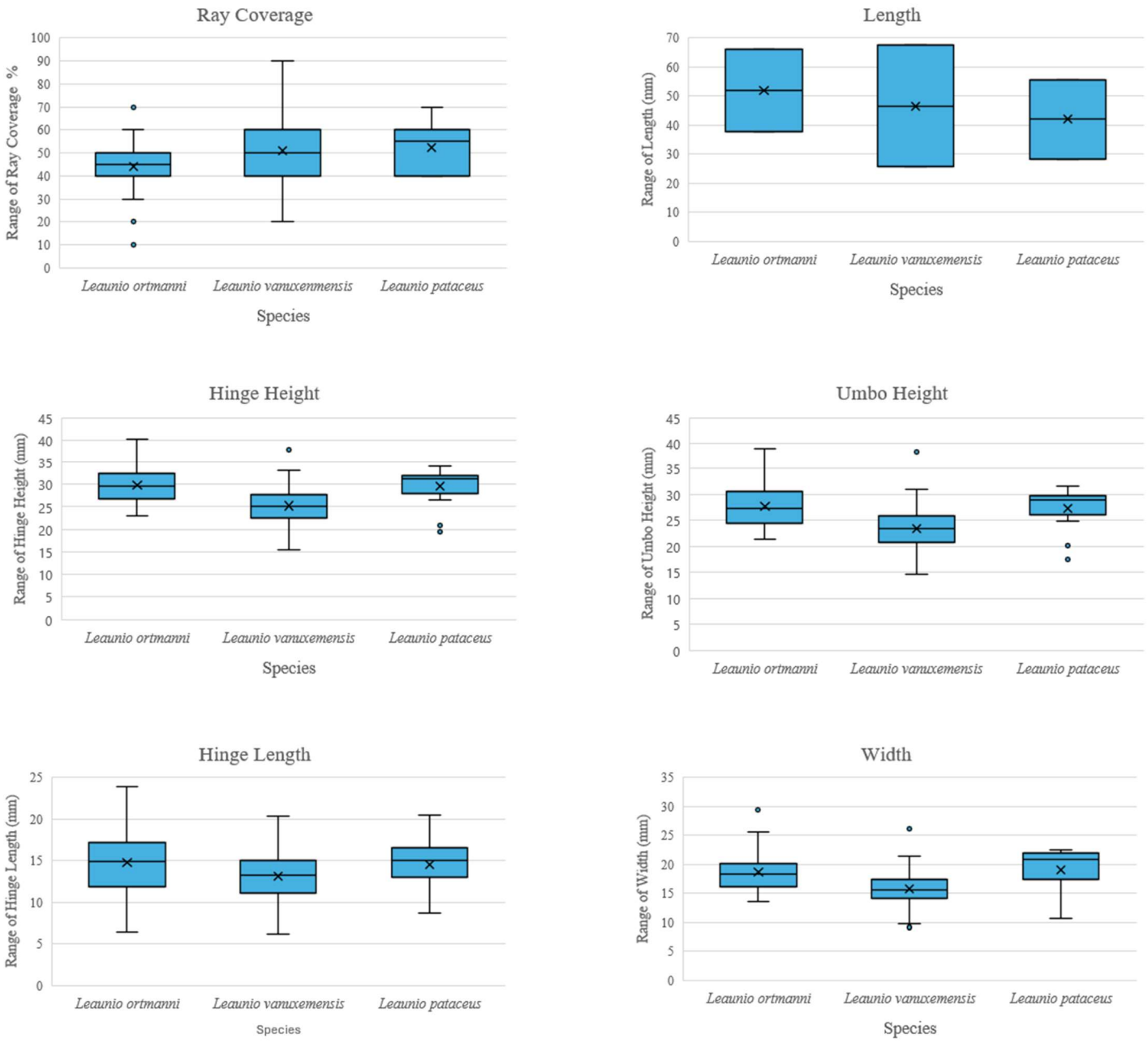

Figure 9. Morphological categorical characteristics showing periostracum color as brown or yellow and nacre color categorized as white, purple, or salmon.

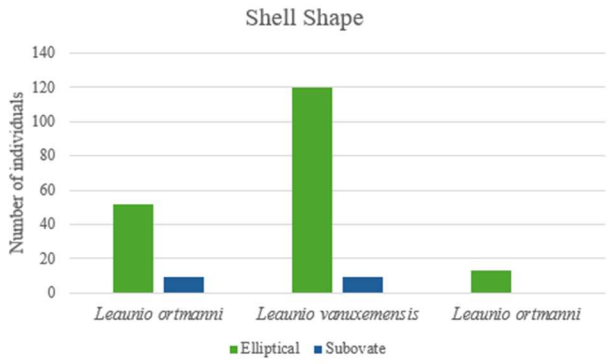

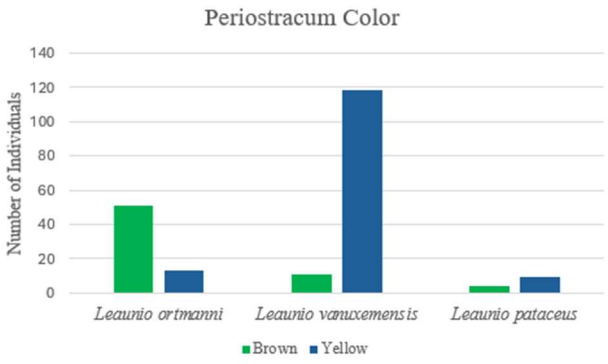

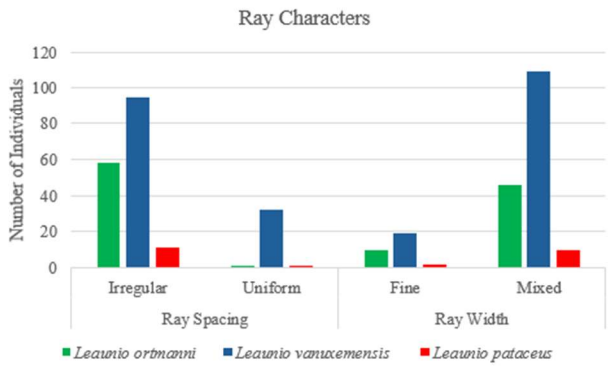

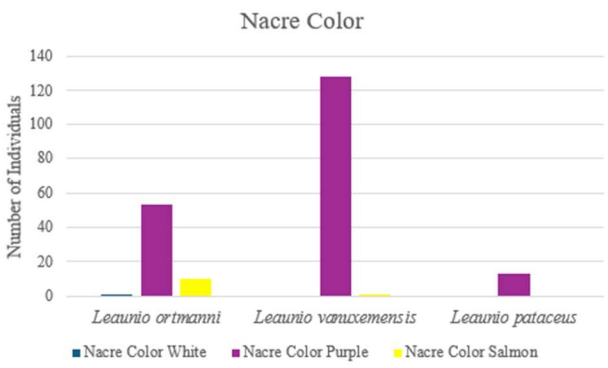

Figure 10. Haplotype network based on *ND1* mitochondrial DNA sequences of *Leaunio ortmanni* from the Green River drainage in bright green, *Leaunio vanuxemensis* from the Cumberland River drainage in pink, *Cambarunio taeniatus* from the Green River drainage in dark green, *L. vanuxemensis* indicated in orange and *Cambarunio iris* indicated in blue from the Upper Tennessee River Basin collected from 2018 to 2020.

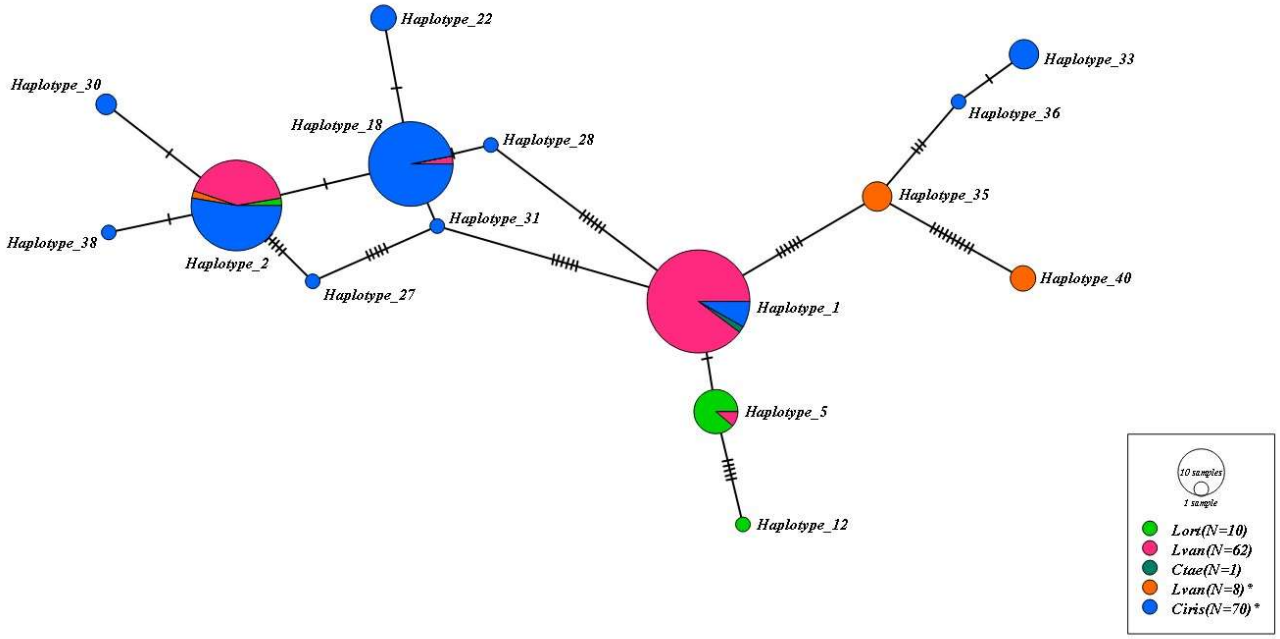

Figure 11. Mitochondrial DNA, *ND1* sequence, phylogenetic tree constructed using Bayesian inference. A general time reversible model (Nei and Kumar 2000) with gamma-distributed rate variation including 3,000,000 generations with 4 chains, and a 20,000 burn-in. Individuals are specified by haplotype. *Leaunio ortmanni*, *Leaunio vanuxemensis, Cambarunio taeniatus,* and *Cambarunio iris* were collected from the Green River drainage, Cumberland River drainage, and Upper Tennessee River Basin from 2018 to 2020. Individuals from the Upper Tennessee River Basin are indicated in red, from the Green River drainage in Green, and Cumberland River drainage in Yellow.

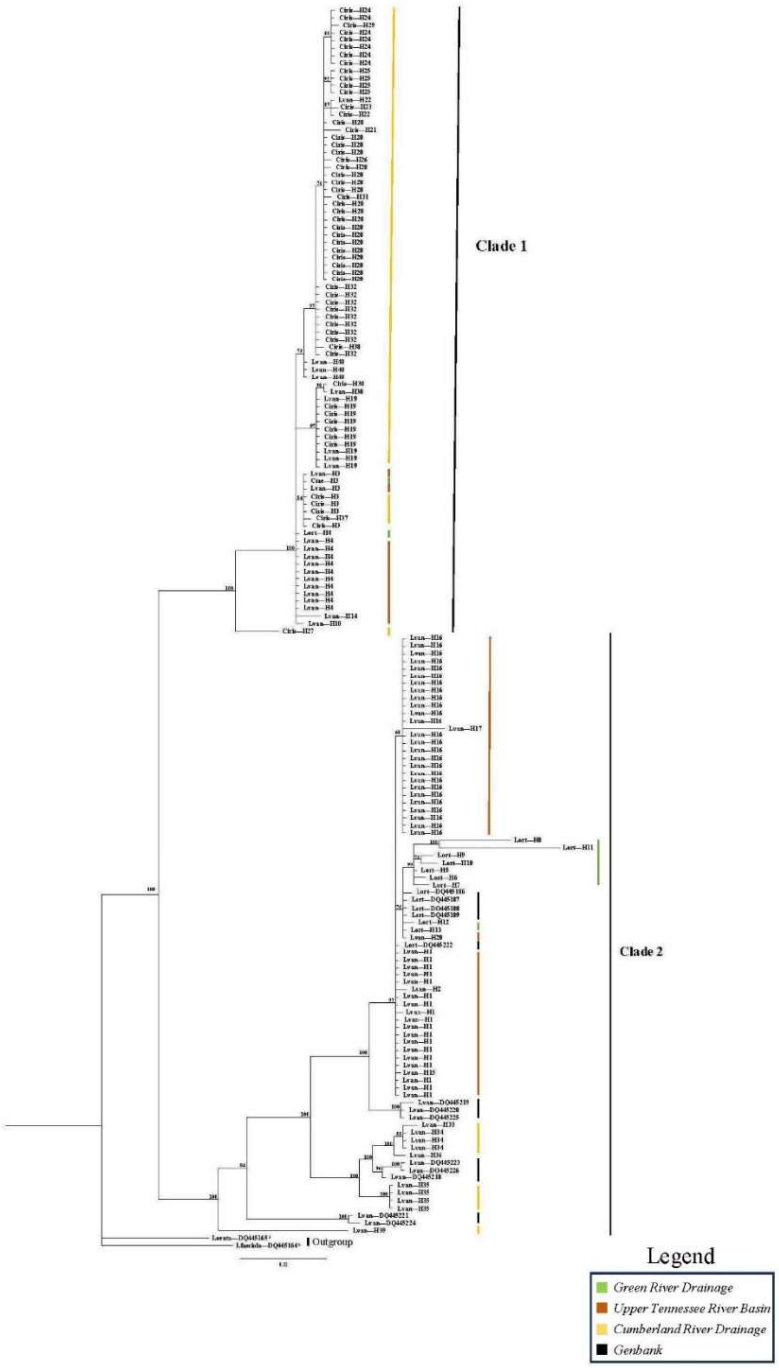

Figure 12. Neighbor-joining (NJ) tree showing relationship between investigated populations of *Leaunio ortmanni* in the Green River drainage collected from 2020 to 2022 and *Leaunio vanuxemensis* from the Cumberland River drainage from 2020 to 2022. The tree was constructed from DNA microsatellite allele frequency data (markers *Eoo_8, Eoo_10, Eoo_22, Eoo_46, Ecap_8, Ecap_7, Ecap_4*, and *LAB_206* from Eackles & King (2002), Jones et al. (2004), and Ortiz et al. (2022)) using Nei's standard genetic distance (D_{ST}).

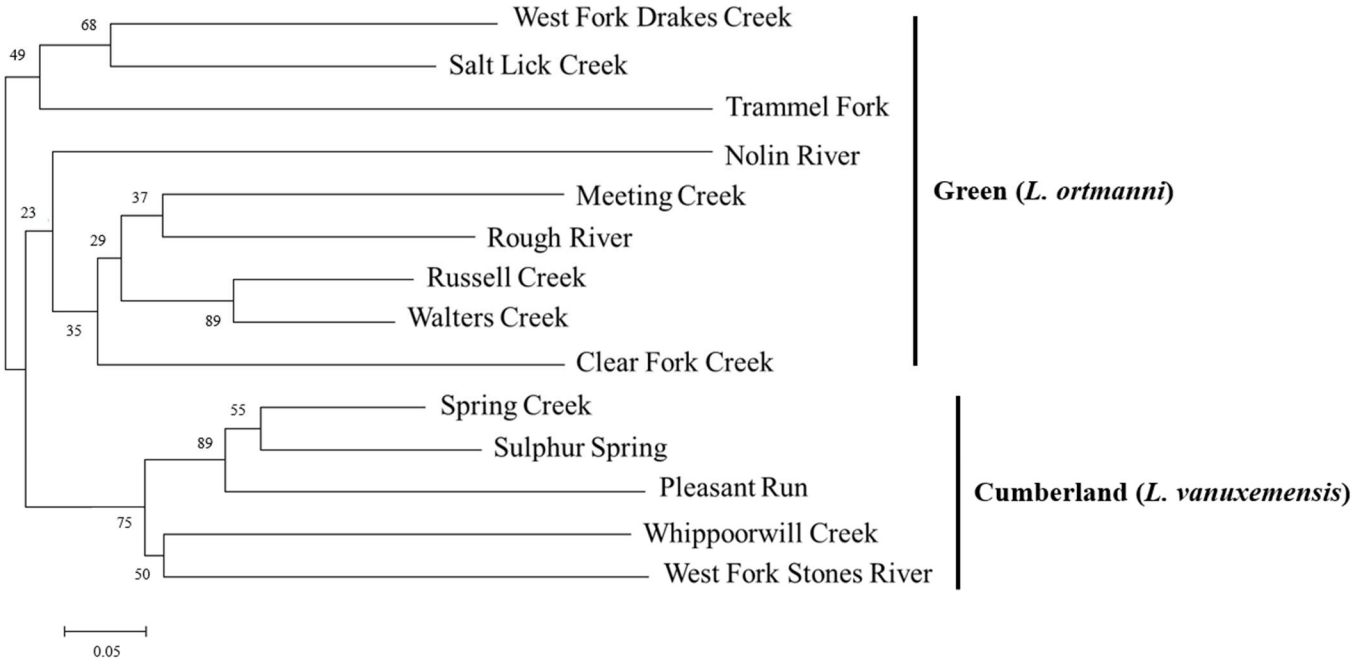

Figure 13. STRUCURE output showing geographic populations along the *x*-axis and population ancestry, i.e., assignment probability to populations on the *y*-axis. STRUCTURE version 2.3.4, using the largest delta *K* value, supports a two population (*K*=2) distinction between drainages. Populations are Meeting Creek (MC), Rough River (RR), Nolin River (NR), Walters Creek (WC), Green River (GR), Russell Creek (RC), West Fork Drakes Creek (WFD), Trammel Fork (TF), Salt Lick Creek (SLC), Clear Fork Creek (CFC) collected from 2018 to 2022 in the Green River drainage indicated in green; Spring Creek (SC), Pleasant Run (PR), Sulphur Spring Creek (SULP), Whippoorwill Creek (WHIP), West Fork Stones River (WFS) collected from 2018 to 2021 in the Cumberland River drainage indicated in red; *Leaunio pataecus* from Sinking Fork (SF) in the Cumberland River drainage collected in 2022 indicated in red; and *L. vanuxemensis* from Locust Cove Creek (LCC) from the Upper Tennessee River drainage collected in 2020 indicated in red. *Indicates species *C. taeniatus*.

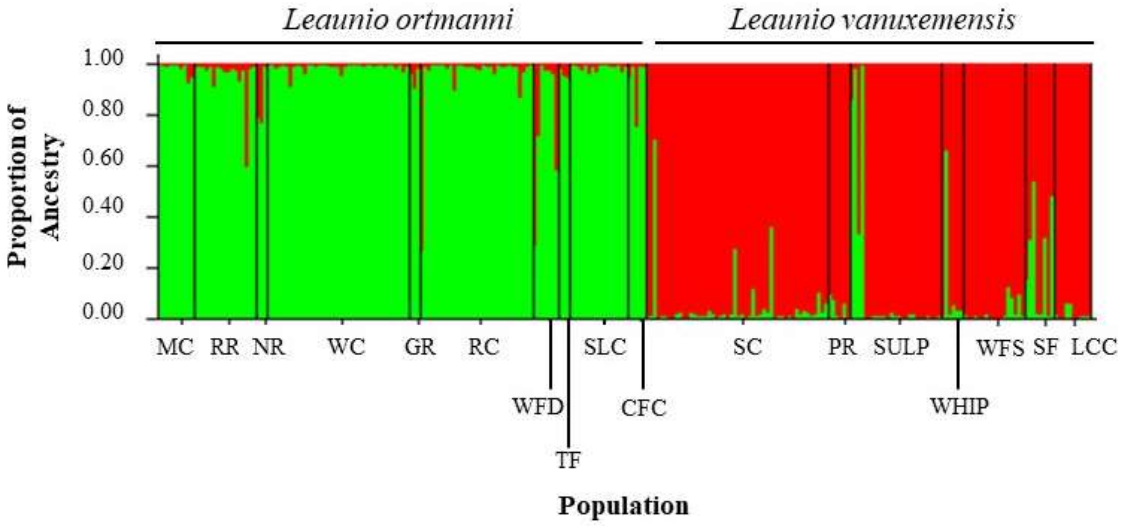

Figure 14. Canonical Variate Analysis and shell landmark variation used to assess differences among species at three size classes (A) Green and Cumberland River drainage specimens regardless of size class, (Panel B) small (<40mm), (Panel C) medium sized mussel specimens (40.1>50 mm), (Panel D) large sized mussel specimens (≥50.1mm), (Panel E) all specimens regardless of size class and drainage, of *L. ortmanni* of the Green River drainage, *L. vanuxemensis* of the Cumberland River drainage and *L. vanuxemensis* of the Powell and Holston River Drainages. This analysis compares individuals of each species, drainage, and respective size classes.

Panel A.

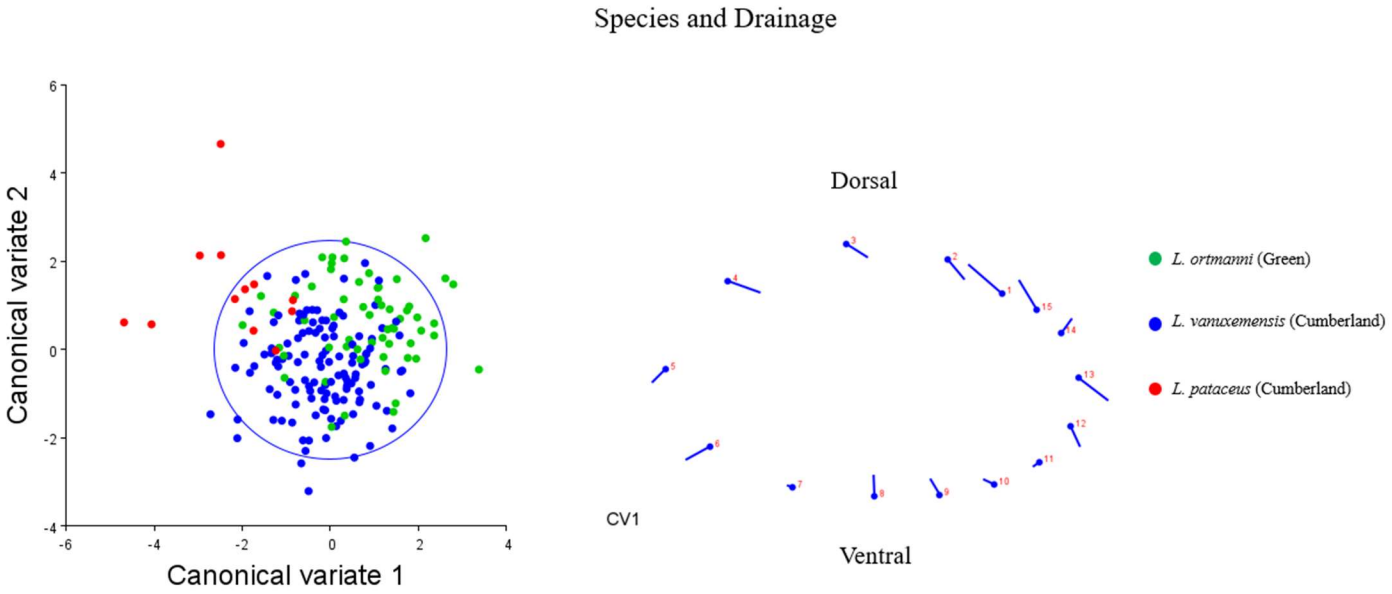

Figure 14. Panel B.

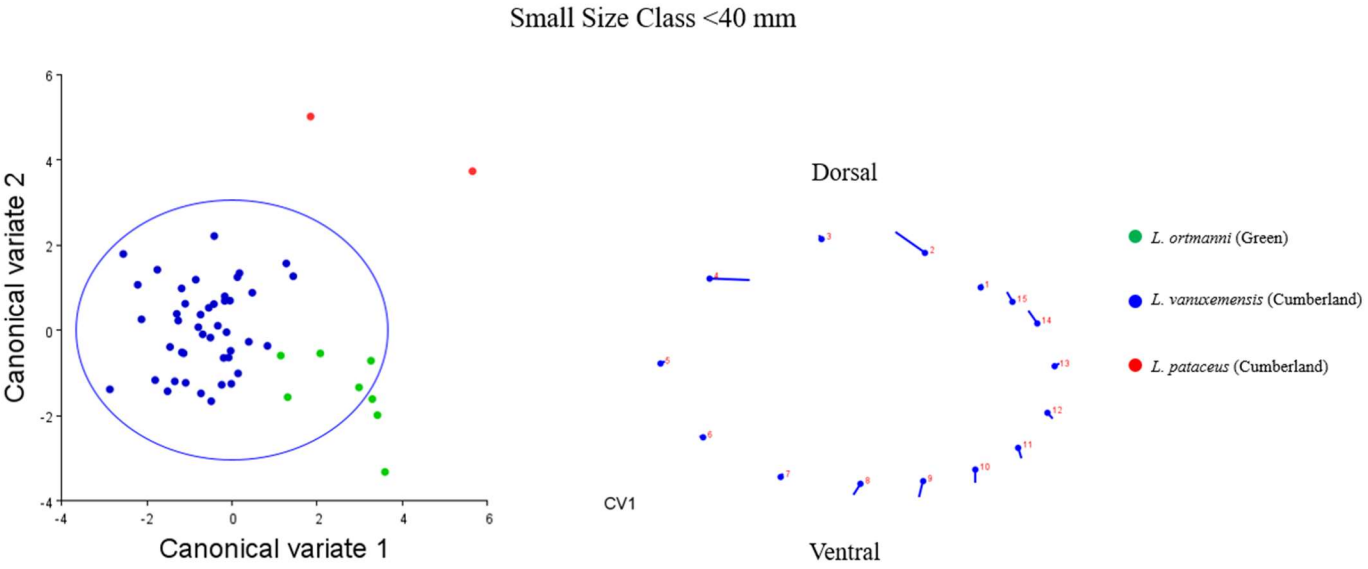

Figure 14. Panel C.

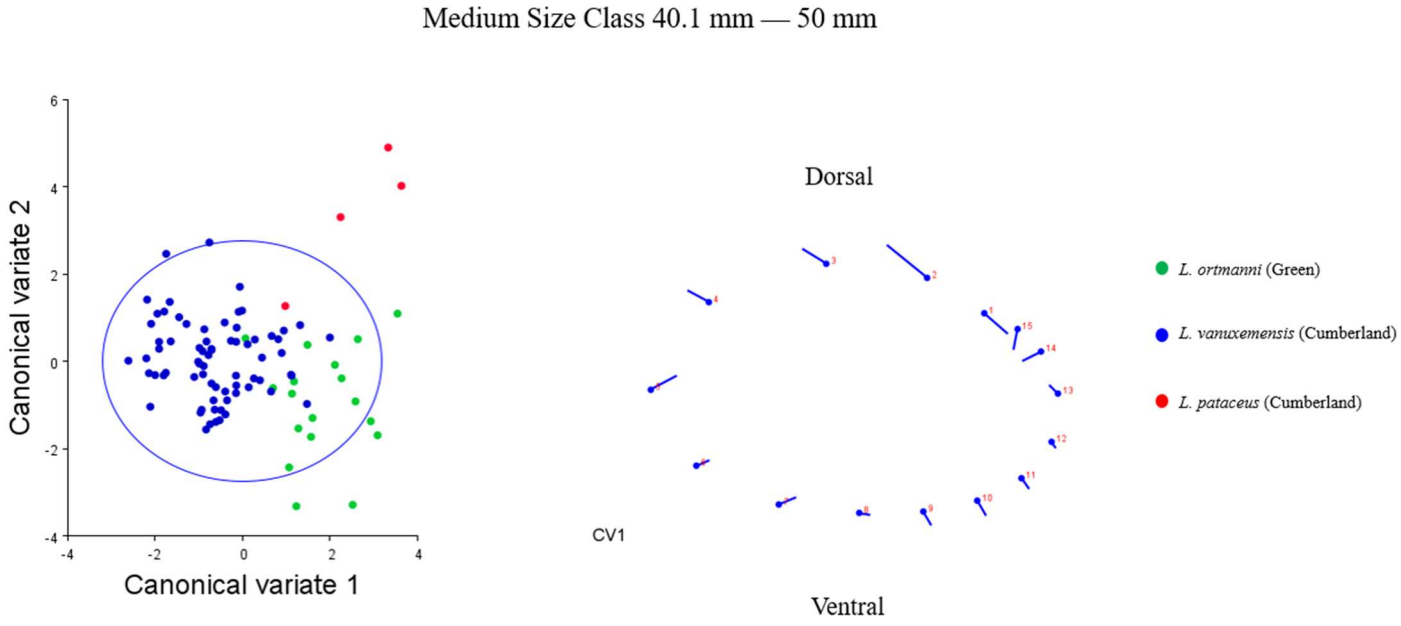

Figure 14. Panel D.

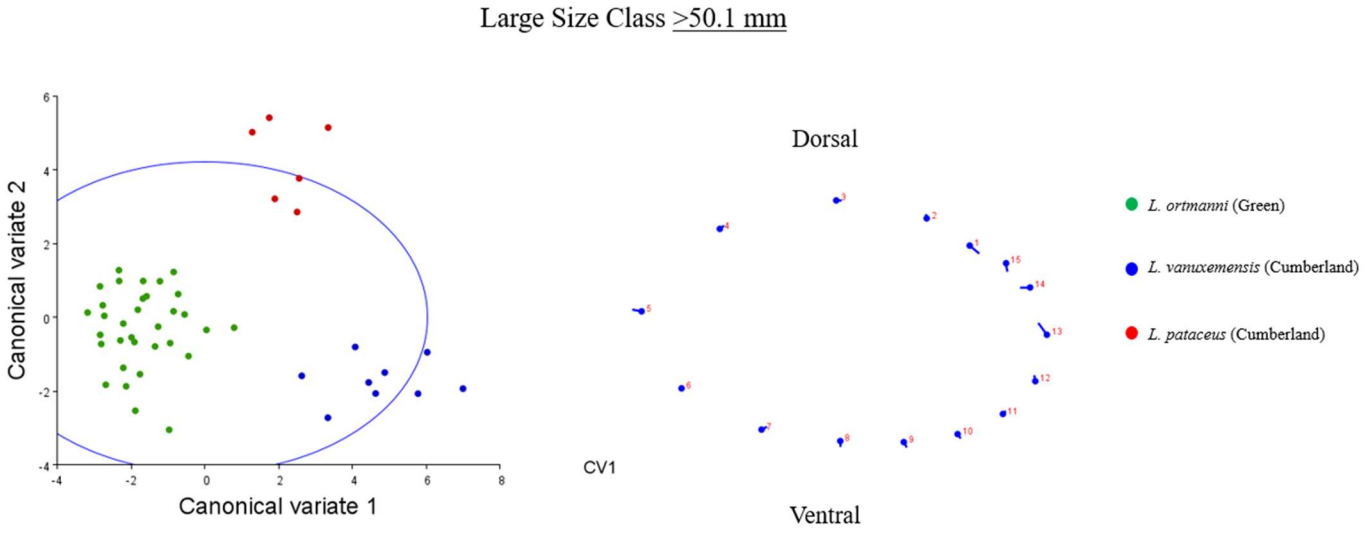

Figure 14. Panel E.

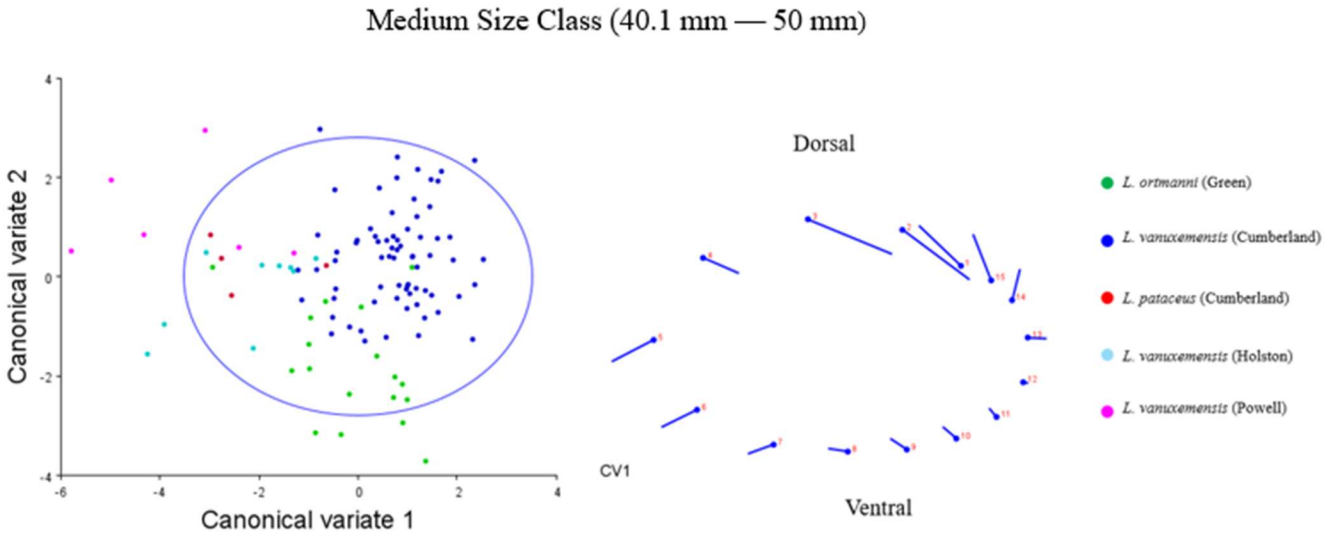

Figure 15. Panel A. Key identifying morphological variables of *L. ortmanni* of the Green River drainage, *L. vanuxemensis* of the Cumberland River drainage, and *L. vanuxemensis* (of the Holston and Powell River Drainages) determined by a mean decrease in identification accuracy and the mean decrease in Gini coefficient including anterior nacre color (Panel A), identification accuracy and the mean decrease in Gini coefficient excluding anterior nacre color (Panel B), which measures the probability of misclassification using random forest analysis.

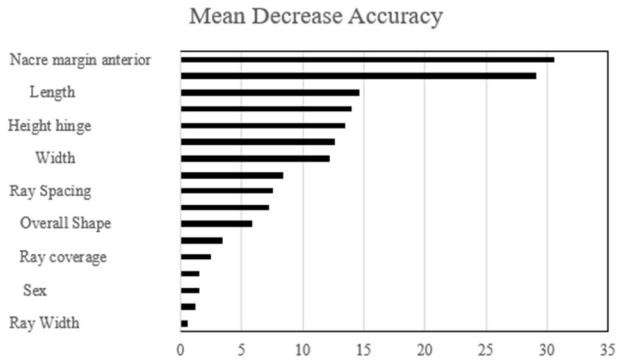

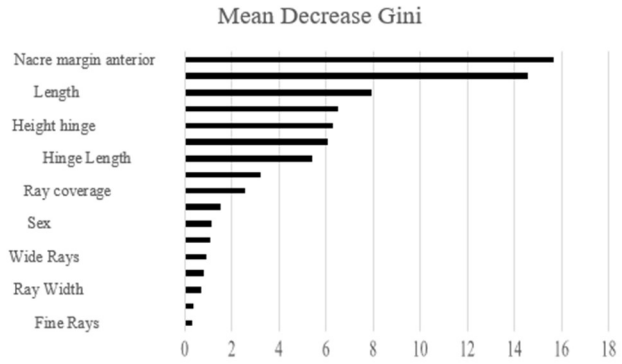

Figure 15. Panel B.

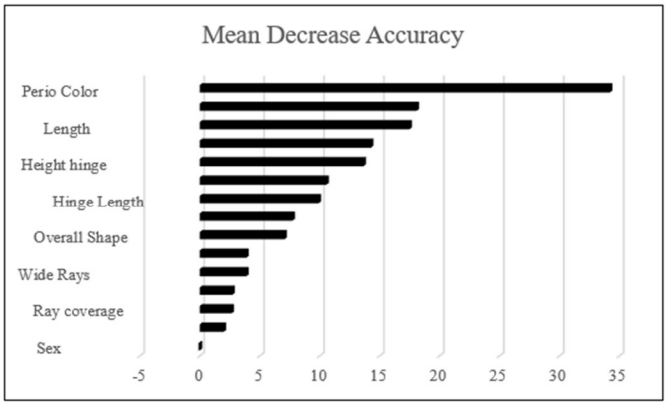

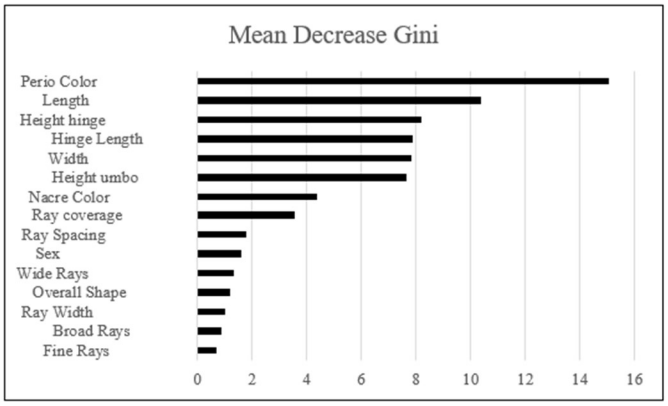

Figure 16. Panel A. Decision tree analysis using internal and external shell variables identifying *L. ortmanni* of the Green River drainage, *L. vanuxemensis* of the Cumberland River drainage, and *L. vanuxemensis* (of the Holston and Powell River Drainages) including anterior nacre color (Panel A), excluding anterior nacre color (Panel B). Tree was constructed using 80% of the data as training data and 20% as validation data.

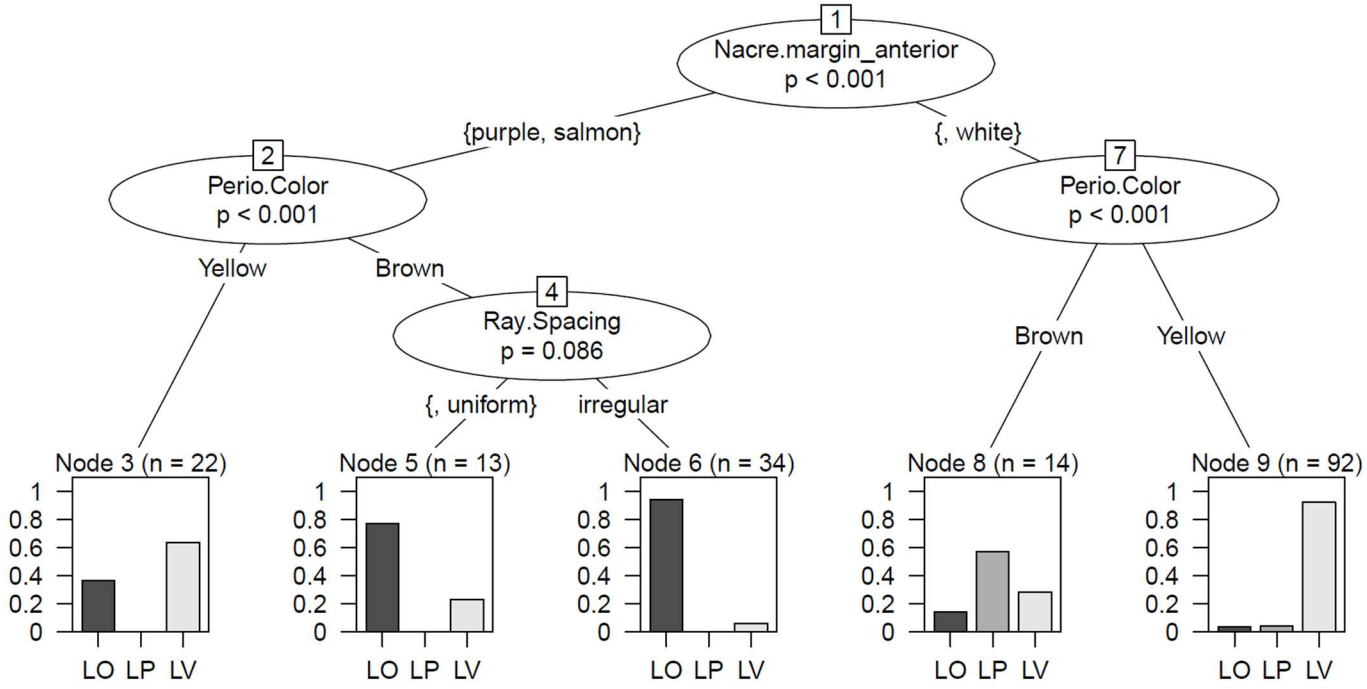

Figure 16. Panel B.

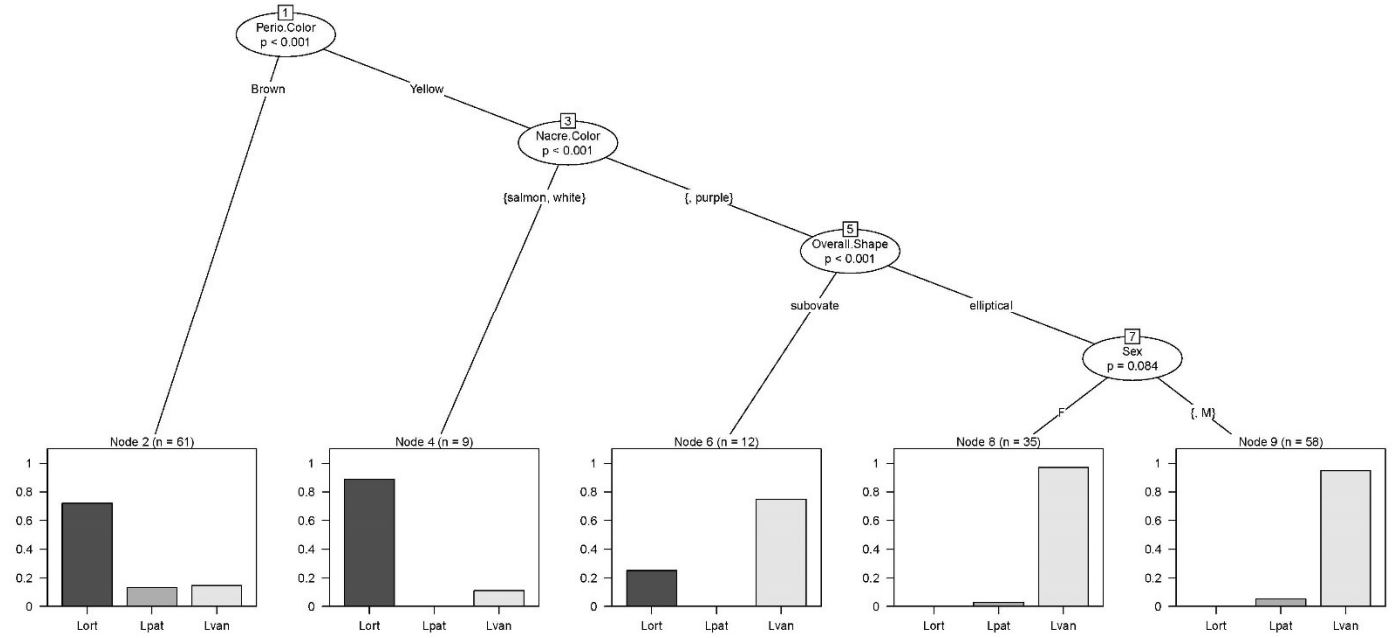

Appendix. Location information for observed haplotypes for each species in the study.

Collection Location						Collected Individuals by Species with Haplotype				Genbank	
Location	Latitude	Longitude	Drainage	County	State	*Leaunio ortmanni*	*Leaunio vanuxemensis*	*Cambarunio taeniatus*	*Cambarunio iris*	*Leaunio ortmanni*	*Leaunio vanuxemensis*
Meeting Creek	37.57589	-86.21584	Green	Hardin	KY	H5, H6					
Nolin River	37.58384	-85.91549	Green	Larue	KY	H8, H9.H10					
West Fork Drakes Creek	36.81139	-86.46045	Green	Simpson	KY	H4		H3			
Salt Lick Creek	36.55167	-85.85698	Green	Macon	TN	H13					
Rough River	37.64184	-86.19804	Green	Hardin	KY	H7					
Russell Creek	37.08715	-85.25097	Green	Adair	KY	H11					
Wiggington Creek	36.91036	-86.75076	Green	Logan	KY	H12				DQ445187	
Spring Creek	36.7619	-86.72829	Cumberland	Simpson	KY		H1, H3, H16, H17, H18				
Pleasant Run	36.7687	-86.78897	Cumberland	Logan	KY		H1, H2, H3				
Sulphur Spring	36.6957	-86.72829	Cumberland	Simpson	KY		H1, H4, H13, H14, H15				
Whippoorwill Creek	36.78515	-86.99621	Cumberland	Logan	KY		H1				
Rich Valley	36.9248886	-81.6260268	Holston	Smyth	VA		H35, H40		H20, H25, H32		
Locust Cove Creek	36.9459366	-81.5913793	Holston	Smyth	VA		H19, H30, H33, H34, H35, H36, H40				
Ceres	36.9562594	-81.4928233	Holston	Smyth	VA				H19, H20, H24, H25, H30, H31		
Saltville	36.8956034	-81.7462632	Holston	Smyth	VA				H3, H20, H22, H24, H32, H37, H38		

Beech Creek	36.4090334	-82.7646788	Holston	Greene	TN		H19, H22, H39		H19, H20, H21, H23,		
Chilhowie	36.807357	-81.67143	Holston	Smyth	VA				H20, H32		
Richlands	37.0940717	-81.8026221	Clinch	Tazewell	VA				H3, H20, H24		
Bennett Island	36.9597	-82.097206	Clinch	Russell	VA				H20, H24, H25		
Cavitts Creek	37.1458558	-81.5449801	Clinch	Tazewell	VA				H3, H19, H26, H27, H28		
Copper Creek	36.7286	-82.4684	Clinch	Scott	VA				H24, H29		
Brush Creek			Green	Warren	KY					DQ445189	
Dry Fork			Cumberland	Logan	KY					DQ445222	
Rock Bridge Branch			Cumberland	Christian	KY						DQ445219, DQ445220
Spring Creek			Hiwassee	Polk	TN						DQ445221
Little River			Tennessee	Blount	TN						DQ445226

CHAPTER 2

SEARCHING FOR RAINBOWS: A GENETIC AND MORPHOLOGICAL ASSESSMENT OF CRYPTIC BIODIVERSITY IN THE RAINBOW MUSSEL (*CAMBARUNIO IRIS*) SPECIES COMPLEX THROUGHOUT THE UPPER TENNESSEE, CUMBERLAND AND GREEN RIVER BASINS

ABSTRACT

The rainbow mussel (*Cambarunio iris*) is a common freshwater mussel species that occurs in streams of the Mississippi River drainage across the Midwest and Eastern United States. Within and among river drainages of the Upper Tennessee River Basin (UTRB), *C. iris* is morphologically highly variable, with shell forms that have periostracum color ranging from yellow to green, and shell shape ranging from elliptical to sub-ovate. Given the species' broad distribution, populations isolated in headwater streams, and known morphological variation, a population genetic study was needed to inform managers of potential cryptic species in the UTRB. We collected and assessed genetic and morphological data within and between sites in the UTRB, from the Clinch (N=46), Powell (N=35), and Holston River (N=21) drainages, and collected individuals of *C. iris* (N=6) and *C. taeniatus* (N=10) from the Green and Cumberland River drainages of Kentucky and Tennessee as closely related outgroup taxa for analysis. We used an 888 base-pair sequence of mitochondrial NADH dehydrogenase 1 (*ND1*), a suite of eight nuclear DNA microsatellite loci to assess patterns of genetic diversity and differentiation, and a suite of internal and external shell characters to quantitatively assess morphological differences among shell forms. Mitochondrial DNA sequences revealed high genetic diversity in the UTRB, with a total of 20 haplotypes with numerous polymorphic nucleotide sites. However, nuclear DNA microsatellites revealed low genetic diversity within populations, with observed heterozygosity (H_o) being lower than expected heterozygosity (H_e) for all populations. Genetic differentiation (quantified as F_{ST} and Jost's D) between populations ranged from very low, effectively 0, to high (F_{ST}=0.2 and Jost's D=0.9) within respective river basins. Morphological morphometrics demonstrated character overlap among species and drainages, especially when analyzed by size-classes and shell morphotypes. The results of this study did not show evidence of cryptic diversity or potential hybridization, of *C. iris* in the UTRB but did support a previous hypothesis that populations of *C. iris* in the Green and Cumberland rivers may represent cryptic species.

INTRODUCTION

The Rainbow mussel (*Cambarunio iris*) is one of the few remaining mussel species in the upper Tennessee River Basin (UTRB) that is widely distributed and abundant. *Cambarunio iris* is one of more than 50 mussel species that exists in the Clinch River system and throughout the UTRB (Figure 1, Panel A), which holds the most mussel diversity of any river system in Virginia (Jones 2015). This species typically inhabits streams along edges of *Justicia* beds, in gravel or sand, and in small-to-medium-sized rivers (Parmalee and Bogan 1998; COSEWIC 2006). Due to its non-imperiled conservation status, *C. iris* has not been a high priority for population genetic studies. However, the species has been regularly propagated for restoration and research purposes with little to no genetic information. Populations of *C. iris* and the species as whole are considered secure throughout most of its distribution in the United States, which currently and historically includes eastern Canada, New York, Michigan, Wisconsin, Illinois, Indiana, Ohio, Pennsylvania, West Virginia, Virginia, Missouri, Oklahoma, Arkansas, Kentucky, Tennessee, Virginia, North Carolina, and Alabama (Mathiak 1979; Cummings and Mayer 1997; Parmalee and Bogan 1998; Marangelo and Strayer 2000; Szafoni et al. 2000; Bogan 2002; Schanzle et al. 2004; COSEWIC 2006; Fisher 2006; Spooner and Vaughn 2007; Chapman and Smith 2008). Such a wide distribution suggests the possibility of cryptic lineages occurring in areas with varied geographic and ecological conditions.

Despite the species broad range, there are instances where habitat loss and degradation may be contributing to the loss of genetic diversity within *C. iris*, a common concern among biologists managing for a species' long-term viability and evolutionary potential (Williams et al. 1993; COSEWIC 2006). Furthermore, this species is regularly propagated for research and conservation purposes and several studies have expressed the importance of understanding population genetics and phylogeography of common, co–occurring, and similarly dispersed species (Elderkin et. al 2008; Olson and Vaughn 2020). These studies have found geographical structuring utilizing mitochondrial DNA (mtDNA) and nuclear DNA (nDNA), and determined that there are different conservation needs at a population scale Therefore, it is appropriate that management decisions are based on studies utilizing large sample sizes over a wide geographic area and using a combination of different genetic markers, morphological traits, and data analyses to determine if populations warrant similar or different management strategies.

Kuehnl (2009) found unique phylogenetic partitioning within *C. iris* using mitochondrial DNA sequences and suggested the possibility of cryptic species diversity throughout its eastern range, but sample sizes from the UTRB in the Clinch, Powell, and Holston rivers generally were small, as well as in the Green and Cumberland rivers. To this point, using limited genetic and morphological data, Watters (2018) described populations previously understood to be *C. iris* occurring in Missouri as *C. hesperus* and populations occurring in the Green, Cumberland, and Duck rivers as *C. dactylus*.

Freshwater mussels are primarily identified by external morphological characters of the shell, which can be problematic for a species such as *C. iris* that is wide-ranging and has high phenotypic variation throughout its range (Inoue et al. 2013). Shea et al. (2011) list possible reasons for misidentification to include: the wide and overlapping distributions of similar-looking species, subtle morphological characters based on locality, and even the species' rarity and protected conservation status causing misidentification. Additionally, Shea et al. (2011) found that federally listed species on average were 3.4 times less likely to be falsely identified than non-listed species. All of these reasons could contribute to the misidentification of *C. iris*, as individuals can vary within and between river systems. Over time, field observations of *C. iris* have documented subtle to obvious differences in shell color, ray patterns, and shell shape among river systems in the same basin. The high shell variation between individuals of *C. iris* from the UTRB can be seen in Figures 2 and 3, and differences in the color and pigmentation patterns of the mantle lure in different drainages in Figure 4. Watters (2018) described three shell morphotypes in the UTRB as follows: (1) Form 1 that is large, elongate, dark green or tan, with narrow green rays, (2) Form 2 that is smaller, compressed, less elongate, and yellow with pencil-thin interrupted green lines, and (3) Form 3 that is elongate, with bright, polished yellow shell with bold, dark green rays (Figure 3). These three shell morphotypes have been a source of taxonomic confusion for biologists and at times, some have even considered that they may represent different species. Thus, detailed genetic and morphological analyses are critical for understanding the potential genetic uniqueness of geographically isolated populations so that managers can improve species conservation strategies (Geist and Kuehn 2005). The purpose of this study was to use a combination of maternally inherited, non-recombining mtDNA, along with biparentally inherited recombining nDNA microsatellite markers and morphological characters to assess the genetic and morphological diversity and differentiation of *C. iris* populations in the UTRB, Green and

Cumberland river drainages. While our focus was to assess genetic and morphological diversity of *C. iris* in the UTRB, in addition, we used the three morphotypes outlined by Watters (2018) to test whether these morphotypes represented morphologically distinct lineages. In consideration that *C. iris* from the Green and Cumberland River drainages were used for this study, we chose to include *C. taeniatus* from the Green and Cumberland River drainages due to the overlapping historical distribution and similar morphological traits as *C. iris* in the UTRB. in addition, we included sequences of *C. taeniatus* from Kuehnl (2009), to compare to sequences of *C. iris*.

METHODS

Individuals of *Cambarunio iris*, *C. taeniatus*, and *Leaunio vanuxemensis* were collected from locations in the UTRB, Green River, and Cumberland River drainages from 2018 to 2022. A total of 17 locations were sampled for *C. iris*, 15 in the UTRB and two locations from the Green River drainage; for *C. taeniatus,* 2 localities in the Green River drainage and 5 localities in the Cumberland River drainage; and for *L. vanuxemensis* 7 localities in the UTRB (Table 1). Genetic samples were taken via mantle tissue clip or buccal swabs (DDK-50, Isohelix, Cell Projects, UK). Mantle tissue clips were preserved in 100% ethanol and stored at -20˚ C prior to extraction. Individuals then were preserved in specimen jars containing 100% ethanol and stored at -20˚ C prior to morphological analysis. Samples from the UTRB are now archived at Virginia Polytechnic Institute and State University and samples from the Green and Cumberland River drainages are archived at Eastern Kentucky University. The DNA from mantle tissue samples was isolated and extracted using a DNeasy Blood and Tissue Kit (Qiagen, Germantown, MD). The concentration and purity of each sample was assessed using a μLite PC spectrophotometer (Biodrop, Cambridge, UK) prior to amplification via polymerase chain reaction.

Mitochondrial DNA

Mitochondrial DNA (mtDNA) sequences were amplified using primers for the first subunit of NADH dehydrogenase (*ND1*). Primer sequences for *ND1* were: forward: 5’-TGGCAGAAAAGTGCATCAGATTAAAGC-3’; and reverse: 5’-CCTGCTTGGAAGGCAAGTGTACT-3’ (Serb et al. 2003). Polymerase chain reaction conditions consisted of H_2O, 5x PCR buffer (Promega, Madison, WI), 2.5 mM $MgCl_2$ (Promega), 2.5 mM dNTPs (Thermofisher Scientific, Waltham, MA), 1 mg/ml BSA (ThermoFisher Scientific), 5 uM

of each primer, 0.1 µl Go *Taq* polymerase (New England Biolabs, Ipswich, MA), and 1 µl of genomic DNA at 50 ng/µl, for a total reaction volume of 22 µl. Polymerase cycling conditions were modified from those of Serb et al. (2003) and were as follow: 94℃ for 3 minutes; followed by 35 cycles of 94℃ for 40 sec, 59℃ for 40 sec, and 72℃ for 1 min; followed by a final extension at 72℃ for 5 minutes; and a hold at 4℃. Polymerase chain reaction products were processed and sequenced by the Virginia Biocomplexity Institute (Blacksburg, VA).

DNA sequences were aligned and edited using Geneious Prime 2022 (Biomatters, Inc., San Diego, CA). Intraspecific mtDNA genetic diversity indices were calculated by population and subbasin; these indices included haplotype diversity (*h*), number of polymorphic segregating sites (*s*), mean number of nucleotide differences among sequences (*k*), and nucleotide diversity (π) and were calculated using DNAsp 6.12.03X64 (Rozas et al. 2017).

A phylogenetic tree was reconstructed using Bayesian inference in the program MrBayes (Huelsenbeck and Ronquist 2001; Ronquist et Al. 2012, version 3.2.6). We used two datasets for reconstructed phylogenetic trees, one with *C. iris* from this study, and a second that included sequences downloaded from Genbank of *C. iris* throughout its historical range. A general time reversible model (Nei and Kumar 2000) with gamma-distributed rate variation included 3,000,000 generations with 4 chains, and a 20,000 generation burnin. Every 100^{th}-generation tree was saved. Popart (Leigh and Bryant 2015) was used to visualize a haplotype network for the analyzed sequences.

Nuclear DNA Microsatellites

The nDNA microsatellite loci and primers were selected from previously developed microsatellite libraries (Eackles and King 2002; Jones et al. 2004; Ortiz et al. 2022) (Table 2). These primers were screened for polymorphism, repeat motif, and utility for use in subsequent multiplexing. Polymerase chain reaction conditions consisted of H_2O, 5x PCR buffer (Promega, Madison, WI), 2.5 mM $MgCl_2$ (Promega), 2.5 mM dNTPs (Thermofisher Scientific, Waltham, MA), 1 mg/ml BSA (ThermoFisher Scientific), 5 uM of each primer, 0.1 µl Go *Taq* polymerase (New England Biolabs, Ipswich, MA), and 1 µl of genomic DNA at 50 ng/µl, for a total reaction volume of 22 µl. PCR cycling conditions were modified from those of Eackles and King (2002), and were as follows: 94℃ for 3 minutes; followed by 30 or 35 cycles, dependent on primer used, of 94℃ for 40 sec, 59℃ for 40 sec, and 72℃ for 1 min; followed by a final extension at 72℃ for

5 minutes; and a hold at 4°C. Polymerase chain reaction products were prepared and sent to the Institute of Biotechnology at Cornell University, Ithaca, New York for DNA fragment-size analysis. The resulting fragments were viewed, scored for length, and examined for size polymorphism with Genemarker software (SoftGenetics, State College, PA). The presence of null alleles, allelic dropout, and allelic stuttering was assessed using Microchecker (Van Oosterhout et al. 2004).

Arlequin v3.0 (Excoffier et al. 2005) was used to assess expected heterozygosity, observed heterozygosity, number of observed alleles per locus, total number of alleles, number of private alleles, conformance of genotype frequencies to Hardy-Weinberg equilibrium, linkage disequilibrium (LD), and to calculate the Garza-Williamson (2001) index (*M*-ratio), which indicates evidence of a recent genetic bottleneck at each locus in each population. Phylogenetic trees were reconstructed using a neighbor-joining (NJ) (Saitou and Nei 1987) method and Nei's standard genetic distance (D_{ST}) (Nei 1972) in program POPTREE2 (Takezaki et al. 2010) to assess phylogenetic relationships among populations in the UTRB, Green, and Cumberland rivers and among respective sub-basins within these three watersheds. STRUCTURE version 2.3.4 (Pritchard and Wen 2003), which implements an assignment test-based algorithm to determine population structure based on common ancestry with individuals arranged by drainage and population, and also by the three morphotypes of *C. iris* as defined by Watters (2018). No assumptions or population prior information was used for the analysis. The best-supported number of multilocus genotypic clusters (*K*) was determined by calculating the mean natural logarithm of the probability of *K* [mean Ln*P*(*K*)] with iterations from *K*=2 to *K*=14 then *K*=10 for analysis based on morphotype, which included ten independent runs for each *K*. All runs included 1,000,000 iterations with 100,000 burn-in steps. Lastly, STRUCTURE PLOT was used to create a visualization of the population structure using the highest likelihood estimates (Ramasamy et al. 2014).

Geometric Morphometrics

Photographs of the external shell were used for geometric morphometric analysis. Individuals of *C. iris* (*N*=86) were collected from the Clinch (VA and TN), Powell (VA), Holston (VA), Green (KY), and Cumberland river drainages (KY and TN); individuals of *C. taeniatus* (*N*=9) from the Green and Cumberland river drainages (KY and TN); and individuals of *Leaunio*

vanuxemensis (*N*=17) were collected from the Holston and Powell river drainages (VA and TN) (Table 1). For leveling, mussel shells were fixed within an adhesive square with modeling clay, and photographs were taken using a PULUZ (Shenzhen, PRC) Photo Light Box®. Size-classes were categorized as small (<30 mm), medium (30.1 mm <50 mm), or large (≥50.1 mm). Photographs were overlain with a grid, a 180-degree line on the anterior part of the umbo, and then a digital semicircle divided into 15-degree increments. The anterior umbo aligned as landmark 1 with the 180-degree angle indicating landmark 5 (Figure 5). Landmarks were obtained using tpsDig2 v 2.25 (Rohlf 2001). MorphoJ version 1.06 (Klingenberg 2011) was used to perform Canonical Variate Analysis (CVA) landmark analyses. The data was checked for outliers, and a covariance matrix was used to assess locations of landmarks between species and size-classes. The CVA was used to determine differences in medium and large size-classes between and within species, and to assess differences among the three morphotypes shown in Figure 3.

Decision Trees and Random Forest for morphometric classification

Quantitative shell characteristics – including maximum length, hinge length, maximum perpendicular umbo height, maximum perpendicular hinge height, and width – were measured in millimeters with digital calipers (Figure 6). Categorical characters – including shape, periostracum color, ray width, ray spacing, ray pattern, ray coverage, foot color, and nacre color – were documented for each individual (Figures 7 and 8). The R packages party 1.3-3 (Hothorn et al. 2019) and rpart 4.1-15 (Therneau et al. 2015) were used for decision tree analysis, with species used as the response variable in the decision tree analysis. Random forest analysis was implemented using randomforest (Liaw 2018) and caret (Kuhn 2012) in R to determine the most prevalent morphological characters for identification of *C. iris*, *C. taeniatus*, and *L. vanuxemensis*. For both the decision tree and random forest analyses, the data was partitioned into a training data set (80% with 67 observations) and a validation data set (20% with 28 observations). The confidence level for the decision tree analysis was set to 90% with a branch split of 1, and *K*-fold cross-validation with *K*=10 was used to validate the model. For random forest analysis, the number of trees was set at default *ntree*=500 and then *ntree*=3000 to determine out-of-bag (OOB) error rate and to visualize the decline in the error rate and when it stabilized. The final *ntree*=2100 was used for analysis.

RESULTS

Mitochondrial DNA

We successfully sequenced the mitochondrial *ND1* region of 60 individuals and utilized 33 sequences from Genbank for a total sample size for *C. iris* of *N*=87 and for *C. taeniatus* of *N*=4. Overall, the mtDNA sequences demonstrated a high amount of haplotype and nucleotide diversity, with a total of 70 polymorphic segregating sites, a haplotype diversity (*Hd*) of 0.9 and a nucleotide diversity (*Pi*) of 0.025. A total of 20 haplotypes were observed in the sampled individuals and populations of *C. iris* and *C. taeniatus* (Table 4). Only two haplotypes were observed from the sequences sampled of *C. taeniatus* in the study and downloaded from Genbank. Haplotype 1 was shared between an individual of *C. taeniatus* from the Green River drainage and several individuals of *C. iris* from Saltville, Richlands, and Copper Creek in the UTRB (Table 5). Among the 20 haplotypes, 10 occurred in at least two of the study populations, while 10 occurred in single populations. Further, the larger the sample size, the greater the number of detected haplotypes (Table 5). The haplotype network (Figure 9) showed a high number of mutational steps between haplotypes and focal populations (indicated by hatch marks), indicating that some haplotypes were highly diverged. The phylogenetic analysis showed that the majority of sequences fell within a single large polyphyletic clade (Clade 1) that included individuals of both *C. iris* and *C. taeniatus*. However, three *C. taeniatus* sequences and one *C. iris* sequence from the UTRB fell outside of this clade, and several individuals of *C. iris* and one individual of *C. taeniatus* grouped into highly diverged but smaller clades with high posterior support values (Figure 10, Panel A). With the addition of sequences from Kuehnl (2009) on GenBank, the second phylogenetic tree has a large group of polyphyletic sequences from Virginia, Kentucky, Tennessee, North Carolina, and Alabama. In the second group, there are three clades, one of *C. iris* from Kentucky, the second of *C. taeniatus* from Kentucky and Tennessee, and the third of *C. iris* from Missouri and Arkansas. The third and fourth groups were comprised of a clade of *L. vanuxemensis* from Virginia and a clade of *C. iris* from Alabama (Figure 10, Panel B).

Nuclear DNA Microsatellites

A total of 88 individuals (*C. iris N*=81 and *C. taeniatus N*=7) were successfully genotyped using a suite of 8 nuclear DNA microsatellites. Individuals missing $\geq$30 percent of their data were removed for analysis (Table 3). Allelic diversity ranged from *A*= 3.25 at Jonesville to *A*= 9.50 at

Saltville for *C. iris* and A=3.63 at Sinking Creek to A=4.88 at West Fork Drakes Creek for *C. taeniatus* (Table 6). At each locus, all populations demonstrated lower mean observed heterozygosity than mean expected heterozygosity, suggesting a recent loss of genetic diversity. For example, in *C. iris* mean observed heterozygosity ranged from H_o=0.36 to H_o=0.70 while mean expected heterozygosity ranged from, H_e=0.71 to H_e=0.93, and in *C. taeniatus* mean observed heterozygosity ranged from H_o=0.50 to H_o= 0.58 and mean expected heterozygosity ranged from H_e=0.78 to H_e=0.82 (Table 6). Private alleles were observed in all populations of *C. iris* except the Chilhowie population in the Middle Fork Holston River, and in both populations of *C. taeniatus*. For all populations of *C. iris* and *C. taeniatus,* the M-ratio was <0.60, which suggests recent loss of within-population genetic diversity (Table 6).

The microsatellite marker-based phylogenetic analysis divided populations from the UTRB into two clades with moderate to significant bootstrap values (Figure 11, Panel A). The addition of *C. iris* from the Green River drainage and *C. taeniatus* from the Green and Cumberland River drainages failed to delineate between nominal taxa, with individuals from the respective populations clustering with individuals from opposing drainages (Figure 11, Panel B).

The STRUCTURE analysis showed a best-supported number of K=14 populations and generally showed high admixture among populations, with a high amount of shared ancestry among populations across drainage divides (Figure 12, Panel A). However, individuals of *C. dactylus* from Russell Creek, KY in the Green River drainage had distinct ancestry profiles, as did a few individuals from the upper Clinch River in Indian and Cavitt's creeks. When individuals were arranged by morphotype, the Russell Creek individuals again displayed distinct ancestry, as well as two individuals of *C. taeniatus* from the Cumberland River (Figure 12, Panel B) but overall, no population structure was observed based on morphotype.

Among populations of *C. iris* in the UTRB, allele frequency divergence values ranged from F_{ST}=0.03 (Ceres vs Saltville) to F_{ST}=0.11 (Chilhowie vs Copper Creek). When including *C. iris* and *C. taeniatus* from the Green and Cumberland River drainages F_{ST}=0.02 (Sinking Creek vs Big Stone Gap) to F_{ST}=0.20 (Russell Creek vs Chilhowie). Jost's D values ranged from D=0.09 (Rich Valley vs Saltville) to D=0.72 (Copper Creek vs Kyles Ford). Between populations of *C. iris* and *C. taeniatus*, Jost's D ranged from effectively 0 between West Fork Drakes Creek and Kyles Ford to D=0.9 between Rich Valley and Russell Creek. Overall, divergence values ranged from low to high within the UTRB and between *C. iris* and *C. taeniatus* from the UTRB, Green and

Cumberland River drainages (Table 7). However, we interpret these results with caution, due to small sample sizes in some populations. To resolve these small sample sizes, we pooled populations based on drainage sub-basin. For example, divergence between the Clinch, Holston and Powell river sub-basins after pooling was much lower, with F_{ST} ranging from 0.002 to 0.04 and *D* ranging from 0.33 to 0.24 for *C. iris* (Table 8). Similarly, divergence was lower for *L. vanuxemensis* between the UTRB and Cumberland river drainages F_{ST} was 0.07 and *D* was 0.37 (Table 8).

Geometric Morphometrics

The CVA demonstrated that the majority of individuals per population fell within the 0.90 confidence intervals. The exceptions included medium-sized (30 mm ≤50.1 mm) *C. iris* individuals from the Holston River sub-basin (Figure 13, Panel A) and large (>50.1 mm) *C. iris* individuals from the Clinch River sub-basin (Figure 13, Panel B). The observed shell landmark variation of individuals from different drainages in both canonical variate analyses (Figure 13, Panels A and B) showed some morphological overlap between species and individuals from different drainages. Shell variation of individuals from the three different morphotypes showed high morphological overlap among individuals, but some separation also was evident (Figure 13, Panel C).

Decision trees

Boxplots with the mean values for each measured quantitative (Figure 14, Panels A and B) and barplots for categorical shell characters (Figure 15) for each species generally show that ray coverage, shell length, shell height, and umbo height were greater for *C. taeniatus*. In the decision tree analysis, the misclassification error rate for the training data set and validation data set was 0% and 4%, respectively when *ntree*=500. After adjusting the *ntree* value to *ntree*=1000, based on the decrease in the out-of-box error rate of 11.94% to 10.45%, the error rate in training data set remained effectively 0 and the validation data set increased to 10% (Table 9). The training data set had an accuracy of 1 (0.95, 1), whereas the validation data set had an accuracy of 0.90 (0.72, 0.98). Maximum umbo height was determined to be a crucial character with the largest mean decrease accuracy and largest mean decrease gini (Figure 16, Panels A and B). The decision tree identified

maximum umbo height, width, periostracum color, and ray coverage as defining characters for species identification (Figure 17).

DISCUSSION

In this study, we assessed the phylogenetic, population genetic, and morphological differences of populations of *Cambarunio iris* in the UTRB of Tennessee and Virginia, and in the Green and Cumberland River basins of Kentucky and Tennessee. We also included individuals of *Leaunio vanuxemensis* from populations in the Holston River drainage and individuals of *C. taeniatus* from populations in the Green and Cumberland River drainages as closely related outgroup taxa. Multiple notable findings stand out from our results, to include: (1) The mtDNA phylogenetic tree shows that nearly all haplotypes of *C. iris* analyzed from across the UTRB are closely related with shallow divergence, indicating a lack of cryptic biodiversity in this region based on this marker; however, one haplotype from the upper Clinch River in Cavitt's Creek was highly diverged, (2) The second mtDNA phylogenetic tree that included sequences used in Kuehnl (2009) shows that haplotypes of *C. iris* from the Green and Cumberland River basins are distinct from those in the UTRB, supporting cryptic biodiversity among these two basins based on this marker and the conclusions of Kuehnl (2009) and Watters (2018) that these populations represent separate species (now *C. dactylus*) from the *C. iris* populations residing in the UTRB; (3) The nuclear DNA microsatellites generally show high admixture within and among sampled populations of *C. iris* throughout the UTRB with minimal geographic structuring among sub-basins (e.g., Powell, Clinch and Holston rivers), but individuals from the Green and Cumberland river's exhibit distinct ancestry profiles from those in the UTRB; and (4) Morphological analyses generally do show differences among lineages and sub-basins in the UTRB and especially between the UTRB, Green and Cumberland river basins.

Mitochondrial DNA

The haplotypes sampled from the major sub-basins within the UTRB generally showed shallow divergence, with ~25% of haplotypes shared across sub-basins. However, a single individual from Cavitt's Creek was highly diverged from the other haplotypes in this study. Interestingly, that particular haplotype (H10) had fewer mutational steps away from the

Cumberland River drainage *C. taeniatus* haplotypes than it did from all other observed haplotypes of *C. iris* throughout the UTRB. While the three *C. taeniatus* mtDNA sequences from the Cumberland River drainage obtained from GenBank from the Kuehnl (2009) study were many mutational steps diverged from the majority of *C. iris* in the UTRB, a single *C. taeniatus* individual in this study sampled from the Green River drainage shared a haplotype with *C. iris* individuals in the UTRB. Haplotype sharing between related freshwater mussel species previously has been documented in the genus *Epioblasma* of the Cumberland and Tennessee River basin and in the genus *Elliptio* for various species occurring along the Atlantic and Gulf slopes of North America; for example, individuals from different species of *Epioblasma* which are clearly differentiated based on morphology and life history traits shared some mtDNA haplotypes (Jones et al. 2006).

Our mtDNA tree is quite similar to that of Kuehnl (2009) in that both trees show a large clade with many closely related haplotypes from the UTRB, but they also show a handful of highly diverged haplotypes from other regions throughout the range of *C. iris* and *C. taeniatus* that do not group with this main clade. Whether or not these divergent haplotypes represent separate species is challenging to put into perspective without complementary data from nuclear markers and morphology. Further, the use of mtDNA with low samples sizes limits our understanding of the diversity within the *C. iris* and *C. taeniatus* species' complex in the UTRB, Green, Cumberland, and other river drainages. Small sample sizes do not support confidently discerning how widely or narrowly distributed certain haplotypes or lineages throughout a species range may be. A close examination of these two phylogenetic trees illustrates two key points. First, while highly divergent mtDNA haplotypes exist in different drainages throughout the range of *C. iris*, the sample sizes are low from some drainages, and some of these divergent lineages occur broadly over the species' range. Second, at least one large clade exists where divergence is low among haplotypes, and these haplotypes also occur broadly (e.g., VA, TN, NC, AL, KY, OH, WV, PA, MI, AR) (Kuehnl 2009). This clade may be indicative of a post-Pleistocene population expansion into the UTRB and upper Ohio River watersheds. Such complex phylogeographic relationships are not unique to mussels. Spinks et al. (2015) provide an example of the Manning River snapping turtle (*Myuchelys purvisi*), which was returned to its original genus by using 13 nuclear and one mtDNA gene whereas it was presumptuously split into another genus using relatively sparse geographic and genetic coverage by a previous study. Therefore, without knowledge of how variation in mtDNA haplotypes matches up with variation at nuclear markers and with unique morphological and life history traits, it is

difficult to use mtDNA alone to delineate species. Recently, Chong et al. (2016) demonstrated the incongruence between mtDNA and nuclear data in the genus *Cyprogenia*. Another mussel example from Sano et al. (2022), found that while mtDNA and nuclear DNA were consistent in *Beringiana*, the mtDNA and nuclear DNA were not concordant for *Sinanodonta*.

Nuclear DNA Microsatellites

Our analyses using nuclear DNA microsatellites allowed us to make strong inferences regarding cryptic biodiversity occurring within and among the sub-basins of the UTRB and at a broader geographic scale in the Green and Cumberland river drainages. First, admixture in the STRUCTURE plots was high, with similar ancestry profiles seen in individuals of *C. iris* at sites within and among the main UTRB sub-basins of the Powell, Clinch, and Holston watersheds, and further, many of the *C. taeniatus* individuals in the Cumberland River basin had ancestry profiles similar to *C. iris*. However, the two individuals of *C. taeniatus* from West Fork Drake, Green River drainage both had highly distinct nuclear DNA ancestry profiles and distinct shell morphologies relative to those in the Cumberland River basin. One of these two individuals (Tag #A64) had the same mtDNA haplotype as many of the *C. iris* in the UTRB, again indicating that some haplotype sharing over a broad geographic area is occurring between these two species. Individuals of *C. iris* from Russell Creek in the Green River have a highly distinct nuclear DNA ancestry profiles, as well as distinct mtDNA and shell morphologies, again supporting Watters (2018) preliminary assessment that this population of *C. iris* is deserving of separate species status (*C. dactylus*), with a distribution that spans the Green, Cumberland and Duck rivers, but with the Green River, KY population being further designated at the subspecies level (*C. dactylus viridensis*). Second, our sample sizes per morphotype were relatively high (Form1=15, Form2=23, Form3=12), and demonstrate high admixture amongst these three forms. Third, population divergence based on F_{ST} and D_{EST} among sites within UTRB subbasins generally was high. These high values are in part due to small sample sizes per site that are inflating the estimated divergence values, but when sites within a basin are combined and then compared as a whole among the basins, these same divergence values decline. This again emphasizes the need for larger sample sizes to estimate these values. Despite its small sample size, the Russell Creek population of *C. iris* in the Green River still stands out as having high divergence relative to the other populations in the study.

Morphological analyses

External morphological traits of the shell, especially the overall shape, ray pattern, and periostracum color, among other traits, are the primary way that biologists identify species in the field. For species that look different based on a suite of external traits, external morphology has generally been a reliable method for identifying freshwater mussel species. However, when species are closely related with high trait similarity, then reliable identifications between species can be harder. Based on the Decision-tree and Random Forest Analysis, we found the key external shell characteristics that were the most informative for differentiating between *C. iris*, *C. taeniatus*, and *L. vanuxemensis,* to include: (1) maximum height from the umbo to the ventral margin, (2) periostracum color (brown vs. yellow), (3) shell width, and (4) ray coverage. These character sets generally show that *C. iris* is smaller than *C. taeniatus* for height from the umbo to the ventral margin, that *C. taeniatus* periostracum color is yellow, *C. iris* periostracum is yellow to brown, and *L. vanuxemensis* is brown, and that *C. iris* has a greater width than *L. vanuxemensis*, and lastly, *C. taeniatus* has more ray coverage than *C. iris*. However, these traits can be difficult to observe and utilize in the field if a practitioner is not cognizant and trained in how to use these traits to identify species. Some traits are highly variable, such as nacre color. While white nacre color was the most common color for *C. iris* and *C. taeniatus* and even occasionally present in *L. vanuxemensis,* salmon nacre color was also present in individuals of *C. iris* and C. *taeniatus,* with purple nacre color also being present in *C. iris* and *L. vanuxemensis*. The varying nacre color of *C. iris* was present in all three forms previously highlighted and was common across all localities. Hence, nacre color is not a useful trait to identify these species. Similarly, Lane et al. (2019) found that nacre color formerly used to distinguish *Venustaconcha trootensis* and *Venustaconcha trabalis* was not reliable, causing taxonomic confusion in the past. To the trained eye, *C. iris* and *L. vanuxemensis* periostracum color (yellow vs. brown) is a key external trait to reliably identify the two species. However, *C. iris* is variable in this trait and can occasionally have brown periostracum. However, the ray pattern of *C. iris* generally is defined by wide green rays, whereas the ray pattern of *L. vanuxemensis* is fine and "pencil-thin", and frequently the periostracum is so dark that the rays are not even visible. Based on our samples and results from construction of the Decision Tree, *C. taeniatus* has greater ray coverage anterior to posterior than *C. iris*. In addition, results of the classification and regression trees (CART) analysis identified height from the umbo to the ventral margin of the shell as the most important diagnostic character, i.e., it is greater in *C.*

taeniatus relative to *C. iris*. Canonical variate analysis (CVA) of species and drainage, first organized by size-class, and then used to further compare species and morphotype demonstrated differences of mussels between sub-basins in the UTRB. This ecophenotypic plasticity has been reported in other taxa and is not surprising for the widely distributed *C. iris* (Morrison et al. 2021; Inoue et al. 2013). These traits can be used for field identification, however, experience level of the practitioner vary's greatly and can lead to difficulty using these traits for identification.

Summary and Conclusions

Our combined use of mtDNA, nDNA, and morphological traits to search for cryptic biodiversity in the *C. iris* complex in the UTRB and other geographical areas has revealed several key findings. First, our nDNA dataset partitioned by the three morphotypes of *C. iris* in the UTRB and analyzed in program STRUCTURE generally did not support a hypothesis that these three shell forms represent cryptic species. Further, the canonical variate analysis (CVA) of the three morphotypes showed a high level of overlap, but with a few individuals per morphotype falling outside of the confidence interval ellipse. These individuals likely represent morphological divergence based on size class or more extreme phenotypic plasticity. The three morphotypes as arranged in the STRUCTURE plot clearly show high admixture and no structure based on morphotype or presumed cryptic species, and therefore the nDNA was congruent with the CVA plot showing high morphological overlap of the three forms. In addition, our nDNA sample sizes per UTRB sub-basin were high and adequate to address this question. Second, individuals of *C. iris* from the Green River drainage stood out across all three data sets. While samples sizes for *C. iris* (now *C. dactylus* recognized by the Freshwater Mollusk Conservation Society) in the Green River drainage for the mtDNA and nDNA datasets were small (N=5), both of the molecular marker datasets were diverged and unique. The morphological characteristics of individuals in this population, i.e., shell shape with *C. dactylus* being more elongate, exterior morphological characters such as periostracum color and ray pattern, and differences in mantle lure, also demonstrate divergence from *C. iris* in the UTRB. If sample sizes using these three datasets could be increased, and afterwards this form of *C. iris* remains characterized as genetically and morphologically divergent and unique, then this Green River endemic form may warrant listing. Third, across the mtDNA, nDNA, and morphological data sets *C. taeniatus* from the Green River

drainage also demonstrated genetic and morphological distinctiveness from *C. taeniatus* in the Cumberland River drainage. Again, more sampling is needed to better characterize these potential genetic and morphological differences in *C. taeniatus* in the Cumberland and Green river drainages. At a broader geographic level, our data shows that mussel species in the *Cambarunio* and *Leaunio* genera in the Green River drainage appear to be genetically and morphologically distinct from individuals in the UTRB and the Cumberland River Drainage, and supports an overall hypothesis that cryptic species likely occur in these two genera. To us, *L. vanuxemensis* in the UTRB has a periostracum color that is evenly brown with fine rays, whereas *L. vanuxemensis* in the Cumberland River system does not match this pattern, suggesting that these populations could be different species.

Finally, the combined use of mtDNA, nDNA, and morphological data was helpful for understanding the genotypic and phenotypic variation of the *C. iris* complex in the UTRB, Green River Drainage, Cumberland River Drainages. Future management should include identifying management units in order to increase the genetic diversity of populations and determine other augmentation and restoration needs of *C. iris* within the UTRB and assess the need for listing *C. dactylus* and *C. taeniatus* in the Green River drainage. Continued use of multiple datasets to understand biological diversity and species level relationships is of the highest importance. Limited sampling sizes and use of just one dataset poses the risk of over or under evaluating the relationships between genera of freshwater mussels and therefore can lead to promulgating even more taxonomic uncertainty.

LITERATURE CITED

Bandelt, H., P. Forster, and A. Röhl. 1999. Median-joining networks for inferring intraspecific phylogenies. Molecular Biology and Evolution 16:37–48.

Bogan, A.E. 2002. Workbook and key to the freshwater bivalves of North Carolina. North Carolina Museum of Natural Sciences, Raleigh, North Carolina. 101 pp.

Chapman, E.J., and T.A. Smith. 2008. Structural community changes in freshwater mussel populations of Little Mahoning Creek, Pennsylvania. American Malacological Bulletin 26: 161–169.

Chong, J.P., J.L. Harris, K.J. Roe. 2016. Incongruence between mtDNA and nuclear data in the freshwater mussel genus *Cyprogenia* (Bivalvia: Unionidae) and its impact on species delineation. Ecology and Evolution 6:2439–2452.

COSEWIC. 2006. COSEWIC assessment and status report on the rainbow mussel *Villosa iris* in Canada. Committee on the Status of Endangered Wildlife in Canada. Ottawa, Canada. 38 pp.

Cummings, K.S. and Mayer 1997. Distributional Checklist and Status of Illinois Freshwater Mussels (Mollusca: Unionacea). Conservation and Management of Freshwater Mussels II: Proceedings of the UMRCC Symposium, Illinois Natural History Survey, Center for Biodiversity, Champaign, IL. Pages 129–145.

Eackles, S.M., and T.L. King. 2002. Isolation and characterization of microsatellite loci in *Lampsilis abrupta* (Bivalvia: Unionidae) and cross-species amplification within the genus. Molecular Ecology Notes 2:559–562.

Earl, D.A., and B.M. vonHoldt. 2011. STRUCTURE HARVESTER: a website and program for visualizing STRUCTURE output and implementing the Evanno method. Conservation Genetics Resources 4:359–361.

Elderkin, C.L., A.D. Christian, J.L. Metcalfe-Smith, and D.J. Berg. 2008. Population genetics and phylogeography of freshwater mussels in North America, *Elliptio dilatata* and *Actinonaias ligamentina* (Bivalvia: Uniondae). Molecular Ecology 17:2149–2163.

Evanno, G., S. Regnaut, and J. Goudet. 2005. Detecting the number of clusters of individuals using the software STRUCTURE: a simulation study. Molecular Ecology 14:2611–2620.

Excoffier, L., G. Laval, and S. Schneider. 2005. Arlequin ver. 3.0: An integrated software package for population genetics data analysis. Evolutionary Bioinformatics Online 1:47–50.

Falush, D., M. Stephens, and J.K. Pritchard. 2003. Inference of population structure using multilocus genotype data: linked loci and correlated allele frequencies. Genetics 164:1567–1587.

Falush, D., M. Stephens, J.K Pritchard. 2007. Inference of population structure using multilocus genotype data: dominant markers and null alleles. Molecular Ecology Notes.

Garza, J.C., and E.G. Williamson. 2001. Detection of reduction in population size using data from microsatellite loci. Molecular Ecology 10:305–318.

Geist, J., and R. Kuehn. 2005. Genetic diversity and differentiation of central European freshwater pearl mussel (*Margaritifera margaritifera L.*) populations: implications for conservation and management. Molecular Ecology 14:425–439.

Hothorn, T., A. Zeileis, and K. Hornik. 2019. Package 'party'. Available online: cran.r-project.org/web/packages/party/party.pdf.

Hubisz, M.J., D. Falush, M. Stephens, and J. K. Pritchard. 2009. Inferring weak population structure with the assistance of sample group information. Molecular Ecology Resources 9:1322–1332.

Inoue, K., D.M. Hayes, J.L. Harris, and A.D. Christian. 2013. Phylogenetic and morphometric analyses reveal ecophenotypic plasticity in freshwater mussels *Obovaria jacksoniana* and *Villosa arkansasensis* (Bivalvia: Unionidae). Ecology and Evolution 3:2670–2683.

Jones, J.W., R.J. Neves, S.A. Ahlstedt, and E.M. Hallerman. 2006. A holistic approach to taxonomic evaluation of two closely related endangered freshwater mussel species, the oyster mussel *Epioblasma capsaeformis* and tan riffle shell *Epioblasma florentina walkeri* (Bivalvia: Unionidae). Journal of Molluscan Studies 72:267–283.

Jones, J.W. 2015. Freshwater mussels of Virginia (Bivalvia: Unionidae): An introduction to their life history, status and conservation. Virginia Journal of Science 66:309–331.

Jones, J.W., M. Culver, V. David, J. Struthers, N.A. Johnson, R.J. Neves, S.J. O'Brien, and E.M. Hallerman. 2004. Development and characterization of microsatellite loci in the endangered oyster mussel *Epioblasma capsaeformis* (Bivalvia: Unionidae). Molecular Ecology Notes 4:649–652.

Jost, L., 2008. G_{ST} and its relatives do not measure differentiation. Molecular Ecology 17:4015–4026.

Klingenberg, C.P., 2011. MorphoJ: an integrated software package for geometric morphometrics. Molecular Ecology Resources 11:353–357.

Kuehnl, K. 2009. Exploring levels of genetic variation in the freshwater mussel genus *Villosa* (Bivalvia: Unionidae) at different spatial and systematic scales: Implications for biogeography, taxonomy, and conservation. Ph.D. Dissertation, Ohio State University, Columbus, Ohio.

Kuhn, M. 2012. The caret package. Available online: cran.r-project.org/package=caret.

Lane, T.W., E.M. Hallerman, and J.W. Jones. 2016. Phylogenetic and taxonomic assessment of the endangered Cumberland bean, *Villosa trabalis* and purple bean, *Villosa perpurpurea* (Bivalvia: Unionidae). Conservation Genetics 17:1109-1124.

Leigh, J.W., and D. Bryant. 2015**.** PopART: Full-feature software for haplotype network construction. Methods in Ecololy and Evolution 6:1110–1116.

Liaw, A. 2018. Package 'randomForest'. Available online: cran.r-project.org/web/packages/randomForest/randomForest.pdf.

Morrison, C.L., N.A. Johnson, J.W. Jones, M.S. Eackles, A.W. Aunins, D.B. Fitzgerald, E.M. Hallerman, T.L. King. 2021. Genetic and morphological characterization of the freshwater mussel clubshell species complex (*Pluerobema clava* and *Pleurobema oviforme*) to inform conservation planning. Ecology and Evolution 11:15325–15350.

Newton, T.J., D.A. Woolnough, and D.L. Strayer. 2008. Using landscape ecology to understand and manage freshwater mussel populations. The North American Benthological Society 27:424–439.

Olson, P.J., and C. Vaughn. 2020. Population genetics of a common freshwater mussel, *Amblema plicata*, in a southern U.S. river. Freshwater Mollusk Biology and Conservation 23:124–133.

Ortiz, K., J.W. Jones and E.M. Hallerman. 2022. Development and characterization of microsatellite loci in the Purple Cat's Paw Pearlymussel *Epioblasma obliquata* (Bivalvia:Unionidae). Freshwater Mollusk Biology and Conservation 25:1–6.

Parmalee, P.W., and A.E. Bogan. 1998. The Freshwater Mussels of Tennessee. University of Tennessee Press: Knoxville, Tennessee. 328 pp.

Peakall, R., and P.E. Smouse. 2006. GENALEX 6: genetic analysis in excel. Population genetic software for teaching and research. Molecular Ecology Notes 6:288–295.

Pritchard, J.K., and W. Wen. 2003. Documentation for STRUCTURE Software: Version 2. Chicago: University of Chicago Press. Retrieved from: http://web.stanford.edu/group/pritchardlab/software/structure2_1.html.

Rambaut, A. 2006–2018. FigTree v1.4.4. Institute of Evolutionary Biology. University of Edinburgh.

Rohlf, F.J. 2001. TPSDig2: a program for landmark development and analysis. http://life.bio.sunysb.edu/morph/index. Html.

Ronquist, F., M. Teslenko, P. van der Mark, D.L. Ayres, A. Darling, S. Hohna, B. Larget, L. Liu, M.A. Suchard, and J.P. Huelsenbeck. 2012. MrBayes 3.2: Efficient Bayesian phylogenetic inference and model choice across a large model space. Systematic Biology 61:539–542.

Rozas, J., A. Ferrer-Mata, J.C. Sánchez-DelBarrio, S. Guirao-Rico, P. Librado, S.E. Ramos-Onsins, and A. Sánchez-Gracia. 2017. DnaSP v6: DNA Sequence Polymorphism Analysis of Large Datasets. Molecular Biology And Evolution. 34:3299–3302.

Saitou, N., and M. Nei. 1987. The neighbor-joining method: a new method for reconstructing phylogenetic trees. Molecular Biology and Evolution 4:406–425.

Sano, I., T. Saito, S. Ito, B. Ye, T. Uechi, T. Seo, V.T. Do, K. Kimura, T. Hirano, D. Yamazaki, A. Shirai, T. Kondo, O. Miura, J. Miyazaki, S. Chiba. 2022. Resolving species-level diversity of *Beringiana* and *Sinanodonta* mussels (Bivalvia: Unionidae) in the Japanese archipelago using genome-wide data. Molecular Phylogenetics and Evolution 175: 107563.

Schanzle, R.W., G.W. Kruse, J.A. Kath, R.A. Klocek, and K.S. Cummings. 2004. The Freshwater Mussels (Bivalvia: Unionidae) of the Fox River Basin, Illinois and Wisconsin. Illinois Natural History Biological Notes 141:1–35.

Schwalb, A.N., K. Cottenie, M.S. Poos, J.D. Ackerman. 2011. Dispersal limitation of unionid mussels and implications for their conservation. Freshwater Biology 56:1509–1518.

Serb, J.M., J.E. Buhay, C. Lydeard. 2003. Molecular systematics of the North American freshwater bivalve genus *Quadrula* (Unionidae: Ambleminae) based on mitochdonrial ND1 sequences. Molecular Phylogenetics and Evolution. 28:1–11.

Shea, C.P., J.T. Peterson, J.M. Wisniewski, and N.A. Johnson. 2011. Misidentification of freshwater mussel species (Bivalvia: Unionidae): Contributing factors, management

implications, and potential solutions. The North American Benthological Society 30:446–458.

Spinks, P.Q., A. Georges, and H. B. Shaffer. 2015. Phylogenetic uncertainty and taxonomic re-revisions: an example from the Australian short-neck turtles (Testudines: Chelidae). Copeia 103:536–540.

Spooner, D.E., and C.C. Vaughn. 2007. Mussels of the Mountain Fork River, Arkansas and Oklahoma. Publications of the Oklahoma Biological Survey, 2nd series 8:14–18.

Szafoni, R.E., K.S. Cummings, and C.A. Mayer. 2000. Freshwater Mussels (Mollusca: Unionidae) of the Middle Branch, North Fork Vermillion River, Illinois, Indiana. Transactions of the Illinois State Academy of Science 93:229–237.

Takezaki, N., M. Nei, and K. Tamura. 2010. POPTREE2: Software for constructing population trees from allele frequency data and computing other population statistics with Windows-interface. Molecular Biology and Evolution 27:747–752.

Therneau, T., B. Atkinson, B. Ripley, and Ripley, M.B. 2015. Package 'rpart'. Available online:cran.r-project.org/web/packages/rpart/rpart.pdf.

Van Oosterhout, C., B. Hutchinson, D. Wills, and P. Shipley. 2004. Micro-checker: a software for identifying and correcting genotyping errors in microsatellite data. Molecular Ecology Notes 4:535–538.

Watters, G.T. 2018. A Preliminary Review of the Nominal Genus *Villosa* of Freshwater Mussels (Bivalvia, Unionidae) in North America. Conchology, INC.

Williams, J.D., M.L. Warren, Jr., K.S. Cummings, J.L. Harris, and R.J. Neves. 1993. Conservation status of freshwater mussels of the United States and Canada. Fisheries 18:6–22.

TABLES

Table 1. Species, river drainages, sub-basin system, specific site location information and year of DNA samples obtained for *Cambarunio iris*, *Cambarunio taeniatus*, and *Leaunio vanuxemensis* used in this study.

Species	River Drainage	Sub-basin System	Site Location name	Year(s) sampled	Latitude	Longitude	Collectors
C. iris	Tennessee	Clinch	Bennett Island, Russell County, VA	2019, 2022	36.9597	-82.097206	K. Ortiz, R. Belcher and K. Howard
			Cavitt's Creek, Tazewell County, VA	2018	37.1458558	-81.5449801	K. Ortiz, A. Ganser and J. Jones
			Copper Creek, Scott County, VA	2018	36.7286	-82.4684	K. Ortiz, A. Ganser, T. Lane, S. Colletti, T. Leach
			Indian Creek, Tazewell County, VA	2018	37.088	-81.7591	K. Ortiz and A. Ganser
			Kyles Ford, Hancock County, TN	2021	36.566368	-83.04182	J. Jones and Z. Taylor
			Richlands, Tazewell County, VA	2019	37.0940717	-81.8026221	K. Ortiz, D. Phipps, D. Neves, A. Ganser and B. Henley
		Holston	Beech Creek, Greene County, TN	2019	36.4097	-82.7638	K. Ortiz, A. Ganser, T. Lane and T. Leach
			Middle Fork Holston, Smyth County, VA	2020	36.807357	-81.67143	K. Ortiz and A. Binner
			North Fork Holston, Smyth County, VA	2020	36.8956034	-81.7462632	K. Ortiz and A. Binner
			North Fork Holston, Smyth County, VA	2020	36.9248886	-81.6260268	K. Ortiz and A. Binner
			North Fork Holston, Smyth County, VA	2020	36.9562594	-81.4928233	K. Ortiz and A. Binner
			Locust Cove Creek, Smyth County, VA	2020	36.9459366	-81.5913793	K. Ortiz and A. Binner
		Powell	Powell River, Lee County, VA	2020	36.621005	83.284522	K. Ortiz, T. Lane and T. Leach
			Wallen Creek, Lee County, VA	2022	36.936871	-82.166001	K. Ortiz and K. Howard
			South Fork Powell River, Wise County, VA	2022	36.865529	-82.7714967	K. Ortiz and K. Howard
	Green	Rough	Rough River, Hardin County, KY	2021	37.67553	-86.17361	M. Compton and K. Howard
		Russell	Russell Creek, Adair County, KY	2021	37.07182	-85.25097	M. Compton and K. Howard
	Cumberland	Rockcastle	Sinking Creek, Laurel County, KY	2022	37.09785	-84.22369	M. Compton and J.C. Miller
C. taeniatus	Green	Barren	West Fork Drakes Creek, Simpson County, KY	2020	36.81139	-86.46045	M. Compton and V. Jones

			West Fork Drakes Creek, Simpson County, KY	2022	36.80881	-86.45611	M. Compton and K. Howard
	Cumberland	Rockcastle	Sinking Creek, Laurel County, KY	2022	37.09785	-84.22369	M. Compton and J.C. Miller
		Red	Sulphur Spring Creek, Simpson County, KY	2019	36.6957	-86.72829	M. Compton and D. Smith
			Sulphur Spring Creek, Simpson County, KY	2022	36.69581	-86.72647	M. Compton, J.C. Miller and L. Massar
		Stones	West Fork Stones River, Rutherford County, TN	2022	35.72173	-86.44735	M. Compton and J.C. Miller
			Middle Fork Stones River, Rutherford County, TN	2022	35.76713	-86.37588	M. Compton and J.C. Miller
L. vanuxemensis	Tennessee	Clinch	Bennett Island, Russell County, VA	2019	36.9597	-82.097206	K. Ortiz and R. Belcher
			Richlands, Tazewell County, VA	2019	37.0940717	-81.8026221	K. Ortiz, D. Phipps, D. Neves, A. Ganser and B. Henley
		Holston	Beech Creek, Greene County, TN	2019	36.4097	-82.7638	K. Ortiz, A. Ganser, T. Lane and T. Leach
			North Fork Holston, Smyth County, VA	2020	36.9248886	-81.6260268	K. Ortiz and A. Binner
			North Fork Holston, Smyth County, VA	2022	36.9562594	-81.4928233	K. Ortiz, I. Boyce and K. Howard
			Locust Cove Creek, Smyth County, VA	2020	36.9459366	-81.5913793	K. Ortiz, A. Binner, I. Boyce and K. Howard
		Powell	Wallen Creek, Lee County, VA	2022	36.936871	-82.166001	K. Ortiz and K. Howard

Table 2. Nuclear DNA microsatellite loci sequence, melting temperature (˚C), repeat motif, and base-pair size range from Eackles and King (2002), Jones et al. (2004), and Ortiz et al. (2022).

Locus	Primer Sequence (5'-3')	Melting Temp. ˚C	Repeat Motif	Size Range (bp)	Source
EOO_8	F: TATCCCTCCGCTGCTGTAAG	59.7	$ACT_{(16)}$	125-173	Ortiz et al. 2022
	R:CCCTGGCCTGTAACAATCTTG	59.7			
EOO_10	F:CTGGTTGTTCGGTCTTGTGG	59.4	$ATC_{(8)}$	137-161	Ortiz et al. 2022
	R:ACTTTACATCCTGTCCAACTGC	59.8			
EOO_22	F:CAGTCCAAGTCATCTCTCAGG	58.4	$AGAT_{(15)}$	91-151	Ortiz et al. 2022
	R:GCATACGTGTAGCTTTATCGTG	58.2			
EOO_24	F:TCACAAGTCCTACACCCTCTC	59	$AATC_{(6)}$	169-193	Ortiz et al. 2022
	R:TCTTATCAGTTGGGTTTGGTGG	59.2			
EOO_46	F:CAGTCGGGCGTCATCACTGTAACGAG	58.9	$ATCC_{(6)}$	223-247	Ortiz et al. 2022
	R:GTTTGTTAGTTGGGCGGATGGTTG	59.9			
ECAP_8	F: TGCAGACATCGTAGCGATATG	59.9	$(CA)_{15}$	127-159	Jones et al. 2004
	R: ATTTCCAGTTGCAAGTCTCATT	57.9			
ECAP_4	F: GTGCCCCAGTGCTAGACATT	60.1	$(CA)_{10}$	98-120	Jones et al. 2004
	R: AGAACAAAACACCCGTGTCC	59.9			
LAB_206	F: AAGTGTAGAGGCAGAGAACTGAC	58*	$(ATCT)_9$	191-231	Eackles & King 2002
	R: TCACTGATACAGCATACATAATATAC	58*			

Table 3. Total sample sizes (*N*) of individuals genotyped per mitochondrial DNA sequences and DNA microsatellite loci for Rainbow Mussel (*Cambarunio iris*), Painted Creekshell (*Cambarunio taeniatus),* and Mountain Creekshell (*Leaunio vanuxemensis*). Individuals were collected from Kyles Ford (KF), Beech Creek (BC), Cavitts Creek (CAV), Copper Creek (CC), Indian Creek (IN), Bennett Island (BI), Saltville (SAL), Ceres (CER), Rich Valley (RV), Locust Cove Creek (LCC), Jonesville (JON), Wallen Creek (WAL), Big Stone Gap (BIG) all streams in the Upper Tennessee River Drainage and West Fork Drakes Creek (WFD), Sinking Creek (SINK), West Fork Stones River (WFS), and Middle Fork Stones River (MFS) all streams in the Green and Cumberland River drainages. – means locus not analyzed for population.

					mtDNA	nDNA Microsatellite Loci								
Species	***N***	**Site**	**Drainage**	**Year**	***ND1***	***Eoo08***	***Eoo10***	***Eoo22***	***Eoo24***	***Eoo46***	***Ecap08***	***Ecap04***	***LAB206***
C. iris	5	KF	Clinch	2021	–	5	5	2	5	5	5	5	5
C. iris	9	CAV	Clinch	2018	5	9	8	9	9	9	8	9	9
C. iris	9	CC	Clinch	2018	3	9	6	8	9	9	9	8	9
C. iris	3	IN	Clinch	2018	–	3	3	3	3	3	3	3	2
C. iris	9	BI	Clinch	2019	5	9	9	9	9	9	9	9	9
C. iris	3	RIC	Clinch	2019	3	–	–	–	–	–	–	–	–
C. iris	8	BC	Holston	2019	8	–	–	–	–	–	–	–	–
C. iris	18	SAL	Holston	2020	18	8	8	8	8	8	8	8	8
C. iris	11	CER	Holston	2020	11	8	8	8	8	8	8	8	8
C. iris	6	RV	Holston	2020	6	3	3	3	3	3	3	3	3
C. iris	5	JON	Powell	2020	–	3	3	2	3	3	3	–	2
C. iris	6	WAL	Powell	2022	–	6	6	6	6	6	6	6	6
C. iris	10	BIG	Powell	2022	–	10	10	10	10	10	10	10	10
C. iris	3	RC	Green	2021	–	3	3	3	3	3	3	3	–
C. iris	3	SINK	Cumberland	2022	–	3	3	3	3	3	3	3	3
C. taeniatus	5	WFD	Green	2020, 2022	1	5	5	5	5	5	5	4	5
C. taeniatus	3	SINK	Cumberland	2022	–	3	3	3	3	3	3	3	3
C. taeniatus	2	WFS	Cumberland	2022	–	2	2	1	2	2	2	2	2
C. taeniatus	1	MFS	Cumberland	2022	–	1	1	1	1	1	1	1	1
L. vanuxemensis	1	BC	Holston	2019	1	–	–	–	–	–	–	–	–
L. vanuxemensis	3	RV	Holston	2020	3	–	–	–	–	–	–	–	–
L. vanuxemensis	12	LCC	Holston	2020	2	12	12	12	12	11	12	12	12

Table 4. Observed haplotypes and polymorphic sites for mitochondrial DNA sequences of the *ND1* gene used for analyses of *Cambarunio iris, Cambarunio taeniatus*, and *Leaunio vanuxemensis.* Individuals were obtained from West Fork Drakes Creek in the Green River drainage; Beech Creek, Rich Valley, Locust Cove Creek, Ceres, Chilhowie, Saltville, Bennett Island, Cavitts Creek, Copper Creek, Richlands in the Upper Tennessee River drainage from 2018 to 2022.

	Polymorphic Sites and Base-Pair Positions																														
	19	20	20	20	21	21	22	22	23	23	24	25	25	25	25	26	26	27	27	27	27	27	28	28	29	29	31	31	31	32	32
Haplotype	8	1	4	7	1	6	0	5	2	7	3	0	2	3	5	4	7	0	6	7	7	9	2	8	1	5	0	5	8	4	5
Haplotype 1	A	A	A	C	T	C	T	C	T	T	C	C	A	G	T	T	A	T	A	T	A	T	T	C	T	T	A	T	T	C	C
Haplotype 2	.	.	.	.	.	.	.	.	.	.	.	.	.	.	.	.	.	.	G	.	.	.	.	.	.	.	.	.	.	.	.
Haplotype 3	.	.	.	.	.	.	.	.	.	.	.	T	.	.	.	.	.	.	.	.	.	C	.	.	.	.	.	.	.	.	.
Haplotype 4	.	.	.	.	.	.	.	.	.	.	.	T	.	.	.	.	.	.	.	.	.	C	.	.	.	.	.	.	.	.	.
Haplotype 5	G	.	.	.	.	.	.	.	.	.	.	T	.	.	.	.	.	.	.	.	.	C	.	.	.	.	.	.	.	.	.
Haplotype 6	G	.	.	.	.	.	.	.	.	.	.	T	.	.	.	.	.	.	.	.	.	C	.	.	.	.	.	.	.	.	.
Haplotype 7	.	.	.	.	.	.	.	.	.	.	.	T	.	.	.	.	.	.	.	.	.	C	.	.	.	.	.	.	.	.	.
Haplotype 8	.	.	.	.	.	.	.	.	.	.	.	T	.	.	.	.	.	.	.	.	.	C	.	.	.	.	C	.	.	.	.
Haplotype 9	.	.	.	.	.	.	.	.	.	.	.	T	.	.	.	.	.	.	.	.	.	C	.	.	.	.	.	.	.	.	.
Haplotype 10	.	.	.	T	.	.	.	.	.	.	T	.	G	A	.	.	.	C	.	C	.	.	.	.	.	.	.	.	.	T	.
Haplotype 11	.	.	.	.	.	.	C	.	.	.	.	T	.	.	.	.	.	.	.	.	.	C	.	.	.	.	.	.	.	.	.
Haplotype 12	.	.	.	.	.	.	.	.	.	.	.	T	.	.	.	.	.	.	.	C	.	C	.	.	.	.	.	.	.	.	.
Haplotype 13	G	.	G	.	G	T	C	.	C	.	T	.	.	A	C	.	.	C	.	C	G	.	.	C	C	.	.	C	.	T	
Haplotype 14	G	.	G	.	G	T	C	.	.	.	T	.	.	A	C	.	.	C	.	C	G	.	.	C	C	.	.	.	.	T	
Haplotype 15	.	G	.	.	.	.	.	.	.	.	.	.	.	.	.	.	.	.	G	.	.	.	.	.	.	.	.	.	.	.	.
Haplotype 16	.	.	.	.	.	.	.	.	.	.	.	T	.	A	.	.	.	.	.	.	.	C	.	.	.	.	.	.	.	.	.
Haplotype 17	.	.	.	.	.	.	.	.	.	.	.	.	.	.	.	.	.	.	.	.	.	C	.	.	.	.	.	.	.	.	.
Haplotype 18	.	.	G	.	.	T	C	.	.	.	T	.	.	A	C	C	.	C	.	C	.	.	.	C	C	G	.	.	.	T	
Haplotype 19	.	.	.	.	.	.	.	.	.	.	.	.	.	.	.	.	G	.	.	.	.	.	.	.	.	.	.	.	.	.	.
Haplotype 20	.	.	.	.	.	.	.	.	.	.	.	.	.	.	.	.	.	.	.	.	.	C	.	.	.	.	.	.	.	.	.
Haplotype 21	.	.	G	.	.	.	.	T	.	C	T	.	.	A	.	.	.	C	.	C	.	.	T	.	C	.	.	.	T	.	

Table 4. Continued.

	Polymorphic Sites and Base Pair Positions																														
Haplotype	327	330	331	339	342	345	346	351	353	354	396	402	411	417	423	426	432	435	438	441	449	457	468	471	474	475	480	499	501	504
Haplotype 1	A	T	T	C	C	C	C	T	T	T	T	C	T	A	A	C	C	C	T	C	C	T	T	T	C	T	T	A	G	A
Haplotype 2	.	.	.	.	.	.	.	.	.	.	.	T	.	.	.	T	.	.	.	.	.	.	.	.	.	.	.	.	.	.
Haplotype 3	.	.	.	T	.	.	.	.	.	.	.	.	.	.	.	T	.	.	.	.	.	.	.	.	.	.	C	.	.	.
Haplotype 4	.	.	.	.	.	.	.	.	.	.	.	.	.	.	.	T	.	.	.	.	.	.	.	.	T	.	C	.	A	.
Haplotype 5	.	.	.	T	.	.	.	.	.	.	.	.	.	.	.	T	.	.	.	.	.	.	.	.	.	.	C	.	.	.
Haplotype 6	.	.	.	T	.	.	.	.	A	.	.	.	.	.	.	T	.	.	.	.	.	.	.	.	.	.	C	.	.	.
Haplotype 7	.	.	.	T	.	.	.	.	.	.	.	.	.	.	.	T	.	.	.	.	.	.	.	.	.	.	C	.	.	.
Haplotype 8	.	.	.	T	.	.	.	.	.	.	.	.	.	.	.	T	.	.	.	.	.	.	.	.	.	.	C	.	.	.
Haplotype 9	.	.	.	T	.	.	.	.	.	.	.	.	.	.	.	T	.	.	.	.	T	.	.	.	.	.	C	.	.	.
Haplotype 10	.	C	.	.	.	G	T	.	.	.	.	.	.	.	.	T	.	T	.	T	.	.	.	.	.	.	.	G	.	.
Haplotype 11	.	.	.	T	.	.	.	.	.	.	.	.	.	.	.	T	.	.	.	.	.	.	.	.	.	.	C	.	.	.
Haplotype 12	.	.	.	T	.	.	.	.	.	.	.	.	.	.	.	T	.	.	.	.	.	.	.	.	.	.	C	.	.	.
Haplotype 13	G	.	C	T	T	.	T	C	.	C	C	T	C	G	G	T	.	.	.	.	.	C	C	C	.	C	.	.	A	.
Haplotype 14	G	.	C	T	T	.	T	C	.	C	.	T	C	G	G	T	.	.	.	.	.	C	C	C	.	C	.	.	A	.
Haplotype 15	.	.	.	.	.	.	.	.	.	.	.	T	.	.	.	T	.	.	.	.	.	.	.	.	.	.	.	.	.	.
Haplotype 16	.	.	.	T	.	.	.	.	.	.	.	.	.	.	.	T	.	.	.	.	.	.	.	.	.	.	C	.	.	.
Haplotype 17	.	.	.	T	.	.	.	.	.	.	.	.	.	.	.	T	.	.	.	.	.	.	.	.	.	.	C	.	.	.
Haplotype 18	G	C	C	T	T	.	T	C	.	C	C	T	C	G	G	T	.	T	.	.	.	C	C	C	.	C	.	.	A	T
Haplotype 19	.	.	.	.	.	.	.	.	.	.	.	.	.	.	.	.	.	.	.	.	.	.	.	.	.	.	.	.	.	.
Haplotype 20	.	.	.	T	.	.	.	.	.	.	.	.	.	.	.	T	T	.	.	.	.	.	.	.	.	.	C	.	.	.
Haplotype 21	.	C	.	.	.	.	T	.	.	C	.	.	.	.	.	T	.	T	C	T	.	.	.	.	.	.	C	.	.	.

Table 4. Continued.

Polymorphic Sites and Base-Pair Positions										
	5	5	5	5	5	5	5	5	5	5
	1	2	2	2	2	3	4	4	5	6
Haplotype	5	0	3	6	9	2	1	7	4	1
Haplotype 1	A	C	C	C	A	T	T	C	C	T
Haplotype 2	G	.	.	.	.	.	.	.	.	.
Haplotype 3	.	.	.	.	.	.	.	.	.	.
Haplotype 4	.	.	.	.	.	.	.	.	.	.
Haplotype 5	.	.	.	.	.	.	.	.	.	.
Haplotype 6	.	.	.	.	.	.	.	.	.	.
Haplotype 7	.	.	.	.	.	.	.	.	.	C
Haplotype 8	.	.	.	.	.	.	.	.	.	.
Haplotype 9	.	.	.	.	.	.	.	.	.	.
Haplotype 10	.	.	.	.	.	.	.	.	T	.
Haplotype 11	.	.	.	.	.	.	.	.	.	.
Haplotype 12	.	.	.	.	.	.	.	.	.	C
Haplotype 13	.	T	T	G	G	C	.	A	.	.
Haplotype 14	.	T	T	G	G	C	.	A	.	.
Haplotype 15	G	.	.	.	.	.	.	.	.	.
Haplotype 16	.	.	.	.	.	.	.	.	.	.
Haplotype 17	.	.	.	.	.	.	.	.	.	.
Haplotype 18	.	T	T	G	G	C	C	A	A	.
Haplotype 19	.	.	.	.	.	.	.	.	.	.
Haplotype 20	.	.	.	.	.	.	.	.	.	.
Haplotype 21	.	.	.	.	.	C	.	.	T	.

Table 5. Number of observed haplotypes for mitochondrial DNA sequences of the *ND1* gene per population of *Cambarunio iris*, *Cambarunio taeniatus* and *Leaunio vanuxemensis* Individuals were obtained from Beech Creek (BC), Bennett Island (BI), Cavitts Creek (CAV), Richlands (RIC), Copper Creek (CC), Ceres (CE), Chilhowie (CHIL), Rich Valley (RV), Saltville (SAL), Locust Cove Creek (LCC), in the Upper Tennessee River Basin and West Fork Drakes Creek (WFD) in the Green River Drainage, and GenBank.

	Upper Tennessee River Basin												Green River Drainage	Cumberland River Drainage	
	Cambarunio iris										*Leaunio vanxemensis*		*Cambarunio taeniatus*		
Haplotype	BC	BI	CAV	RIC	CC	CE	CH	RV	SAL	LCC	RV	LCC	WFD	Genbank	Total
Haplotype 1			1	1					2				1		5
Haplotype 2	3		1			3				1					7
Haplotype 3	2	2		1		3	2	2	6						18
Haplotype 4	1														1
Haplotype 5	1								1						2
Haplotype 6	1														1
Haplotype 7		2		1	2	1			1						6
Haplotype 8		1				2		1							4
Haplotype 9			1												1
Haplotype 10			1												1
Haplotype 11			1												1
Haplotype 12					1										1
Haplotype 13												1			2
Haplotype 14															1
Haplotype 15						1				1					9
Haplotype 16						1						1			1
Haplotype 17							1	2	6			1			1
Haplotype 18											1	1			1
Haplotype 19									1						1
Haplotype 20									1						1
Haplotype 21														3	
Total	8	5	5	3	3	11	3	5	18	2	1	4	1	3	65

Table 6. Summary of genetic variation among eight microsatellite DNA loci examined for *Cambarunio iris* in the Upper Tennessee River Basin collected from 2018 to 2022; in the Green River drainage from 2020 to 2022; and in the Cumberland River drainage from 2022. *Cambarunio taeniatus* in the Green River drainage and the Cumberland River drainage collected from 2020 to 2022. *Leaunio vanuxemensis* collected from 2020 to 2022 in the Upper Tennessee River Basin. *N*=number of individuals genotyped per locus, H_o= mean observed heterozygosity, H_e= mean expected heterozygosity, *A*= mean number of observed alleles per locus, *Ap*= total number of private alleles observed per locus, mean *M-ratio* = ratio of *A* and number of alleles possible within the range of nucleotide base-pair differences between the shortest and longest microsatellite alleles observed per locus.

Species	Drainage	Population	*N*	H_o	H_e	*A*	*A*p	Mean M-ratio
C. iris	Clinch	Kyles Ford	5	0.70	0.92	7.25	4	0.41
	Clinch	Bennett Island	9	0.50	0.89	8.75	6	0.49
	Clinch	Copper Creek	8	0.48	0.88	7.63	5	0.46
	Clinch	Cavitts Creek	9	0.44	0.87	8.25	4	0.58
	Clinch	Indian Creek	3	0.40	0.79	3.38	1	0.27
	Clinch	SUB-BASIN TOTAL	34	0.50	0.93	18.38	20	0.58
	Holston	Chilhowie	3	0.67	0.85	4.38	0	0.42
	Holston	Saltville	8	0.56	0.92	9.50	6	0.53
	Holston	Ceres	8	0.61	0.86	8.25	7	0.52
	Holston	Rich Valley	3	0.67	0.88	4.63	2	0.36
	Holston	SUB-BASIN TOTAL	22	0.61	0.92	16.25	15	0.56
	Powell	Wallen Creek	6	0.46	0.85	5.88	0	0.62
	Powell	Big Stone Gap	10	0.36	0.82	8.00	3	0.59
	Powell	Jonesville	3	0.63	0.78	3.25	2	0.51
	Powell	SUB-BASIN TOTAL	19	0.42	0.89	12.50	5	0.64
	Green	Russell Creek	3	0.67	0.70	3.29	5	0.52
	Cumberland	Sinking Creek	3	0.38	0.76	3.38	3	0.67
C. taeniatus	Green	West Fork Drakes Creek	4	0.50	0.82	4.88	2	0.49
	Cumberland	Sinking Creek	3	0.58	0.78	3.63	3	0.52
L. vanuxemensis	Holston	Locust Cove Creek	12	0.53	0.87	9.25	3	0.65
	Powell	Wallen Creek	7	0.46	0.86	5.88	3	0.70

Table 7. Microsatellite DNA allelic differentiation F_{ST} values below diagonal and D_{est} values above the diagonal among populations based on eight microsatellite loci for *Cambarunio iris* in Kyles Ford (KF), Bennett Island (BI), Copper Creek (CC), Cavitts Creek (CAV), Saltville (SAL), Ceres (CE), Rich Valley (RV), Wallen Creek (WC), Big Stone Gap (BSG) in the Upper Tennessee River Basin; Russell Creek (RC) in the Green River drainage; Sinking Creek (SINK) in the Cumberland River drainage. For *Cambarunio taeniatus* in West for Drakes Creek (WFD) in the Green River Drainage and Sinking Creek (SINK) in the Cumberland River drainage. NA indicates value could not be obtained due to low sample size.

		Cambarunio iris												*Cambarunio taeniatus*	
Species		KF	BI	CC	CAV	CH	SAL	CE	RV	WC	BSG	RC	SINK	WFD	SINK
Cambarunio iris	KF	—	0.06	0.45	0.23	0.47	0	0.40	0.17	0.26	0.37	NA	0.42	0.09	0.39
	BI	0.03	—	0.48	0.25	0.14	0.17	0.51	0.66	0.53	0.30	NA	.20	0.33	0.29
	CC	0.06	0.06	—	0.29	0.58	0.25	0.42	0	0.41	0.55	NA	0.44	0.60	0.45
	CAV	0.05	0.05	0.06	—	0.28	0.25	0.47	NA	0.46	0.50	NA	NA	0.68	0.52
	CH	0.08	0.06	0.1	0.08	—	0.31	0.18	NA	0.30	0.38	NA	NA	0.54	0.46
	SAL	0.03	0.04	0.04	0.05	0.06	—	0.25	0.04	0.42	0.53	NA	0.30	0.26	0.32
	CE	0.06	0.08	0.06	0.08	0.06	0.05	—	0.13	0.50	0.34	NA	0.79	0.61	0.59
	RV	0.05	0.09	0.05	0.09	0.09	0.05	0.05	—	0.45	0.44	NA	NA	0.64	0.52
	WC	0.06	0.09	0.08	0.09	0.09	0.07	0.10	0.09	—	0.44	NA	0.60	0.46	0.52
	BSG	0.08	0.07	0.10	0.10	0.10	0.09	0.08	0.10	0.10	—		0.31	0.60	0.68
	RC	0.09	0.09	0.09	0.10	0.16	0.06	0.09	0.12	0.12	0.14	—	NA	NA	NA
	SINK	0.10	0.08	0.12	0.13	0.13	0.09	0.16	0.13	0.15	0.11	0.19	—	0.69	NA
Cambarunio taeniatus	WFD	0.04	0.07	0.11	0.10	0.11	0.06	0.11	0.11	0.10	0.12	0.13	0.17	—	0.60
	SINK	0.08	0.08	0.11	0.14	0.12	0.08	0.12	0.12	0.12	0.16	0.16	0.15	0.14	—

Table 8. Nuclear microsatellite DNA based differentiation showing F_{ST} values (below diagonal) and D_{est} values (above the diagonal) among populations based on eight microsatellite loci for *Cambarunio iris* and *Leaunio vanuxemensis* in the Clinch, Holston, and Powell river drainages.

		Cambarunio iris			*Leaunio vanuxemensis*	
Species		Clinch	Holston	Powell	Holston	Powell
Cambarunio iris	Clinch	—	0.21	0.25	0.42	0.36
	Holston	0.023	—	0.22	0.31	0.27
	Powell	0.020	0.03	—	0.22	0.53
Leaunio vanuxemensis	Holston	0.05	0.04	0.04	—	0.36
	Powell	0.05	0.04	0.08	0.070	—

Table 9. Decision tree analysis confusion matrix for *Cambarunio iris* of the Clinch, Powell, Holston, Green, and Cumberland River drainages; *C. taeniatus* of the Green and Cumberland River drainages; and *Leaunio vanuxemensis* of the Powell and Holston River Drainages. Data validations included Hold-Out validation which splits the data into training (80%, 67 observations) and validation data (20%, 28 observations). The matrix shows predicted and actual identification in order to show the misclassification for each species. The misclassification error for training data was 0 and 10% for the validation data.

			Actual		
			Cambarunio iris	*Cambarunio taeniatus*	*Leaunio vanuxemensis*
Prediction	Training data	*Cambarunio iris*	52	0	0
		Cambarunio taeniatus	0	8	0
		Leaunio vanuxemensis	0	0	7
	Validation Data	*Cambarunio iris*	25	1	1
		Cambarunio taeniatus	1	0	0
		Leaunio vanuxemensis	0	0	0

Figure 1, **Panel A.** Map of the upper Tennessee River basin, including the French Broad River drainage (darker grey). (Panel B.) Tissue sample collection locations of *Cambarunio iris* and *Leaunio vanuxemensis* in the Clinch, Powell, and Holston River drainages.

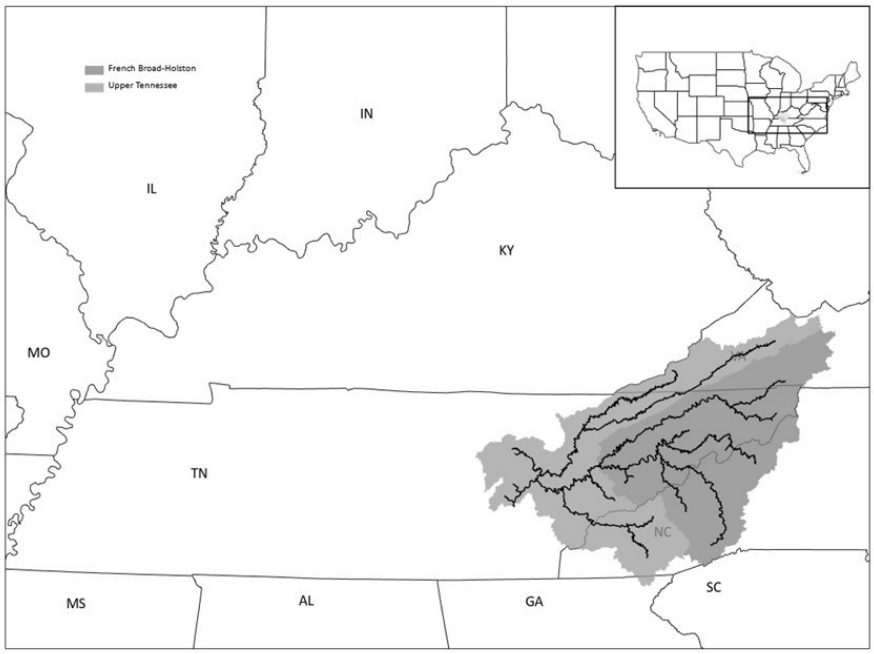

Figure 1, **Panel B**.

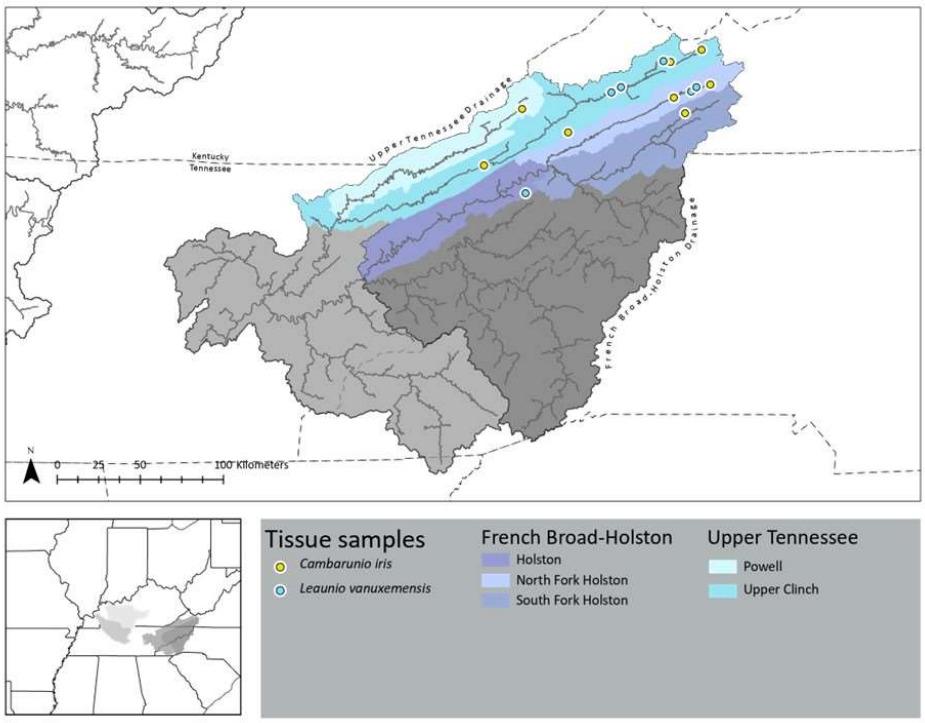

Figure 2. Example of variation among individuals collected for mitochondrial DNA, nuclear DNA, and morphological analyses. *Cambarunio iris* collected from the Holston River drainage in 2020 outlined in yellow. *Cambarunio iris* collected from the Clinch River drainage in 2021 and 2022 outlined in red. *Cambarunio iris* collected from the Powell River drainage in 2022 outlined in blue. *Cambarunio taeniatus* collected from the Green River drainage in 2020 outlined in green. Row A, Columns 1 and 2 indicate right valve periostracum and nacre for one individual, columns 3 and 4 indicate right valve periostracum and nacre for the second individual, and so on.

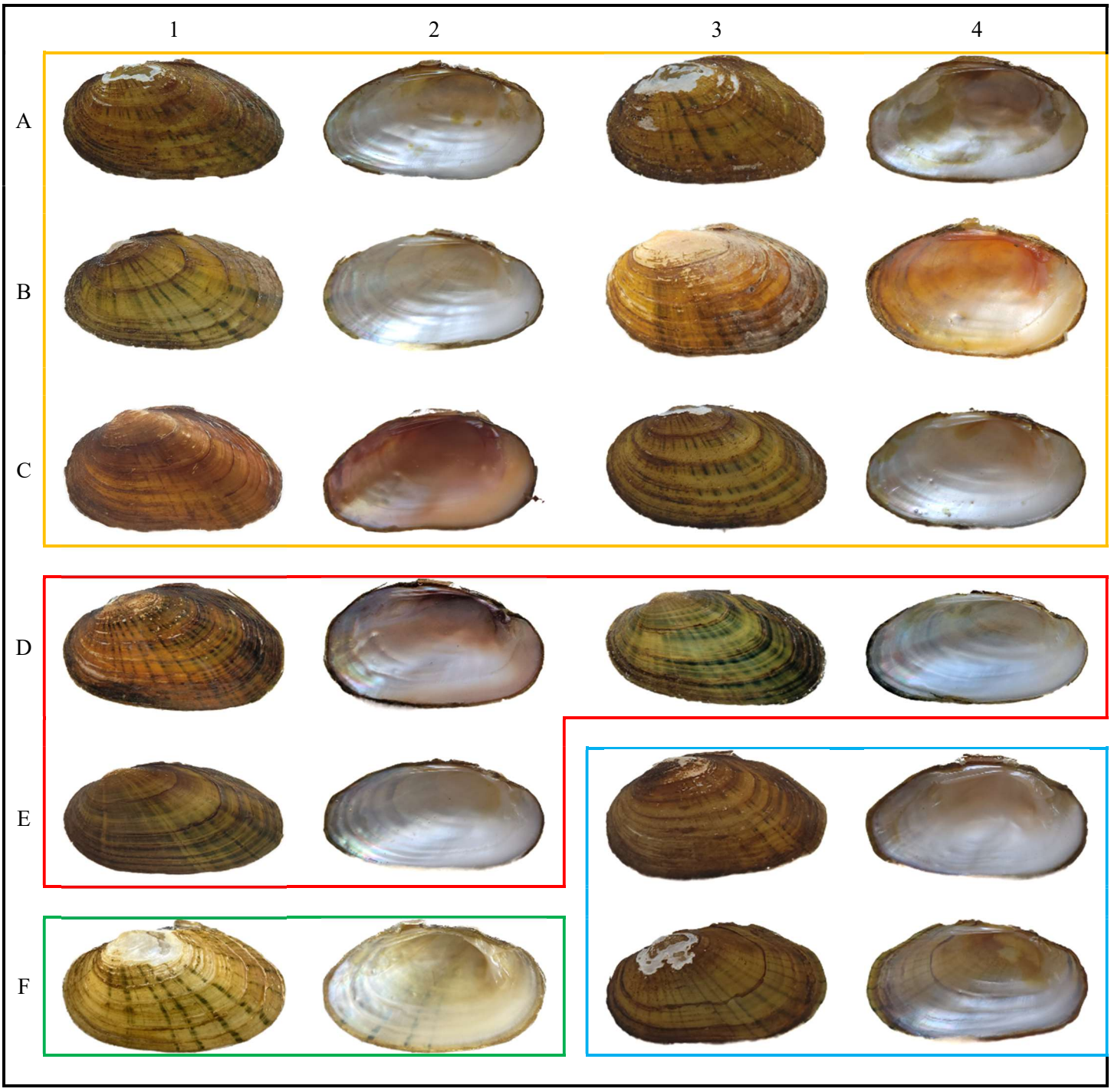

Figure 3. Three morphotypes of *Cambarunio iris* collected in the Upper Tennessee River Basin. Form 1: Elliptical, compressed, yellow with dense green rays. Form 2: Subovate, more inflated, yellow with pencil thin to thick sporadically spaced rays. Form 3: More triangular, compressed, yellow to light brown, with even ray coverage that may be complete or broken.

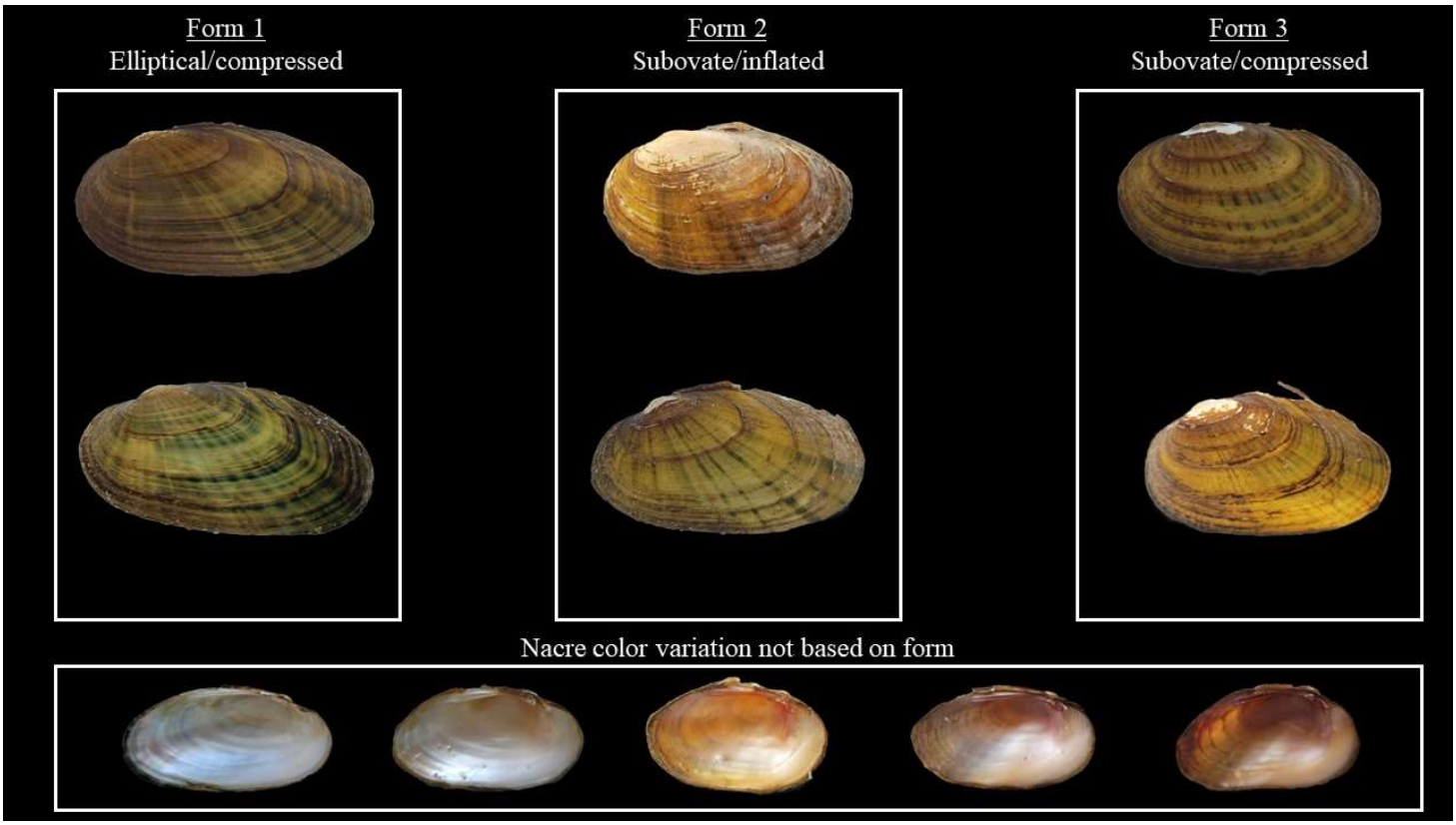

Figure 4. Photographs of mantle lure display for *Cambarunio iris* from Indian Creek in the Clinch River drainage, VA, *Cambarunio dactylus* from the Rough River in the Green River drainage, KY, and *Cambarunio hesperus* from Swan Creek in the White river drainage, MO.

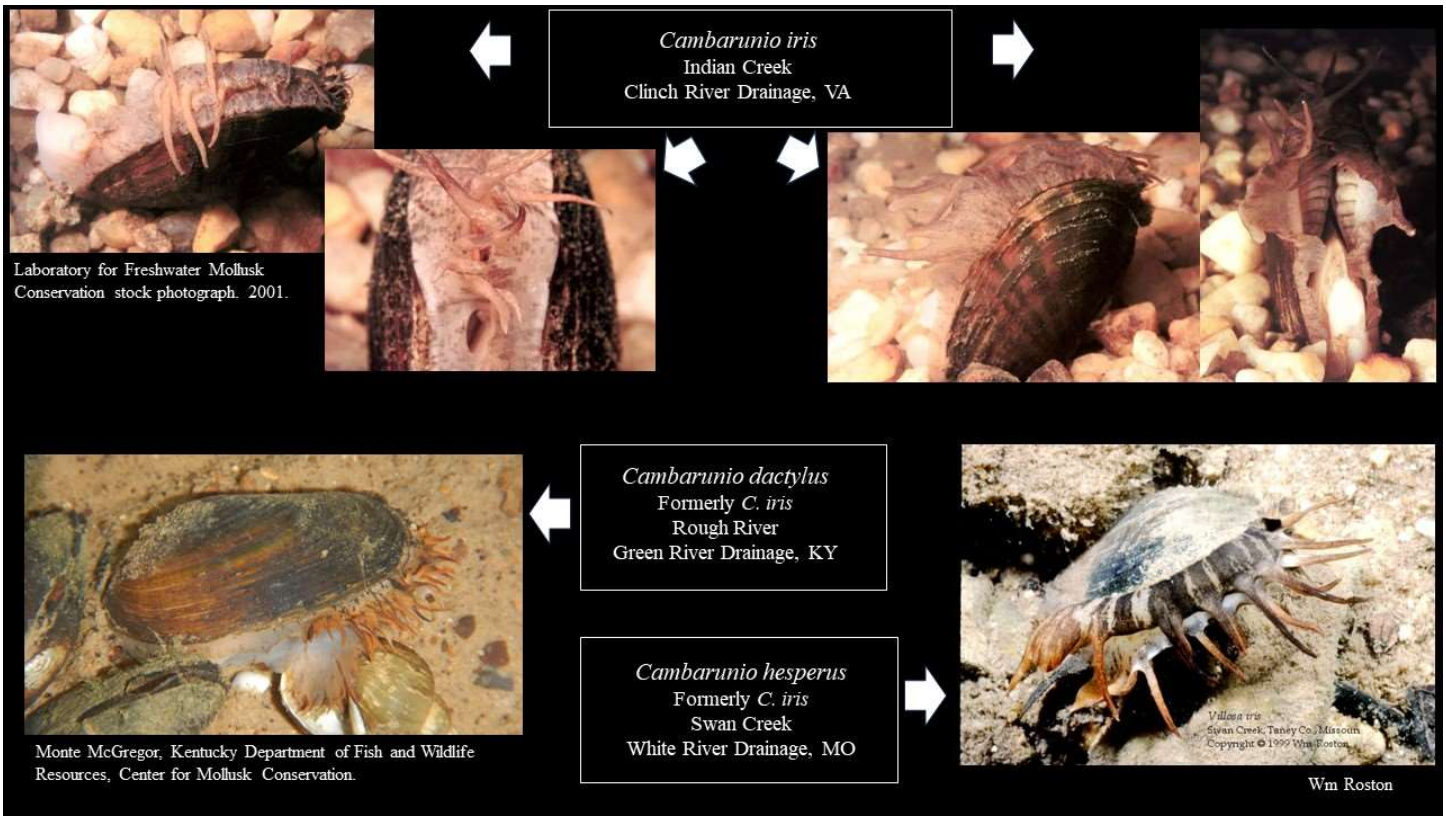

Figure 5. Landmarks used for the geometric morphometric analysis. Two main landmarks were aligned to the anterior part of the umbo (Point 1) and 180 degrees to the longest, posterior of the shell (Point 5). A total of 14 landmarks separated by 15 degrees were used for obtaining shell measurement data.

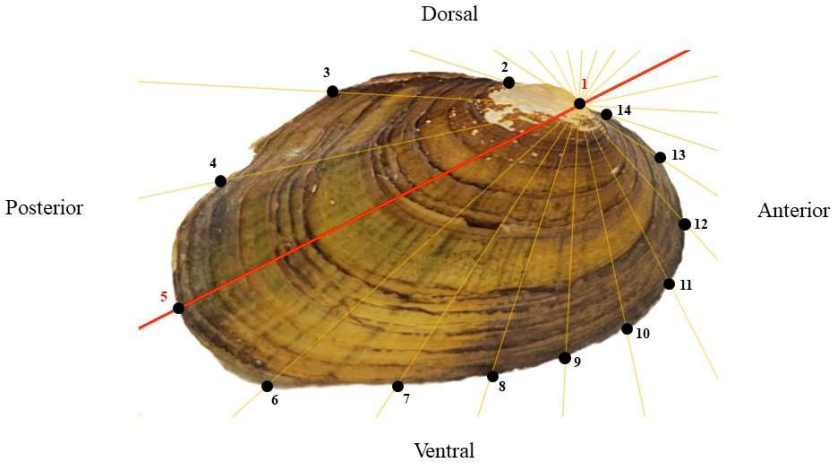

Figure 6. Morphological measurements of a freshwater mussel, showing Max Length, Max hinge height, Max umbo height, and hinge length used for decision-tree and random forest-tree analyses are illustrated. A. Interior of right valve. B. Exterior of right valve.

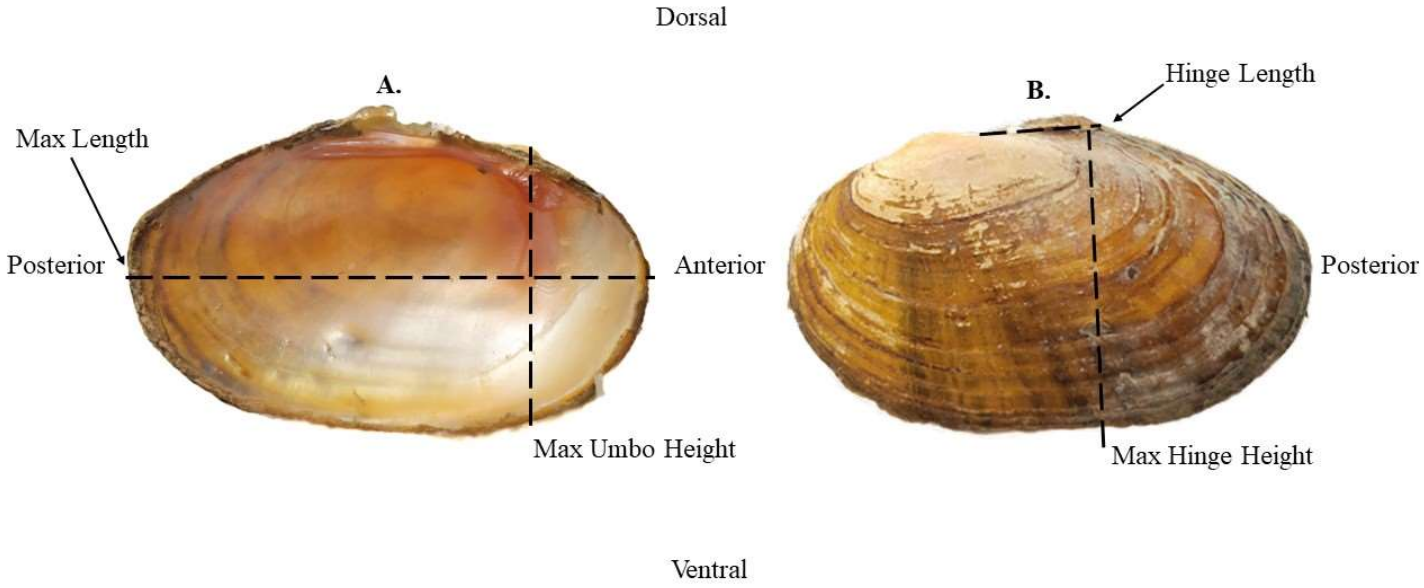

Figure 7. Morphological categorical characteristics. Shell shape categorized as elliptical or subovate, ray pattern categorized as interrupted or uninterrupted, and ray width categorized as fine, wide, or mixed.

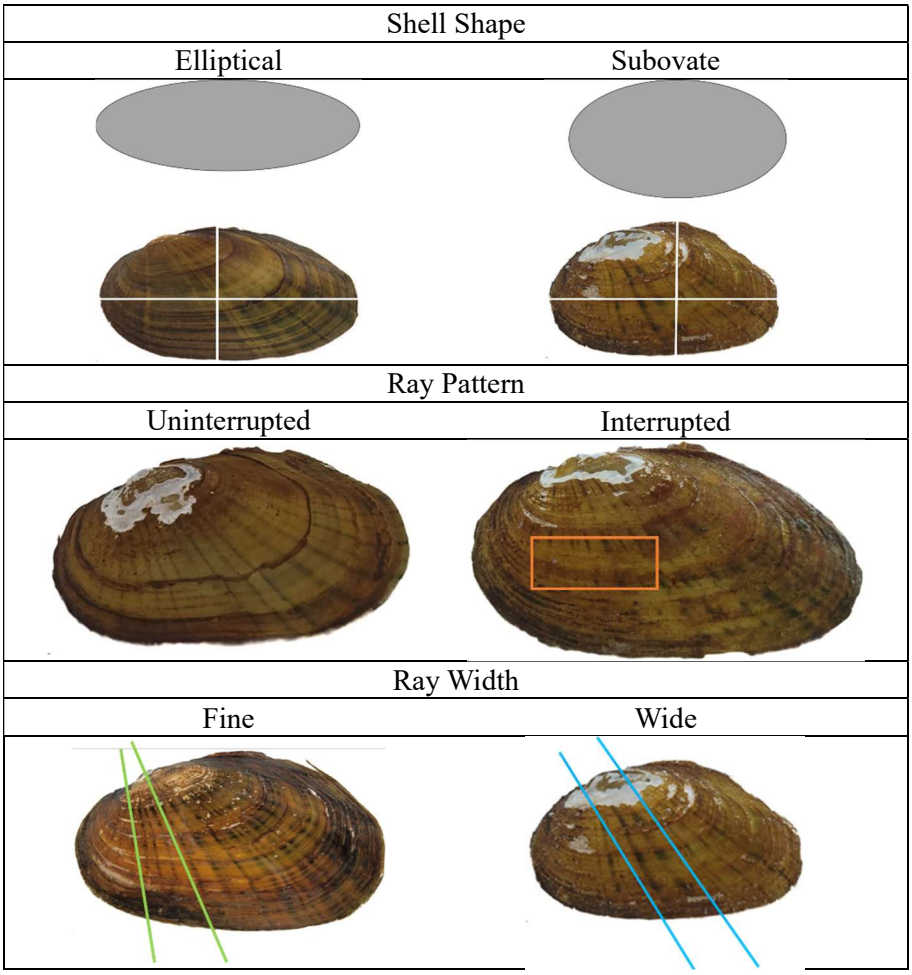

Figure 8. Morphological categorical characteristics. Periostracum color categorized as brown or yellow and nacre color categorized as white, purple, or salmon.

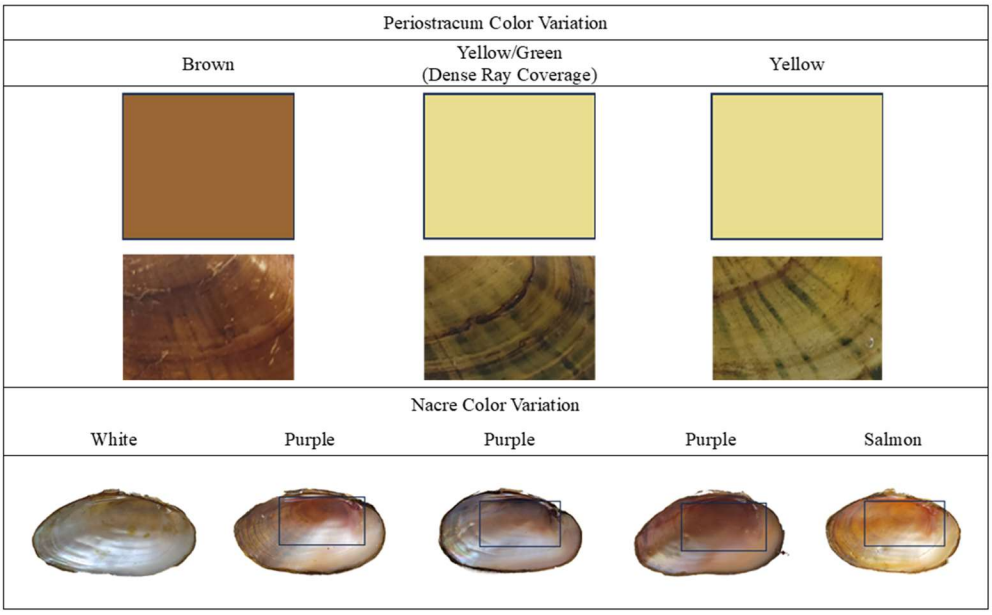

Figure 9. Haplotype network of *Cambarunio iris* indicated in red and *Leaunio vanuxemensis* indicated in purple in the Upper Tennessee River Basin collected from 2018 to 2020; and *Cambarunio taeniatus* (1 individual) of the Green River Drainage, indicated in green, collected in 2020. *Indicates *C. taeniatus* sequences obtained from Genbank which are coded yellow.

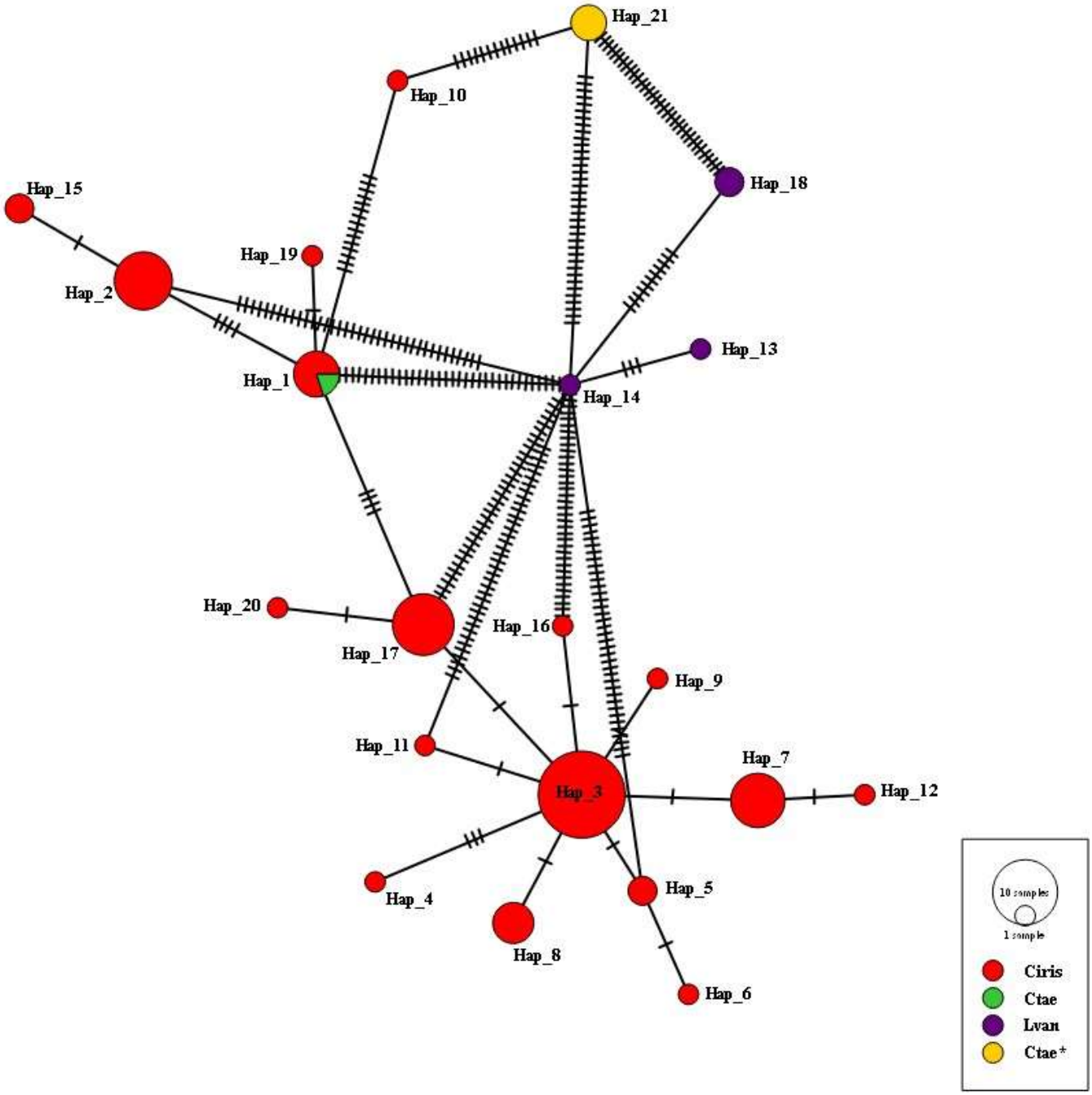

Figure 10, Panel A. Phylogenetic tree constructed using Bayesian inference and a general time reversible model (Nei and Kumar 2000) with gamma-distributed rate variation including 3,000,000 generations with 4 chains with a burnin of 20,000 generations. Posterior probability values less than 0.0040 are not displayed on branch lengths. Individuals are specified by haplotype. Panel A, *Cambarunio iris* and *Leaunio vanuxemensis* were collected from the Upper Tennessee River Basin from 2018 to 2020. *Cambarunio taeniatus* (1 individual) was collected from the Green River drainage in 2020. Additional *C. taeniatus* sequences were obtained from Genbank. Panel B, in addition to the selected sequences per haplotype from the UTRB, sequences from Genbank, included in Kuenhl (2009) were included to increase sample sizes from *C. iris* historic range. States from which sequences originated are in parenthesis with GenBank sequences noted with an asterisk*.

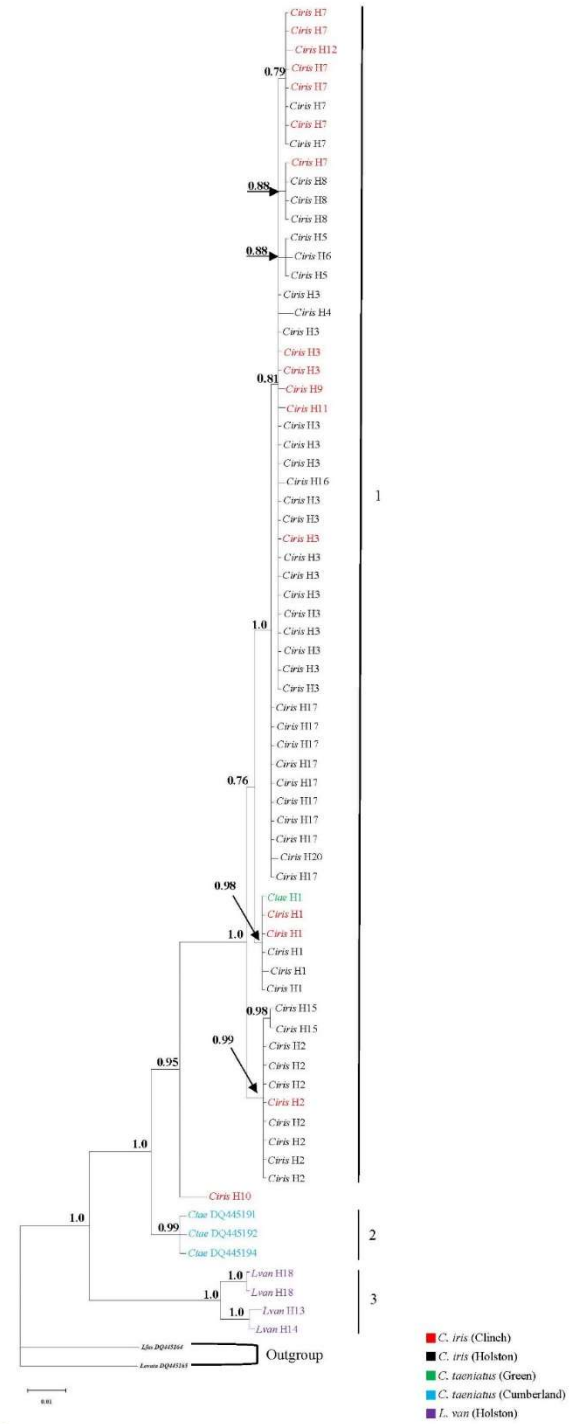

Figure 10, **Panel B**. Phylogenetic tree constructed using Bayesian inference and a general time reversible model (Nei and Kumar 2000) with gamma-distributed rate variation including 3,000,000 generations with 4 chains with a burnin of 20,000 generations. Posterior probability values less than 0.0040 are not displayed on branch lengths. Individuals are specified by haplotype. Panel B, in addition to the selected sequences per haplotype from the UTRB, sequences from Genbank, included in Kuenhl (2009) were included to increase sample sizes from *C. iris* historic range. States from which sequences originated are in parenthesis with GenBank sequences noted with an asterisk*.

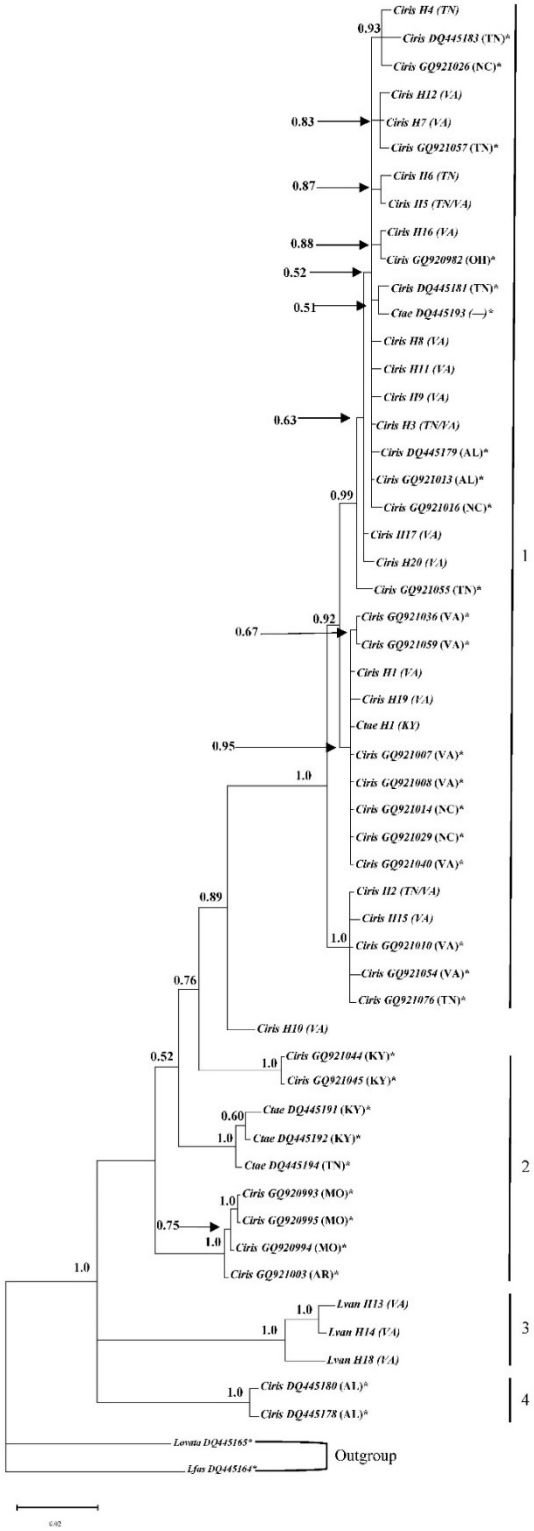

Figure 11. Neighbor-joining (NJ) tree showing relationship between investigated populations of *Cambarunio iris* in the Upper Tennessee River Basin (Panel A) collected from 2020 to 2022; *Cambarunio iris* from the Upper Tennessee River Basin and *Cambarunio taeniatus* collected from the Green and Cumberland River drainages from 2020 to 2022 (Panel B); Individual populations combined per river drainage to increase sample sizes (Panel C). The tree was constructed from DNA microsatellite allele frequency data using Nei's standard genetic distance (D_{ST}). *Indicates *C. taeniatus*.

Figure 11, Panel A.

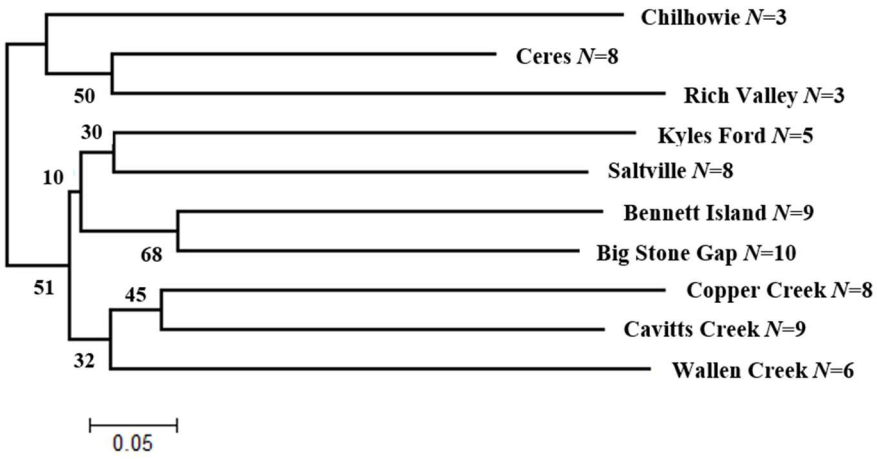

Figure 11, Panel B.

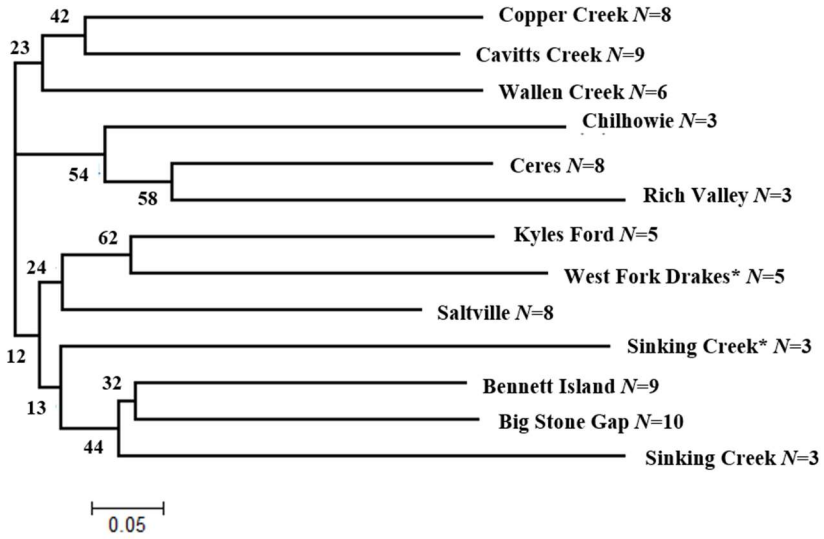

Figure 11, Panel C.

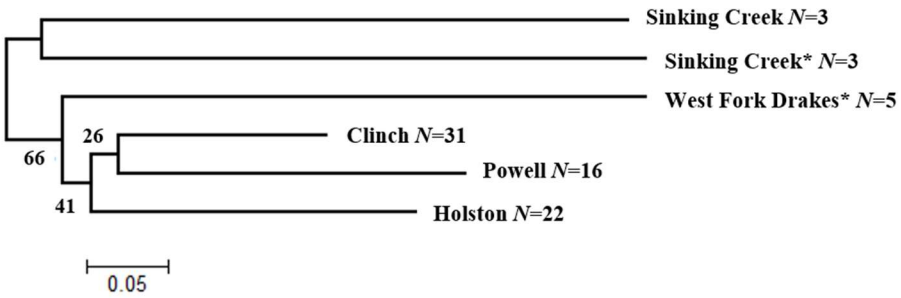

Figure 12. STRUCTURE output bar graph showing geographic populations on the *x*-axis and population ancestry, i.e., assignment probability to populations on the *y*-axis. STRUCTURE version 2.3.4, the smallest mean probability of *K* (Ln*P*(*K*)) supports a fourteen population (*K*=14) distinction (Panel A). We grouped individuals by morphotype and the smallest mean probability of *K* (Ln*P*(*K*)) supports a ten population (*K*=10) distinction (Panel B). *Indicates *C. taeniatus*.

Figure 12, Panel A.

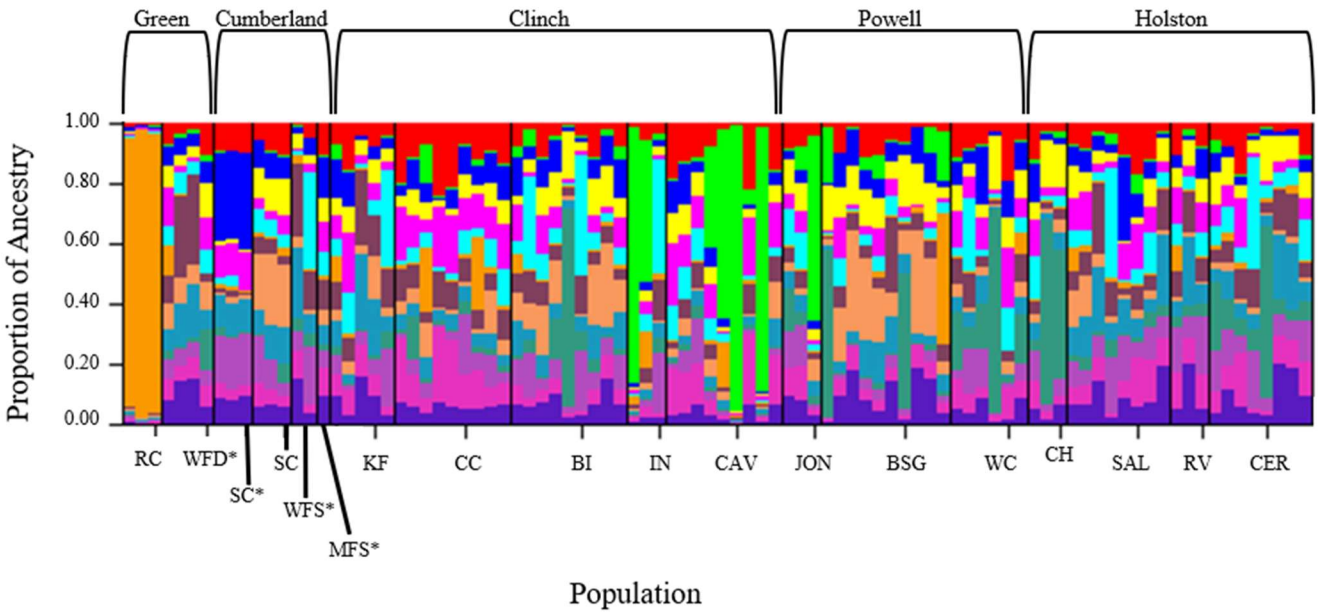

Figure 12, Panel B.

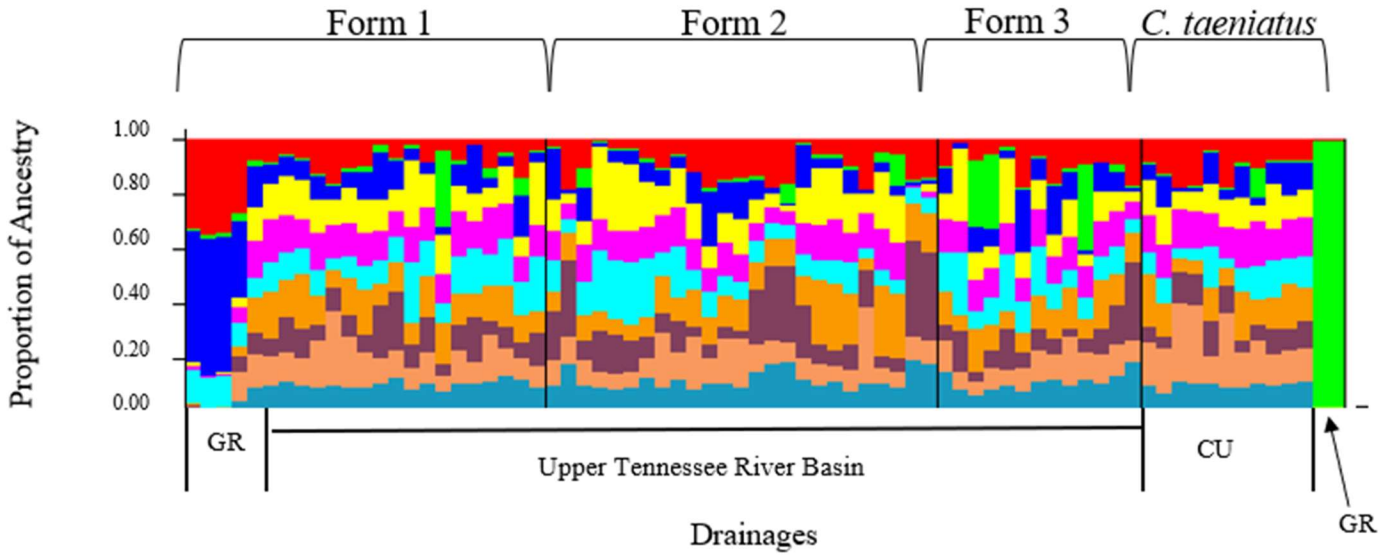

Figure 13. Canonical Variate Analysis and shell landmark variation used to assess differences among species at two size classes (Panel A) medium (30.1 mm ≤50 mm), (Panel B) large sized mussel specimens (>50.1 mm) of *Cambarunio iris* of the Clinch, Powell, Holston, Green, and Cumberland River drainages; *Cambarunio taeniatus* of the Green and Cumberland River drainages; and *Leaunio vanuxemensis* of the Powell and Holston River Drainages. This analysis compares individuals of each species, drainage, and respective size classes. (Panel C) compares individuals based on species and morphotype.

Figure 13, Panel A.

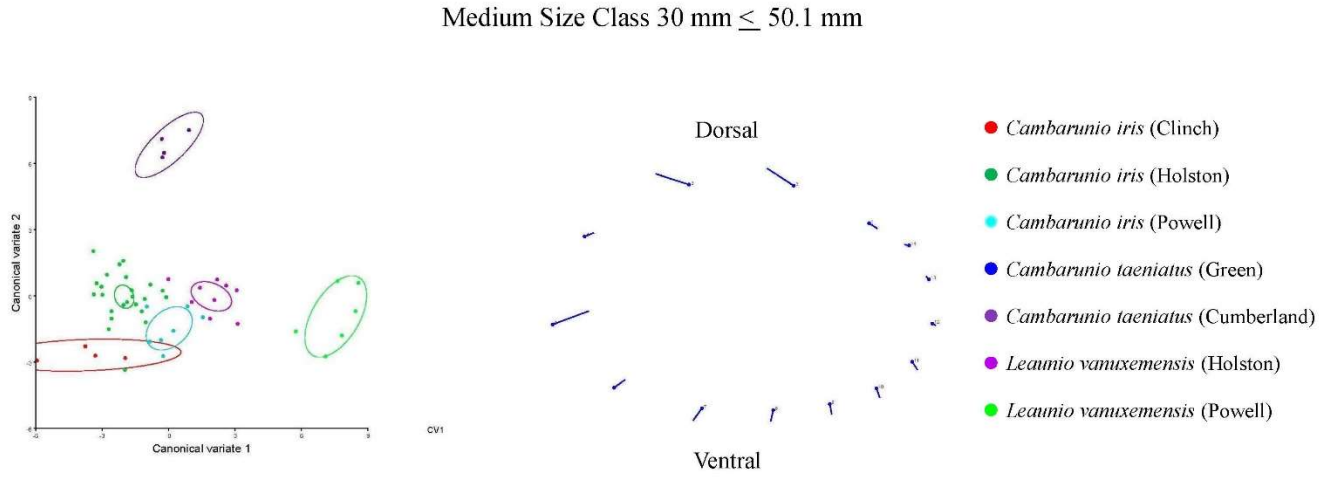

Figure 13, Panel B.

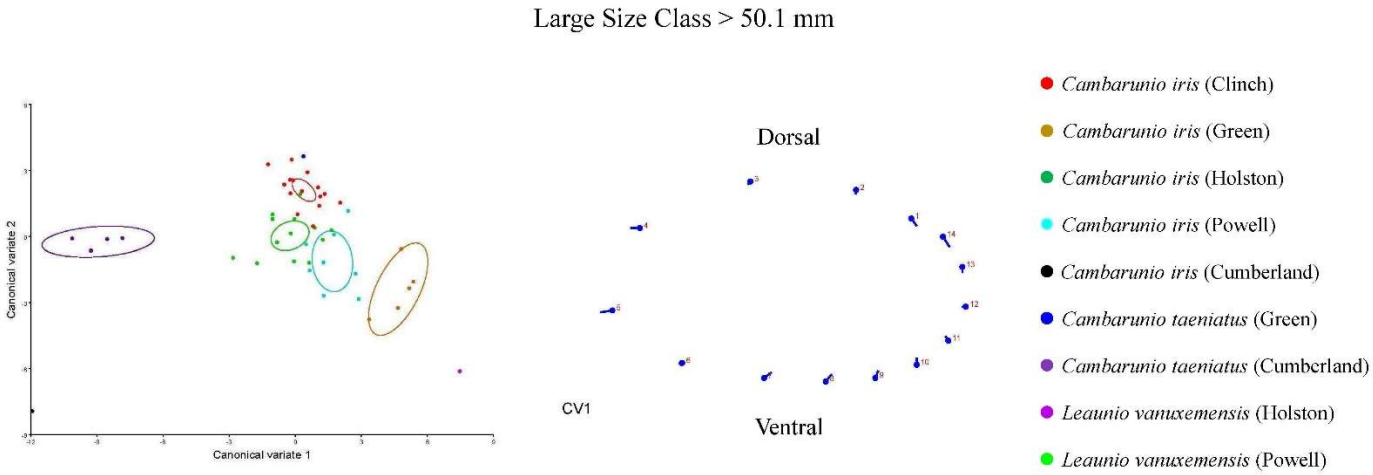

Figure 13, Panel C.

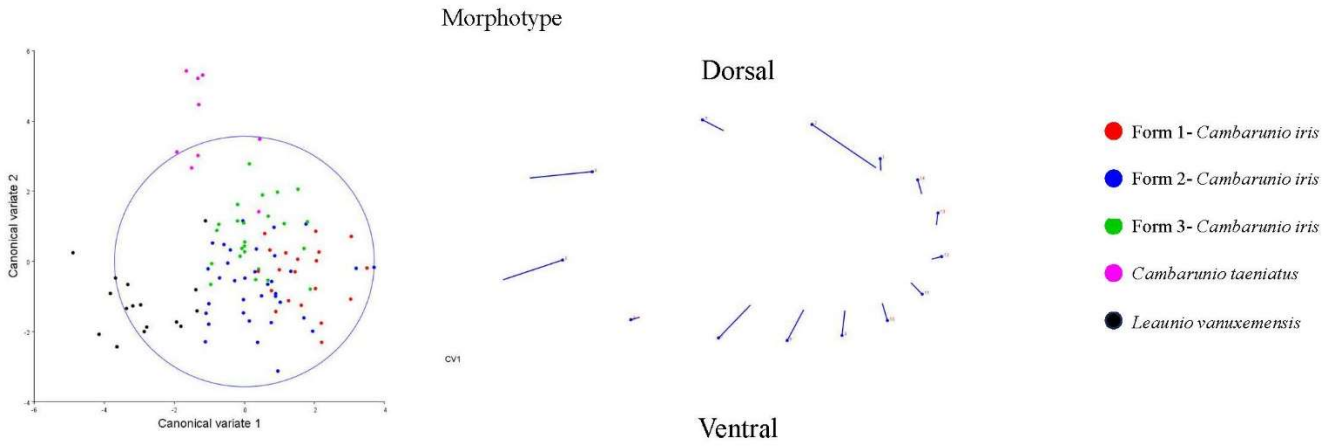

Figure 14. Ranges of quantitative morphological variables recorded for *Cambarunio iris* of the Clinch, Powell, Holston, Green, and Cumberland River drainages; *Cambarunio taeniatus* of the Green and Cumberland River drainages; and *Leaunio vanuxemensis* of the Powell and Holston River Drainages. Quantitative morphological variables include: (1) percentage of Ray Coverage, (2) Maximum Length, (3) Maximum Hinge Height, (4) Maximum Umbo Height, (5) Shell Width, and (6) Hinge Length.

Figure 14. Panel A.

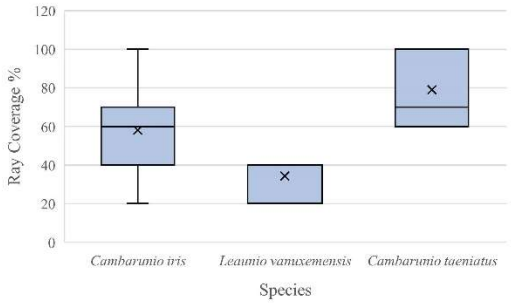

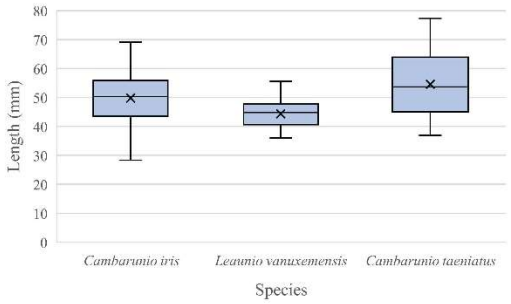

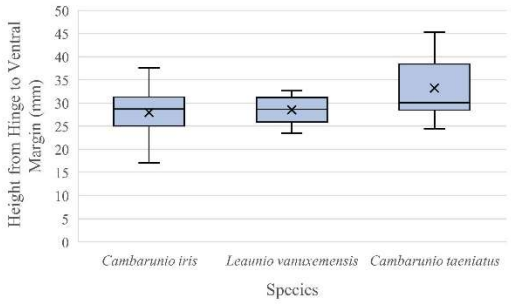

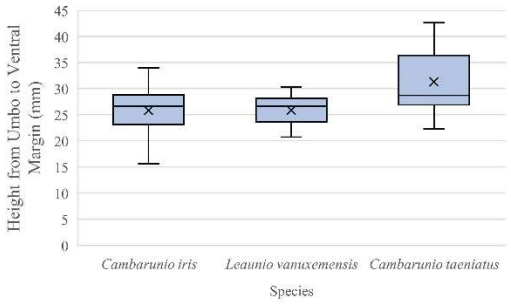

Figure 14. Panel B.

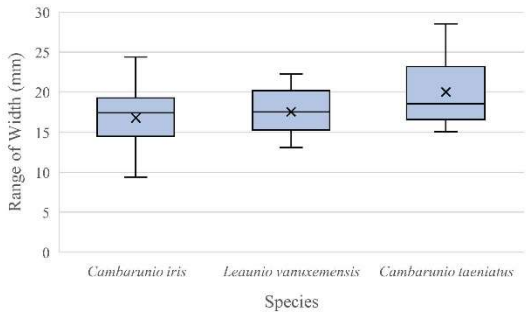

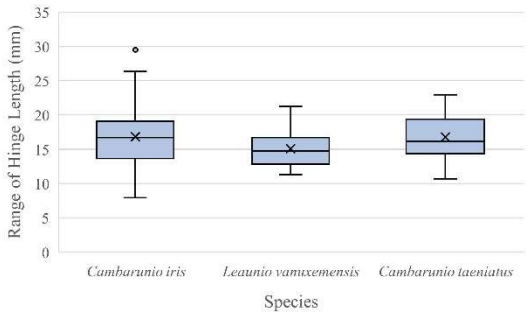

Figure 15. Categorical variables and the number of individuals per species of *Cambarunio iris* of the Clinch, Powell, Holston, Green, and Cumberland River drainages; *Cambarunio taeniatus* of the Green and Cumberland River drainages; and *Leaunio vanuxemensis* of the Powell and Holston River Drainages. Categorical variables recorded for each individual included: (1) Shape, (2) Periostracum Color, (3) Ray Width, (4) Ray Spacing, (5) Ray Pattern, (6) Foot Color, and (7) Nacre Color.

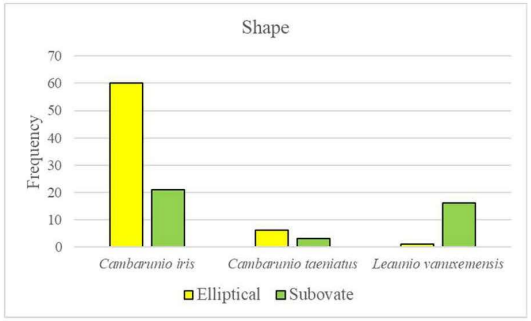

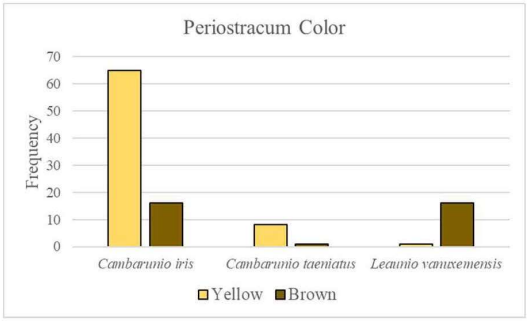

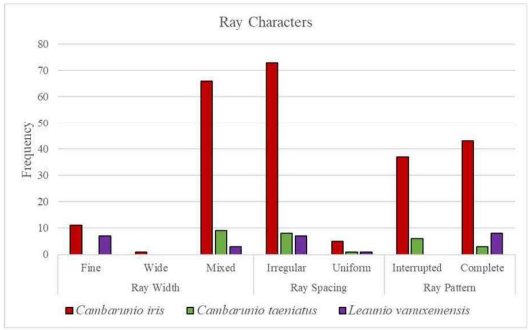

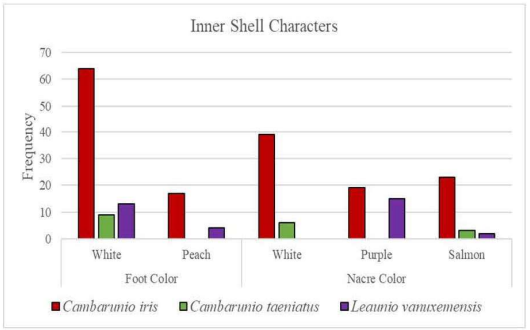

Figure 16. Key identifying morphological variables of *Cambarunio iris* (of the Clinch, Powell, Holston, Green, and Cumberland River drainages), *Cambarunio taeniatus* (of the Green and Cumberland River Drainages), and *Leaunio vanuxemensis* (of the Holston and Powell River Drainages) determined by a mean decrease in identification accuracy (Panel A) and the mean decrease in Gini coefficient (Panel B), which measures the probability of misclassification using random forest analysis.

Figure 16, Panel A.

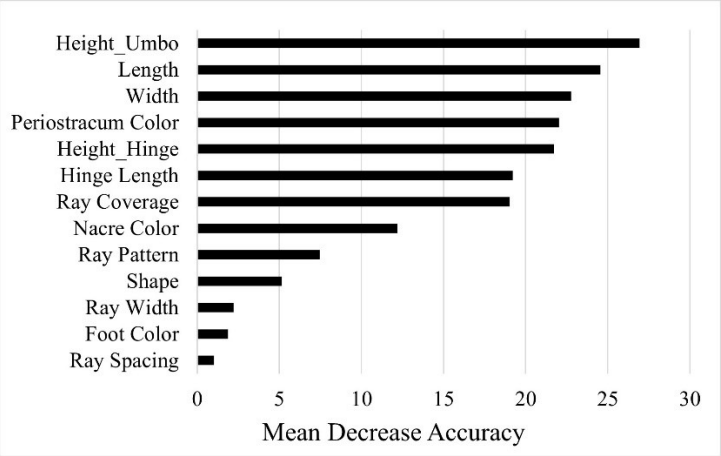

Figure 16, Panel B.

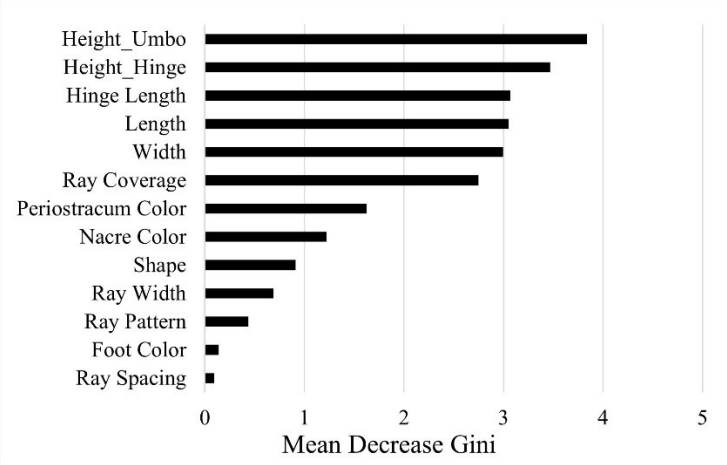

Figure 17. Decision tree analysis using internal and external shell variables identifying *Cambarunio iris* of the Clinch, Powell, Holston, Green, and Cumberland River drainages; *Cambarunio taeniatus* of the Green and Cumberland River drainages; and *Leaunio vanuxemensis* of the Powell and Holston River Drainages. Tree was constructed using 80% of the data as training data and 20% as validation data.

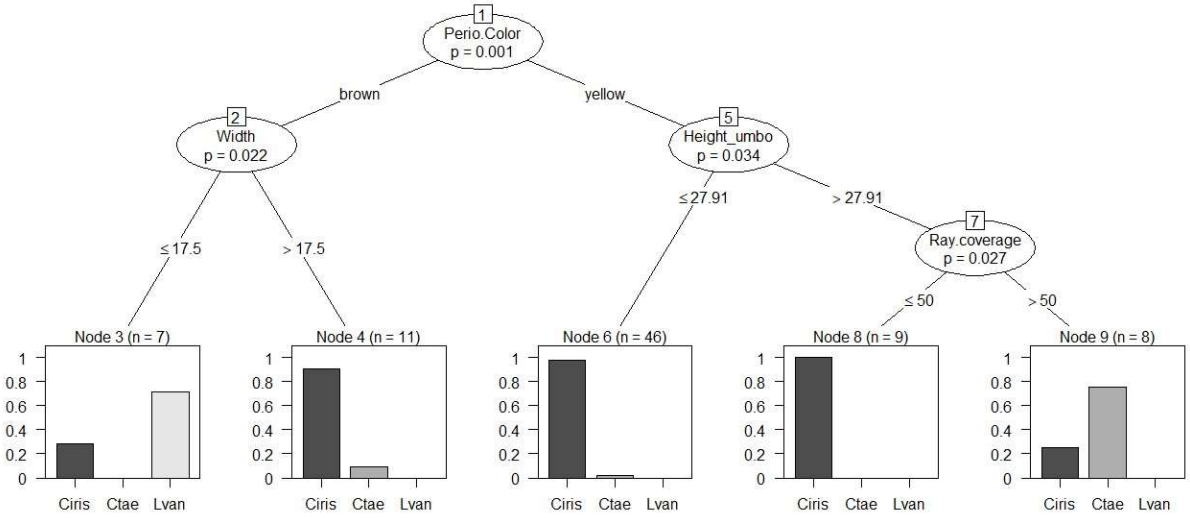

Appendix. GeneBank *ND1* mitochondrial DNA sequences used in Kuhenl (2009) for comparison to sequences from the Upper Tennessee River Basin.

Species	Location	River	County	State	Collector	*ND1* Genbank Ascension Number
Cambarunio iris	Hurricane Creek	Paint Rock	Jackson	AL	J. Godwin, D. Sheldon	DQ445178
Cambarunio iris	Hurricane Creek	Paint Rock	Jackson	AL	J. Godwin, D. Sheldon	DQ445179
Cambarunio iris	Hurricane Creek	Paint Rock	Jackson	AL	J. Godwin, D. Sheldon	DQ445180
Cambarunio iris	Mainstem	Little	Blount	TN	S. Fraley	DQ445181
Cambarunio iris	Daddy's Creek	Obed	Cumberland	TN	J. Buhay	DQ445183
Cambarunio iris	Beaver Creek	White	Douglas	MO	M.C. Barnhart	GQ920993
Cambarunio iris	Beaver Creek	White	Douglas	MO	M.C. Barnhart	GQ920994
Cambarunio iris	Beaver Creek	White	Douglas	MO	M.C. Barnhart	GQ920995
Cambarunio iris	11 point Run	White	Randolph	Arkansas	A.D. Christian	GQ921003
Cambarunio iris	11 point Run	White	Randolph	Arkansas	A.D. Christian	GQ921004
Cambarunio iris	Russell Creek	Green	Adair	KY	K.F. Kuehnl, R. Evans	GQ921044
Cambarunio iris	Russell Creek	Green	Adair	KY	K.F. Kuehnl, R. Evans	GQ921045
Cambarunio iris	Grissom Island	Clinch	Claiborne	TN	J. Jones	GQ921055
Cambarunio iris	Grissom Island	Clinch	Claiborne	TN	J. Jones	GQ921057
Cambarunio iris	Mainstem	Little	Tazewell	VA	J. Jones	GQ921059
Cambarunio iris	Mainstem	Little Darby Creek	Madison	Ohio	G.T. Watters et al.	GQ920982
Cambarunio iris	Mainstem	Tennessee	Jackson	Alabama	J.T. Garner	GQ921013
Cambarunio iris	Peachtree Creek	Hiwassee	Cherokee	NC	S. Fraley et al.	GQ921014
Cambarunio iris	Peachtree Creek	Hiwassee	Cherokee	NC	S. Fraley et al.	GQ921016
Cambarunio iris	Mainstem	Little Tennessee	Swain	NC	S. Fraley et al.	GQ921026
Cambarunio iris	Mainstem	North Fork Holston	Scott	VA	N/A	GQ921054
Cambarunio iris	Beech Creek	Holston	Hawkins	TN	S. Fraley, R.S. Butler, S. Ahlstedt	GQ921076
Cambarunio iris	Mainstem	Hiwassee	Cherokee	NC	S. Fraley et al.	GQ921029
Cambarunio iris	Mainstem	Clinch	Tazewell	VA	N. Eckert	GQ921040
Cambarunio iris	Indian Creek	Clinch	Tazewell	VA	J. Jones	GQ921007
Cambarunio iris	Indian Creek	Clinch	Tazewell	VA	J. Jones	GQ921008
Cambarunio iris	Indian Creek	Clinch	Tazewell	VA	J. Jones	GQ921010
Cambarunio iris	Mainstem	Little	Tazewell	VA	N. Eckert	GQ921036
Cambarunio taeniatus	Mainstem	Rockcastle	Rockcastle	KY	J. Buhay, A. Wethington	DQ445191
Cambarunio taeniatus	Mainstem	Rockcastle	Rockcastle	KY	J. Buhay, A. Wethington	DQ445192
Cambarunio taeniatus	Big South Fork	Cumberland	Scott	TN	S. Ahlstedt	DQ445194
Lampsilis fasciola						DQ445164